AD NUMBER

AD845600

LIMITATION CHANGES

TO:

Approved for public release; distribution is unlimited.

FROM:

Distribution authorized to U.S. Gov't. agencies and their contractors; Critical Technology; OCT 1968. Other requests shall be referred to Air Force Rome Air Development Center, EMATE, Griffiss AFB, NY. This document contains export-controlled technical data.

AUTHORITY

radc, usaf, ltr, 17 sept 1971

RADC-TR-68-557
October 1968, Final Report

HIGH POWER C BAND PHASE SHIFTERS

L. J. Lavedan, Jr.

Contractor: Sperry Rand Corporation
Contract Number: F30602-68-C-0006
Effective Date Of Contract: 11 July 1967
Contract Expiration Date: 15 October 1968
Amount of Contract: $125,134.00
Program Code Number: 7E30

Principal Investigator: L. J. Lavedan, Jr.
Phone: 813-855-4471

Project Engineer: Patsy A. Romanelli
Phone: 315-330-4924

Sponsored by
Advanced Research Projects Agency
ARPA Order No. 550

Rome Air Development Center
Air Force Systems Command
Griffiss Air Force Base, New York

When US Government drawings, specifications, or other data are used for any purpose other than a definitely related government procurement operation, the government thereby incurs no responsibility nor any obligation whatsoever; and the fact that the government may have formulated, furnished, or in any way supplied the said drawings, specifications, or other data is not to be regarded, by implication or otherwise, as in any manner licensing the holder or any other person or corporation, or conveying any rights or permission to manufacture, use, or sell any patented invention that may in any way be related thereto.

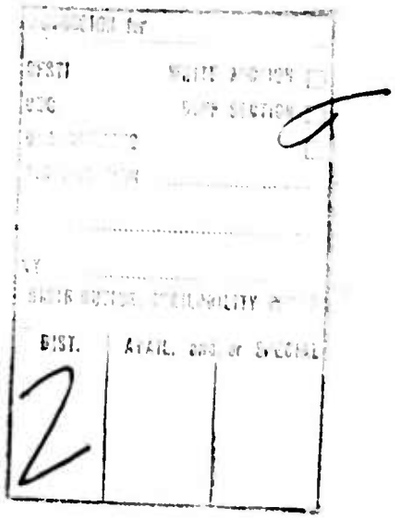

Do not return this copy. Retain or destroy.

HIGH POWER C BAND PHASE SHIFTERS

L. J. Lavedan, Jr.

Sperry Rand Corporation

This research was supported by the Advanced Research Projects Agency of the Department of Defense and was monitored by P. A. Romanelli, RADC (EMATE), GAFB, N.Y. 13440 under Contract No. F30602-68-C-0006

PUBLICATION REVIEW

This report has been reviewed and is approved.

Approved: PATSY A. ROMANELLI
Project Engineer
Electron Devices Section

Approved: LEO M. SULLIVAN
Colonel, USAF
Chief, Surveillance & Control Division

FOR THE COMMANDER:

IRVING J. GABELMAN
Chief, Advanced Studies Group

TABLE OF CONTENTS

TABLE OF CONTENTS (Continued)

TABLE OF CONTENTS (Continued)

LIST OF ILLUSTRATIONS

LIST OF ILLUSTRATIONS (Continued)

LIST OF ILLUSTRATIONS (Continued)

SYNOPSIS

This is the Final Report on this program.

This report outlines all tasks performed under this program and includes techniques performed in developing high power phase shifters and a description of the hardware delivered with test results.

Structural studies have been carried out to assure compatability of designs with phased array requirements. Cross sections have been reduced to a minimum by careful location of cooling structures.

Remote driving techniques were developed with emphasis on switching efficiency. A scheme of triggering a single bit phase shifter is outlined in detail.

Studies of flux drive led to a better understanding of practical and theoretical limitations, these limitations being discussed in detail.

A direct comparison of single and multibit phase shifters is given with emphasis on microwave performance and relative cost.

Memorandum on Final Report
Contract F30602-68-C-0006

20 November 1968

1. The purpose of this program was to design and fabricate high power ferrimagnetic digital phase shifters. Two approaches were followed. These are the multibit type, where each bit is switched to achieve phase, and the single bit unit, where the phase is determined by the level of magnetization within the material. Both types of phase shifters, with their associated drivers, were built.

2. Test results indicate that practical phase shifters can be constructed that will handle 100 Kw peak, 1000 watts average, and 100 microsecond pulse width. The cost for each type of phase shifter is considered to be equivalent; and while the multibit approach is more complex, it exhibits greater phase accuracy and less loss.

Patsy A Romanelli

PATSY A. ROMANELLI
Project Engineer
Electron Devices Section

1. INTRODUCTION

1.1 PROGRAM OBJECTIVES

The purpose of this program was the design and fabrication of high power digital phase shifters capable of continuous operation at 100 KW peak, 1000 watts average, 100 microsecond rf pulse length, with size and performance compatible with operation in a phased array radar.

General system parameters that were extended to the phase shifter included:

- Phase steps of 22.5^{o}
- Close packing of phase shifters for 0.5λ to 0.6λ centers spacing
- Remote drivers required as a result of spacing requirements.

This program included the development of a multibit type of unit wherein each bit is switched between fixed magnetizations, and a single bit device wherein the phase steps are attained by steps in magnetization level of the device. Selection of phase increments when using the single bit phase shifter is attained by flux drive control of the driver.

Of necessity, this program included the following broad categories:

- Evaluation of system needs
- Materials considerations
- Construction and assembly techniques
- High power considerations.

1.2 IMPLEMENTATION AND ATTAINMENT OF OBJECTIVES

After careful evaluation of the state of the art in phase shifter design, the following tasks were determined to be included as part of this program:

- Evaluation of microwave performance of ferrite (garnet) materials in their partially magnetized state with emphasis on peak power performance.
- A study of techniques to reduce and suppress arcing in the phase shifter structure due to high peak powers and/or wide rf pulse width.

- Attainment of stable differential phase at all average powers up to the maximum specified under this program. (This phase included cooling methods and effects of magnetostriction as related to high average power and nonuniform heating.)

- Design of drivers. The single bit driver included flux drive performance and a relatively simple means of programming.

- Construction of phase shifters of the above mentioned types and a direct comparison of performance of the devices. This comparison of necessity included cost comparison and performance-cost tradeoff between the two methods of design.

These objectives have been attained under this program with successful completion of the two designs. Several important engineering advances to the state of the art were attained and because of the similarity of microwave construction of the two types of devices, a reliable comparison of performance was attained.

1.3 RELATED STUDIES OF PHASE SHIFTER DESIGN

As part of this program it was necessary to formulate and confirm a basic understanding of the following areas:

- Remoted drivers . . . Impedance and efficiency effects on driver-phaser performance due to long lead lengths.

- Magnetostriction . . . Study of CVB materials that normally have very low magnetostrictive properties and their use as microwave materials. This study of necessity included a study of all properties of CVB materials.

- Flux drive . . . A thorough understanding of flux drive was attempted with emphasis on the subtle interaction between flux, waveguide cross section, and especially toroid wall thickness.

The results of these studies are given in later sections of this program. The discussion of flux drive phenomena is of special importance in that it indicates a set of limiting circumstances to its use not previously considered.

2. DESIGN

2.1 PHASE SHIFTER CROSS SECTION

A computer program was previously devised at Sperry[1] to precisely predict microwave parameters of loaded waveguide structures including magnetic and dielectric components. This program satisfies the needs of ferrite phase shifter design.

Figures 1 and 2 are typical of the normalized curves generated from this computer program. As can be seen from Figures 1 and 2, minimum insertion loss and maximum phase shift per inch are not compatible in terms of waveguide dimensions. A study of these and other related curves has resulted, however, in a compromise cross section as given in Figure 3.

For certain applications, it is often desirable to deviate from this "optimum" towards an individual parameter optimum, as occurred for the high power phase shifters of this program.

Because of the high average power encountered in conjunction with thermal transfer characteristics of the typical microwave structure, a minimum insertion loss was indicated as most desirable.

Optimization for minimum insertion loss yields several benefits:

- Reduction in overall device insertion loss.
- Reduction in loss/inch of material from overall loss reduction and increase in ferrite length.
- Reduction in microwave coupling to ferrite yielding higher limiting threshold (to be discussed in Section 2.2).

Figures 4 and 5 were computer-generated for this program. Special modifications were made to accept waveguide dimensions and frequency directly (unnormalized), and an additional parameter was introduced, that is, all parameters were plotted for the condition of zero phase-frequency slope. The cross section of Figure 6 was derived from these curves.

In addition, the effects of boron nitride dielectric constant have been included in the calculations of Figures 4 and 5 by deriving an effective dielectric constant for the regions on each side of the magnetic toroid material.

---

[1] J. L. Allen, "The Analysis of Dielectric-Loaded Ferrite Phase Shifters Including the Effects of Losses," Ph. D. dissertation, Georgia Institute of Technology, May 1966

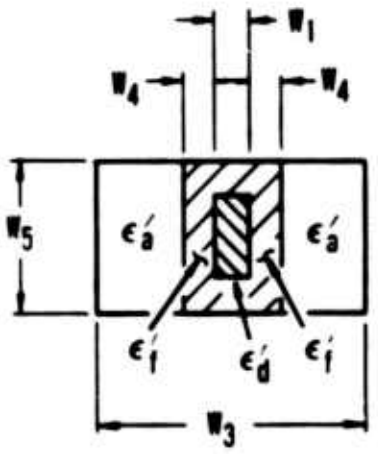

$m_s = \dfrac{\gamma 4\pi M_s}{\omega_c} = 0.8$

f_c = 9 Gc

$m = \dfrac{\gamma 4\pi M_f}{\omega_c} = 0.4$

FR = 1.0

W_1 = PARAMETER

$W_3 = 0.5\ \lambda_c$

W_4 = VARIABLE

$W_5 = 0.294\ \lambda_c$

$R_f = 0.5$

$\epsilon'_a = 1.0$

$\epsilon'_d = 16.0$

$\epsilon'_f = 16.0$

$\tan \delta_a = 0$

$\tan \delta_d = 0.0005$

$\tan \delta_f = 0.0007$

λ_c = 3 33 Cm

HF = 0

ΔH = 65 Oe.

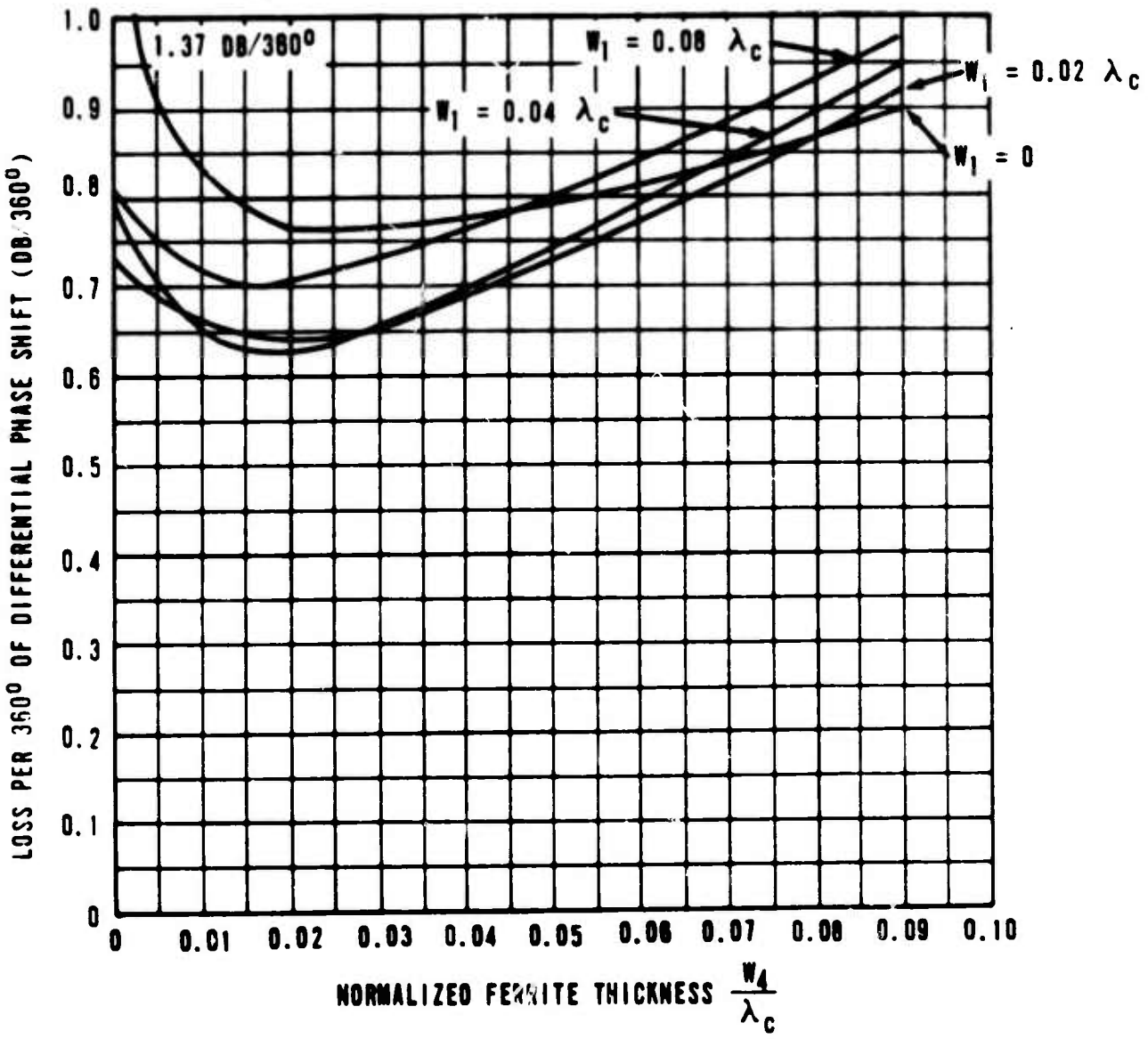

Figure 1. Loss Per 360° of Differential Phase Shift vs Normalized Ferrite Thickness with Dielectric Core Thickness as a Parameter. This plot indicates a minimum loss for a toroid wall thickness $W_4 \approx 0.02\ \lambda_c$.

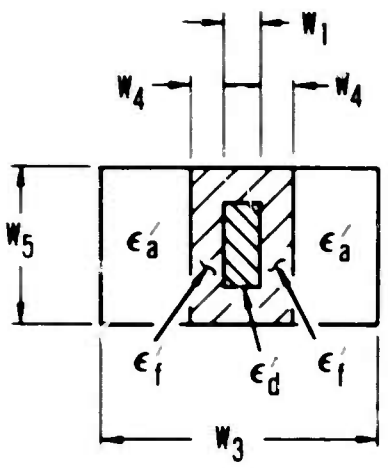

$$m_s = \frac{\gamma 4\pi M_s}{\omega_c} = 0.8$$

f_c = 9 Gc

$$m = \frac{\gamma 4\pi M_f}{\omega_c} = 0.4$$

FR = 1.0

W_1 = PARAMETER

$W_3 = 0.5\ \lambda_c$

W_4 = VARIABLE

$W_5 = 0.294\ \lambda_c$

R_f = 0.5

ϵ'_a = 1.0

ϵ'_d = 16.0

ϵ'_f = 16.0

tan δ_a = 0

tan δ_d = 0.0005

tan δ_f = 0.0007

λ_c = 3.33 Cm

HF = 0

ΔH = 65 Oe.

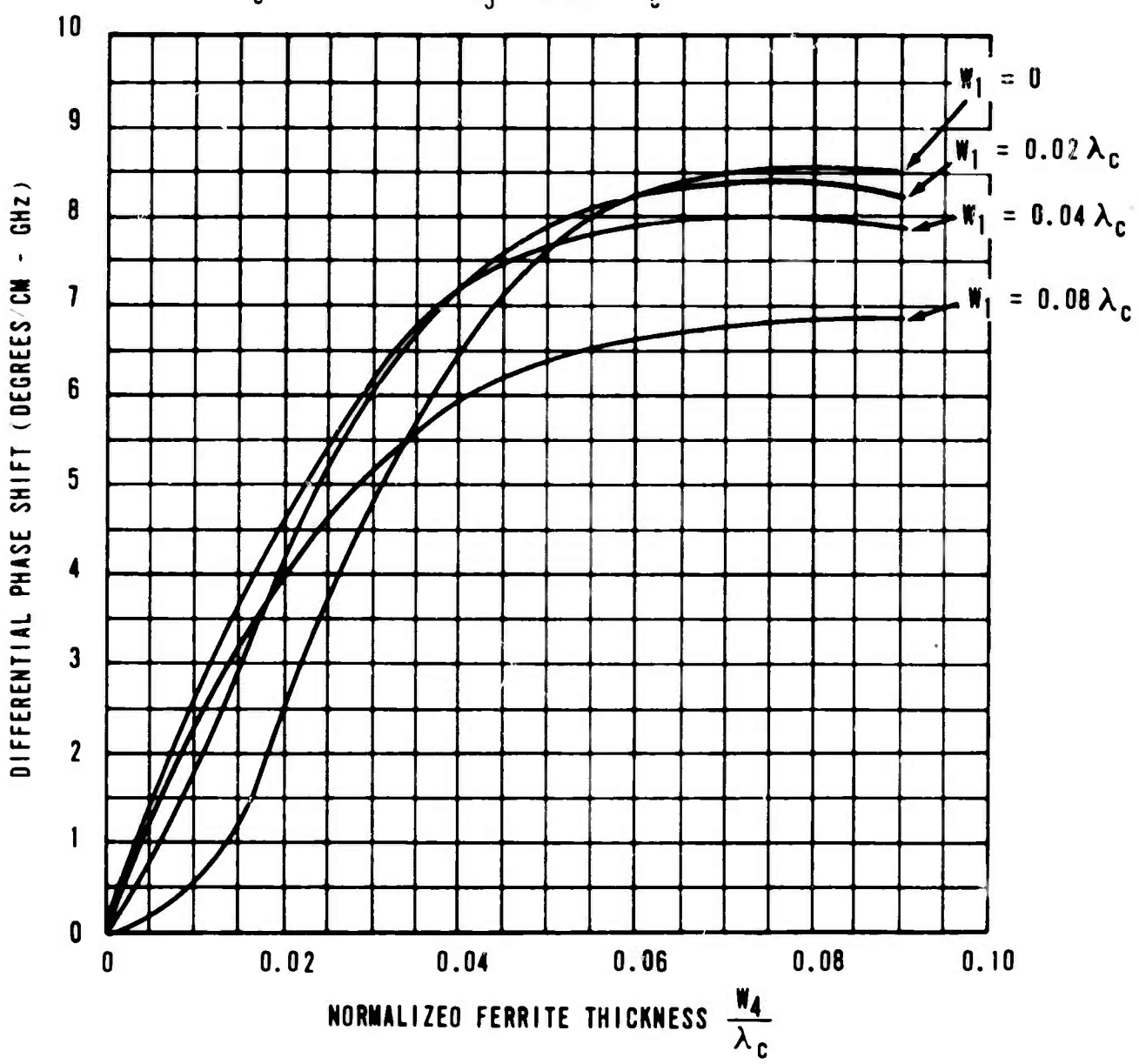

Figure 2. Differential Phase Shift vs Normalized Ferrite Thickness With Dielectric Load Thickness As A Parameter

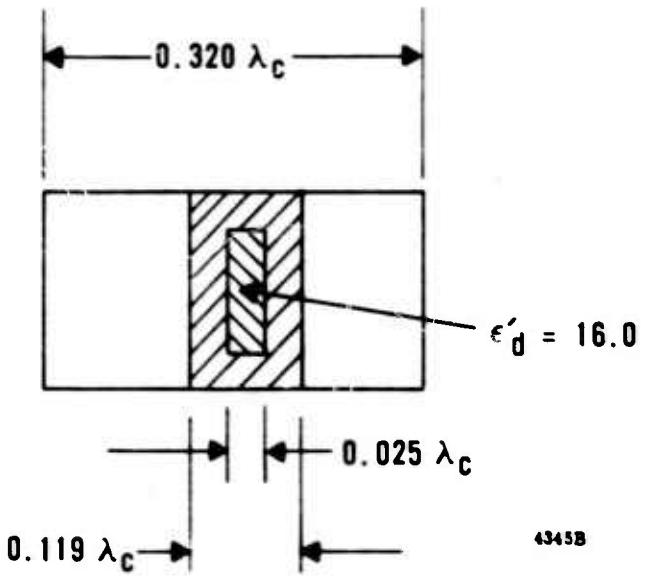

Figure 3. Optimum Cross-Section for Digital Phase Shifter with Zero Phase-Frequency Slope

*NOTE: Waveguide and toroid wall dimensions are shown in Figure 5.

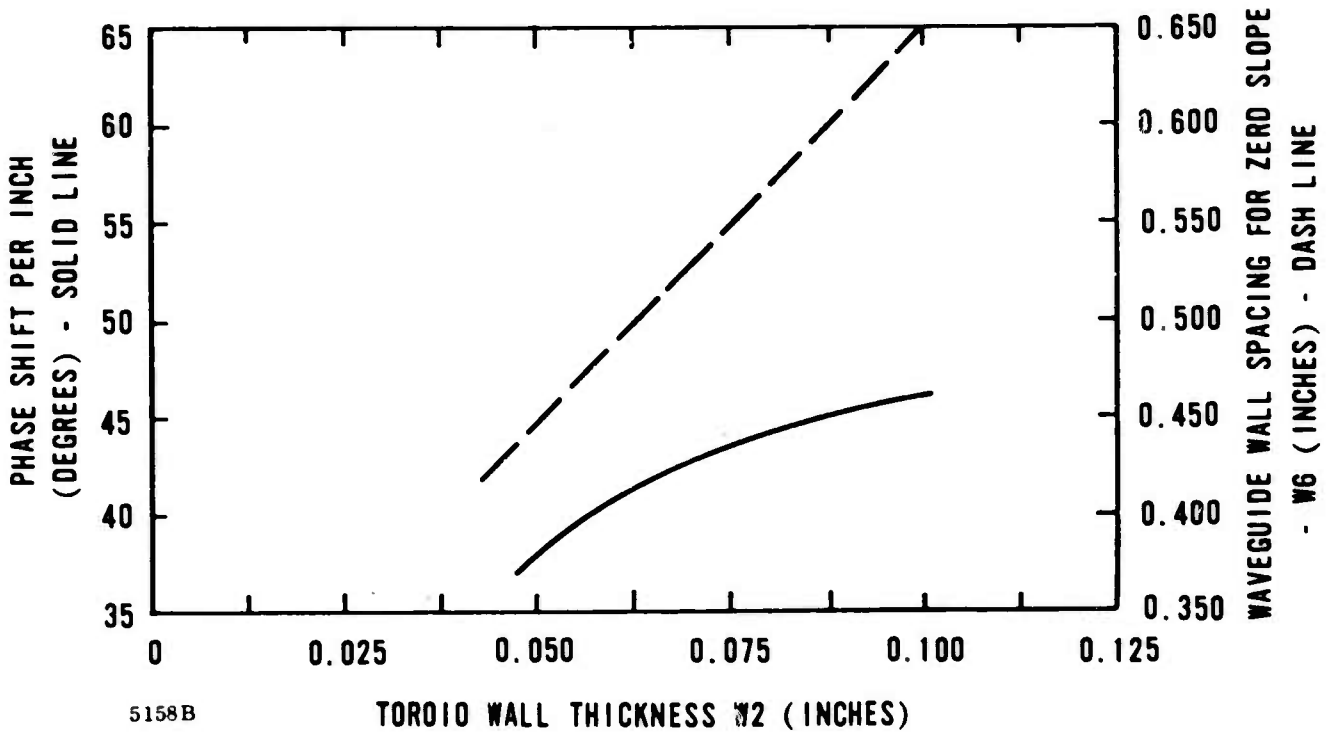

Figure 4. Phase Shift Per Inch versus Toroid Wall Thickness with Waveguide Wall Spacing Adjusted for Zero Phase Slope

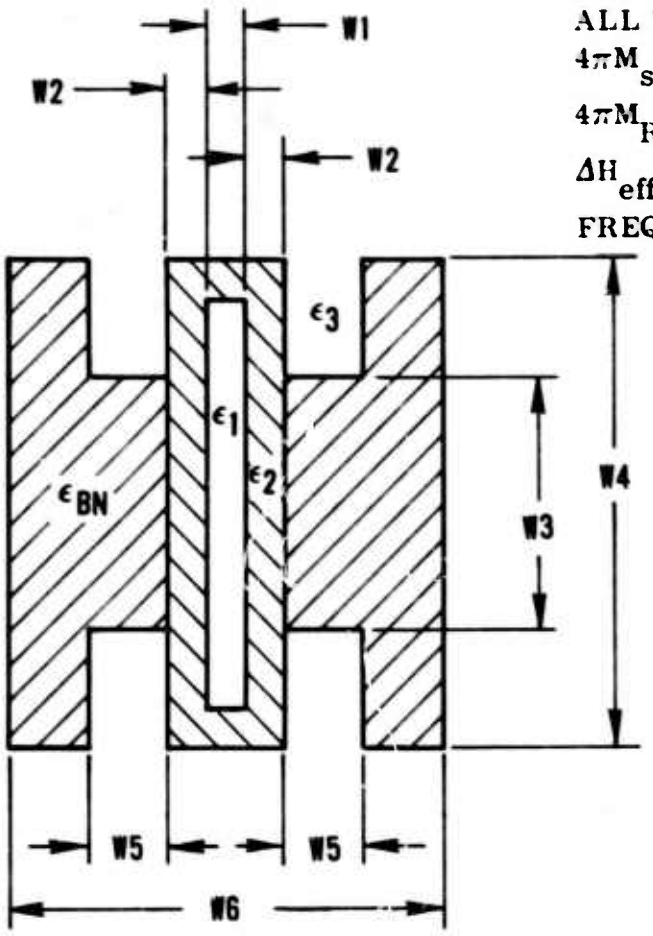

ALL TANδ = 0.0005
$4\pi M_s$ = 620 GAUSS
$4\pi M_R$ = 340 GAUSS
ΔH_{eff} = 25 OER.
FREQ. 5.45 - 5.95 GHz

W1	= 0.045
W2	= VAR
W3	= 0.315
W4	= 0.622
W5	= 0.100
W6	= VAR
ϵ_1	= 16.0
ϵ_2	= 15.4
ϵ_3	= 1.0
ϵ_{BN}	= 4.5

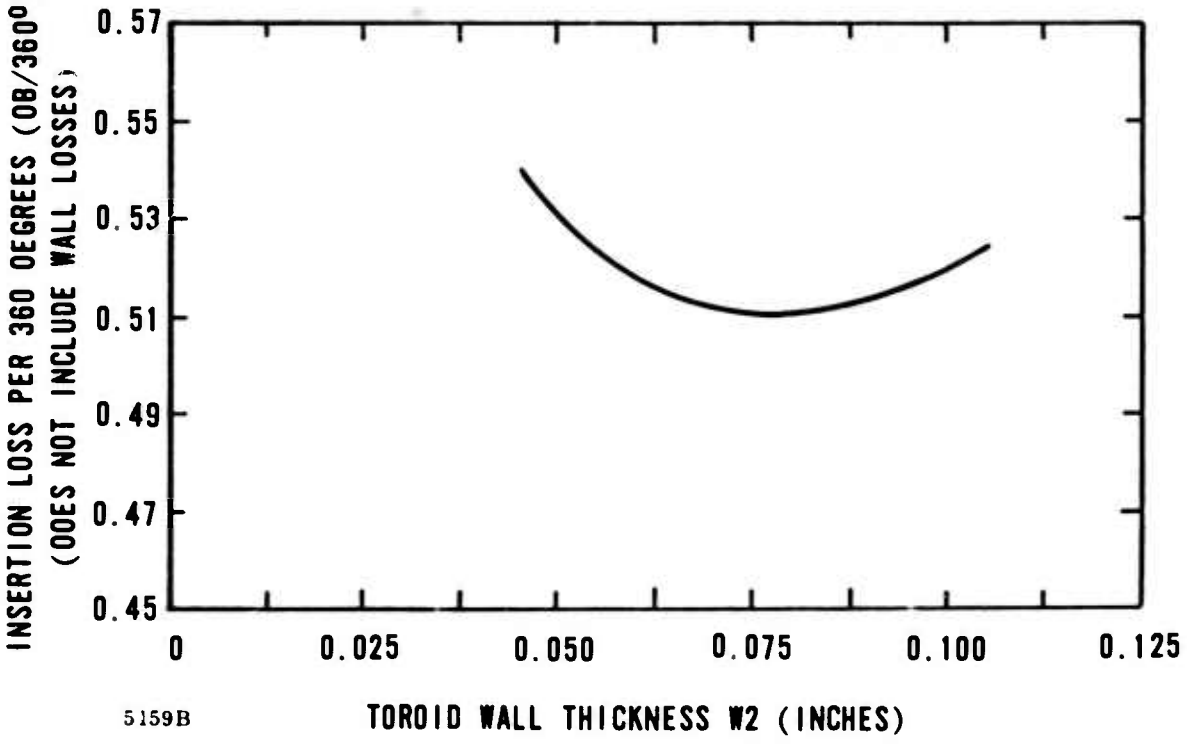

5159B

Figure 5. Insertion Loss Per 360° versus Toroid Wall Thickness with Waveguide Wall Spacing Adjusted for Zero Phase Slope

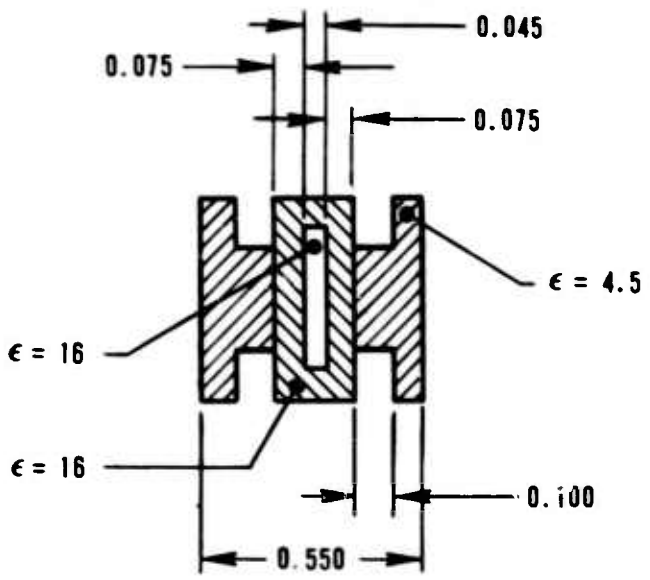

Figure 6. Waveguide Cross Section as Selected from Computer Program

2.2 LIMITING

Figure 7 illustrates experimental data of limiting threshold (and critical H field) in the various waveguide frequency bands as a function of normalized saturation magnetization for aluminum and gadolinium substituted YIG.

This data was generated under the conditions of the "optimum" cross section as described in Section 2.1 for a waveguide height of 0.525 inch in C band.

Any change in waveguide dimensions from the "optimum" would naturally result in a shift in these curves.

As mentioned in Section 2.1, the reduction in wall thickness results in a limiting threshold increase over that stated in Figure 7.

In addition, because of the high probability of arcing at the power levels of this program, the waveguide height was increased to 0.622 inch (standard C band height). Limiting threshold is also a function of waveguide height. The resulting cross section yields a limiting threshold corresponding to a point of $M_S = 0.32$ and $h_{crit} = 63$ oersteds on Figure 7. Note that location of M_S is heavily dependent on accuracy of producing and measuring $4\pi M_S$.

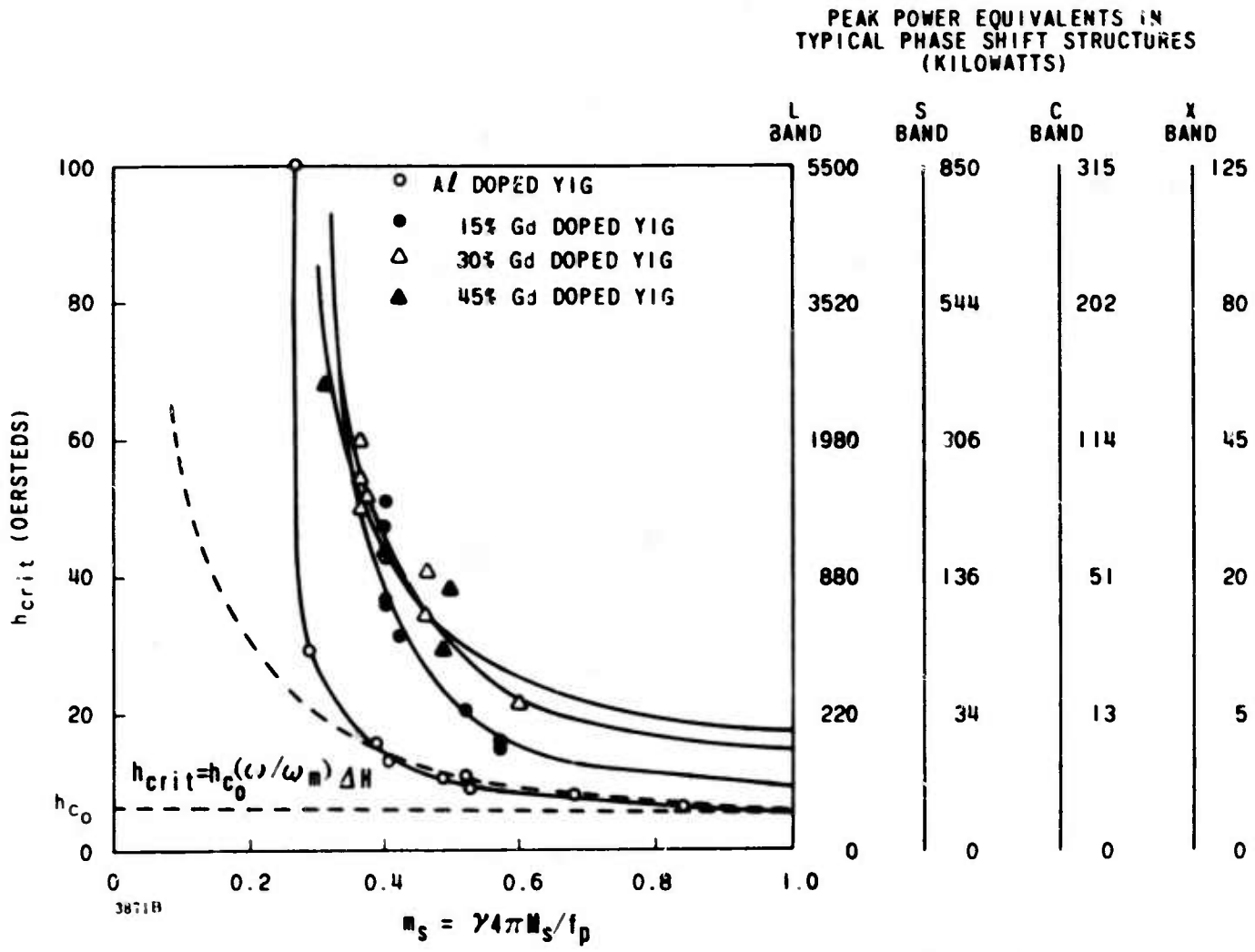

Figure 7. Ferrite Critical Field Dependence on the Frequency Normalized Saturation Magnetization for Aluminum and Gadolinium Substituted YIG

The final cross section showing the boron nitride cooling structures and material parameters is given in Figure 8. It should be noted that no mention of disprosium has been made as a means of increasing limiting threshold. This omission is deliberate since the addition of disprosium to YIG materials causes a sizeable increase in effective linewidth, thus increasing overall insertion loss beyond normally acceptable limits.

The use of disprosium should be limited only to those applications where short length is coupled with high limiting threshold thus requiring the use of high $4\pi M_S$ materials. The loss of such a design would normally exceed the 1.0 db allowable limit (1.5 to 2.0 db usual) and would result in high dissipation per inch, thus limiting the usefulness of the device at high average power.

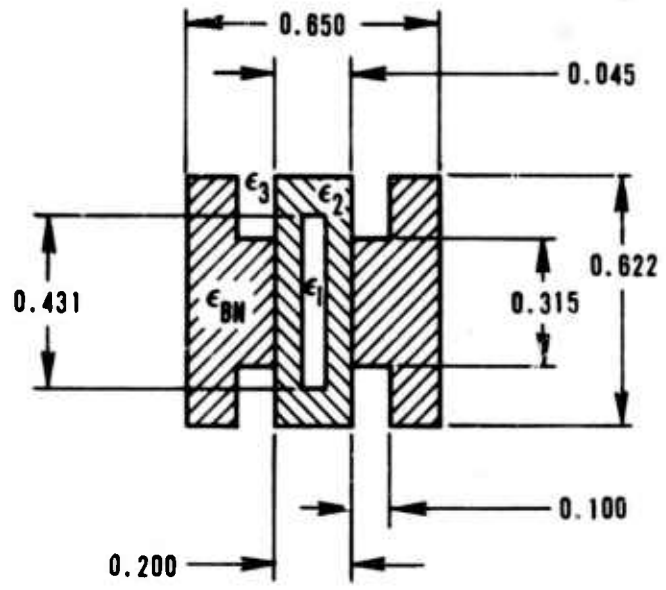

ALL DIMENSIONS IN INCHES

$\epsilon_1 = 16.0$	ALL LOSS TAN'S = 0.0005
$\epsilon_2 = 15.4$	FREQUENCY = 5.45 - 5.95 GHz
$\epsilon_3 = 1.0$	$4\pi M_S$ = 620 GAUSS
$\epsilon_{BN} = 4.5$	$4\pi M_R$ = 340 GAUSS
	ΔH = 75 OERSTEDS (POLYCRYSTALLINE LINEWIDTH)

MATERIAL CHOSEN: YIG + 15% Gd - SPERRY G-317
COOLING STRUCTURE: BORON NITRIDE

5161B

Figure 8. Final Experimental Cross Section of Phase Shifter

2.3 PHYSICAL LIMITATIONS

2.3.1 Array Limitations

The unit designed under this program is intended for use in a phased array radar where the phase shifter spacing shown in Figure 9 is the same as that for the array feed elements. The active portion of the phase shifters was designed to meet this requirement.

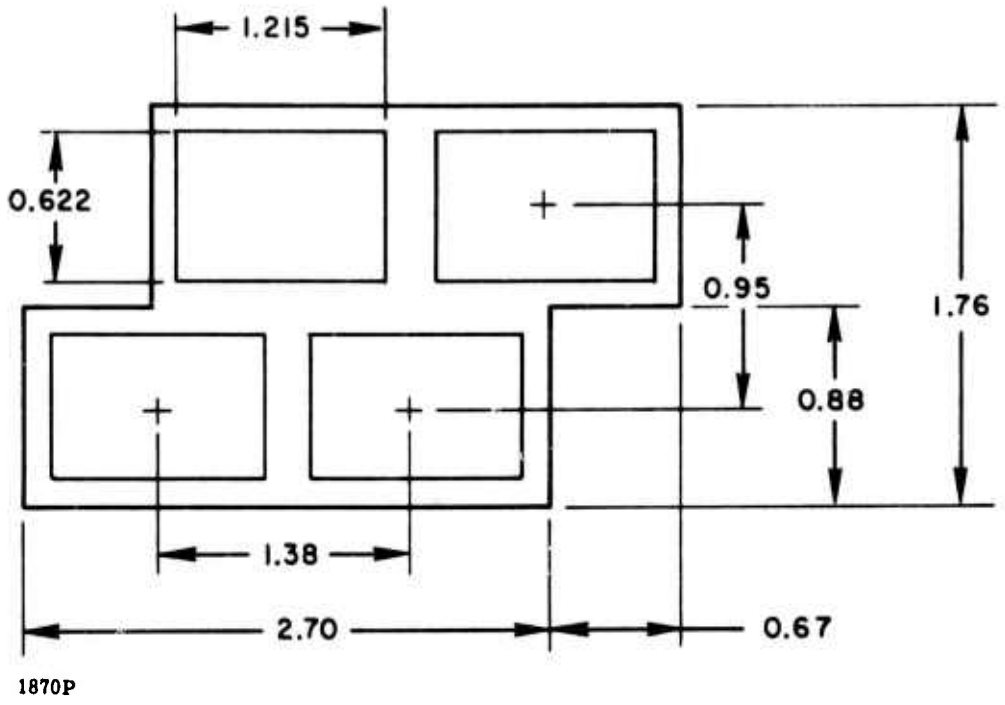

Figure 9. Typical Element Spacing For C Band Array

For practical purposes, however, the units were designed with "unloaded" waveguide input and output. Such a design can not be placed directly on 0.5λ centers since any waveguide wall thickness would imply waveguide below cutoff. This configuration, however, does permit ease of testing.

In practice, the phase shifter output can be matched directly to radiate into space and a loaded waveguide or ridged waveguide input can be developed.

These development features did not directly relate to the phase shifter and were not included in this program.

2.3.1.1 Arcing. The height chosen when used in an unloaded waveguide will normally not arc over at the power levels of this program. However, concentration of fields due to dielectric loading in the active phase shift region will substantially reduce peak power handling of the microwave structure. This reduction in arc over power level in conjunction with the wide pulse length (100 usec) presented a severe design problem. By careful assembly of the phase shifter and selection of the maximum height allowable, the design proved successful. Test results are given in a later section.

2.3.2 Driver - Phase Shifter Packaging

From the array spacing of Figure 9, it is obvious that the phase shifter occupies the full available space. It is therefore necessary to locate the driver at a remote location. In addition, it is necessary to connect the driver and phase shifter through suitable cabling that will not interfere with normal input microwave feed lines.

Although this cabling and driver cross section appear at first to be no problem, a thorough investigation reveals the following:

- High pulse currents (5 to 20 amperes) will flow through driver-phase shifter interconnecting cables.
- Interconnecting line impedance and wire resistance are critical for maximum efficiency of the assembly.
- Because of space limitations, it is advisable that the driver cross section be no greater than that of the phase shifter. This therefore implies that the driver will possess a shape similar to that of the phase shifter, that is, small cross section and moderate length.

2.4 RESULTANT DESIGN

2.4.1 General

A possible array structure is shown in Figure 10. The phase shifters are mounted into a suitable frame possibly from the front of the array. Directly behind this array of phase shifters is a space for interconnecting waveguides. Waveguide interconnection could take the form of sidewall slot couplers, a power divider network or any suitable means of power division. If the phase shifters are inserted from the face of the array, connection between distribution network and phase shifter could take the form of a self-sealing joint. At the power levels of this program, however, this joint must be positive. One solution to the cross section problem may be that of Figure 11 where phase shifters are constructed in pairs with a three-port power divider assembled as part of the phase shifter. Elimination of the fourth terminated port of the power divider is permissable only if out-of-phase reflections are not anticipated.

A cable is routed from the phase shifter to the driver array between the interconnecting waveguide. At the driver end this cable can be rigidly attached to the driver array frame. The driver then can be inserted into the frame from the

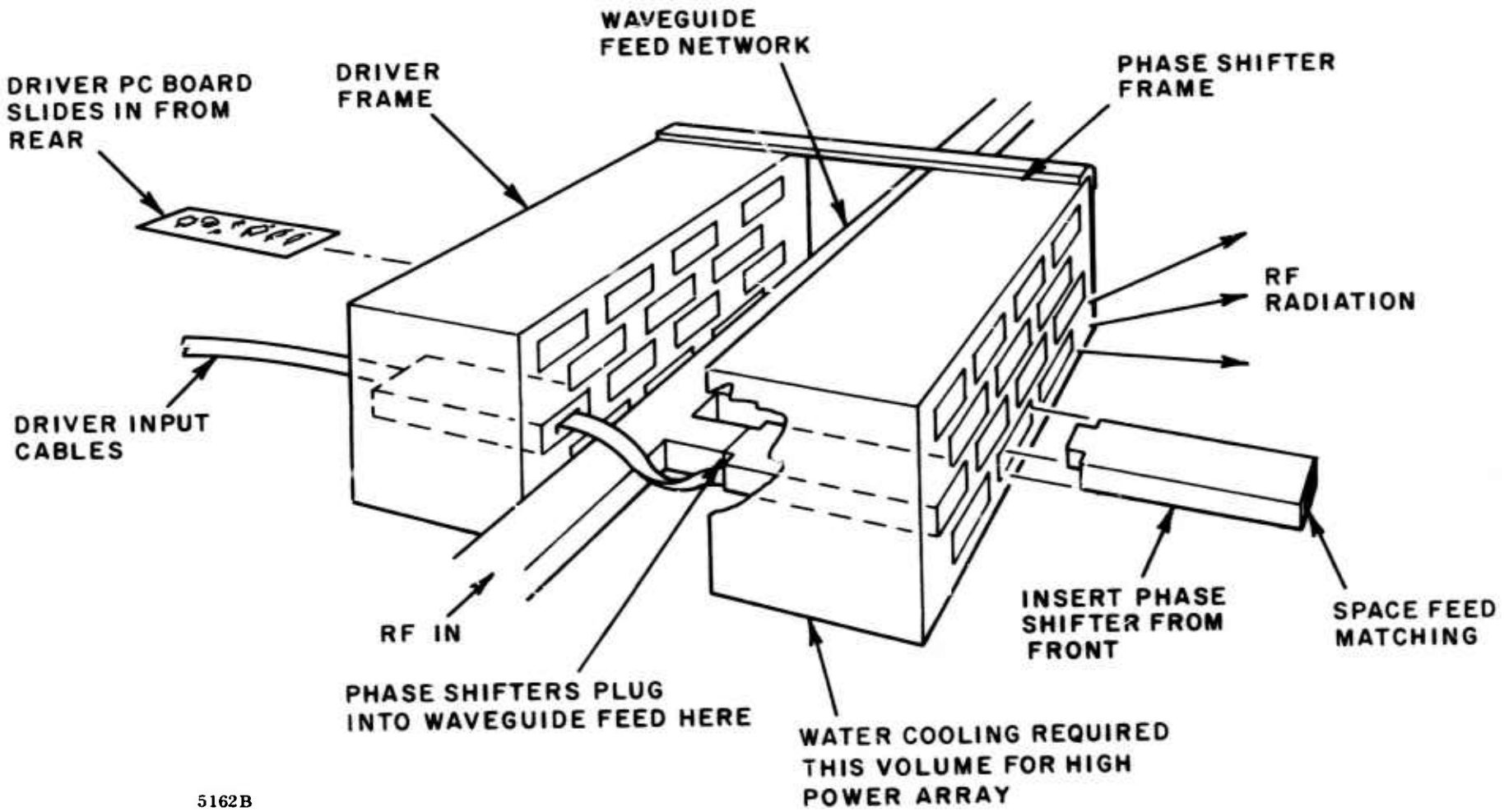

Figure 10. Array Structure-Drivers Separated from Phase Shifters

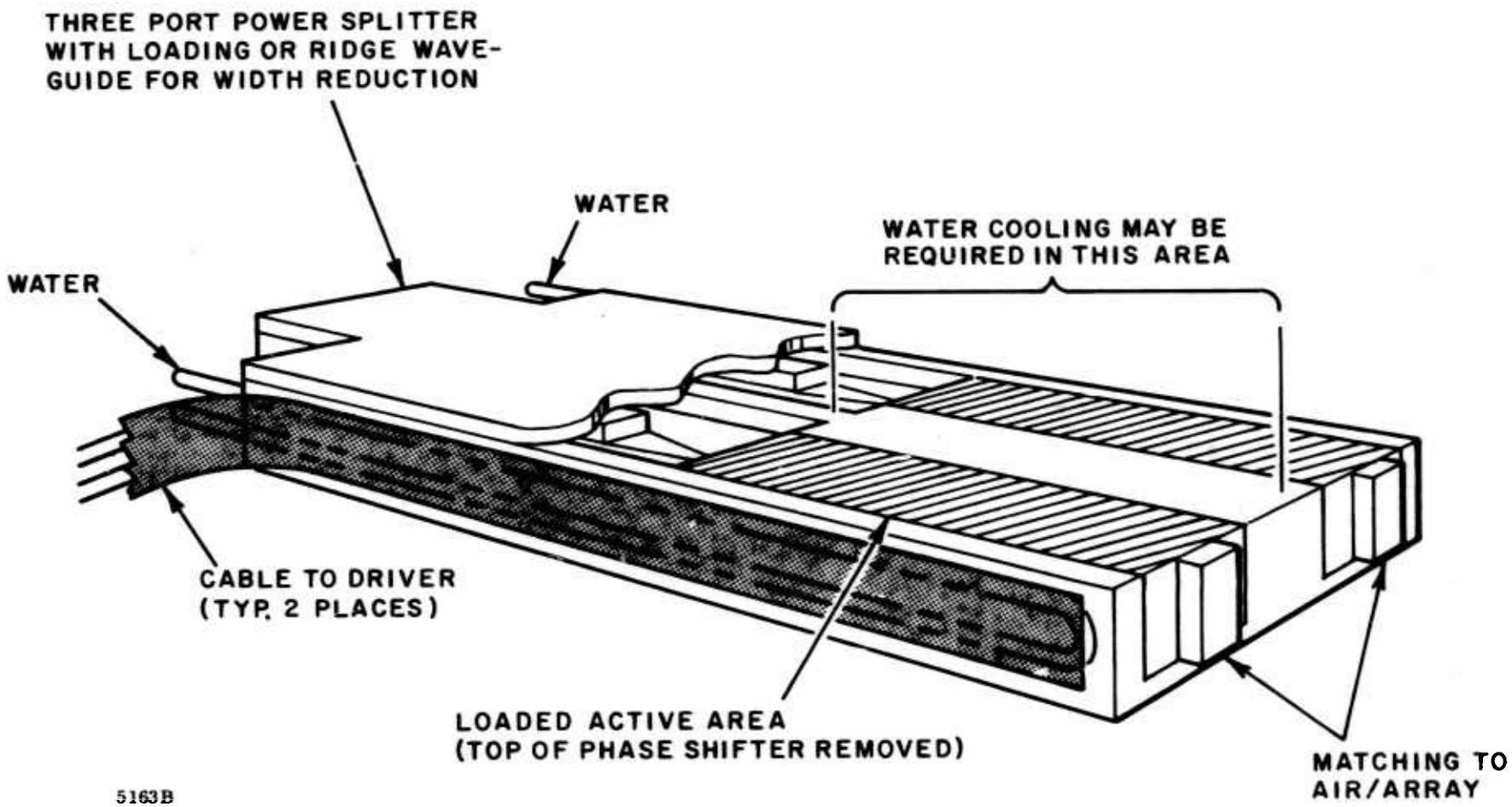

Figure 11. Phase Shifter Assembly Employing Two Phase Shifters and Special Power Splitter in Single Package for Space Reduction

rear. A single cell mockup of such a driver array frame and mounting was designed and constructed as part of this program. Suitable locking devices were provided as part of the driver to prevent accidental disconnect of electronic components and cables. Figure 12 shows this mockup with driver in place.

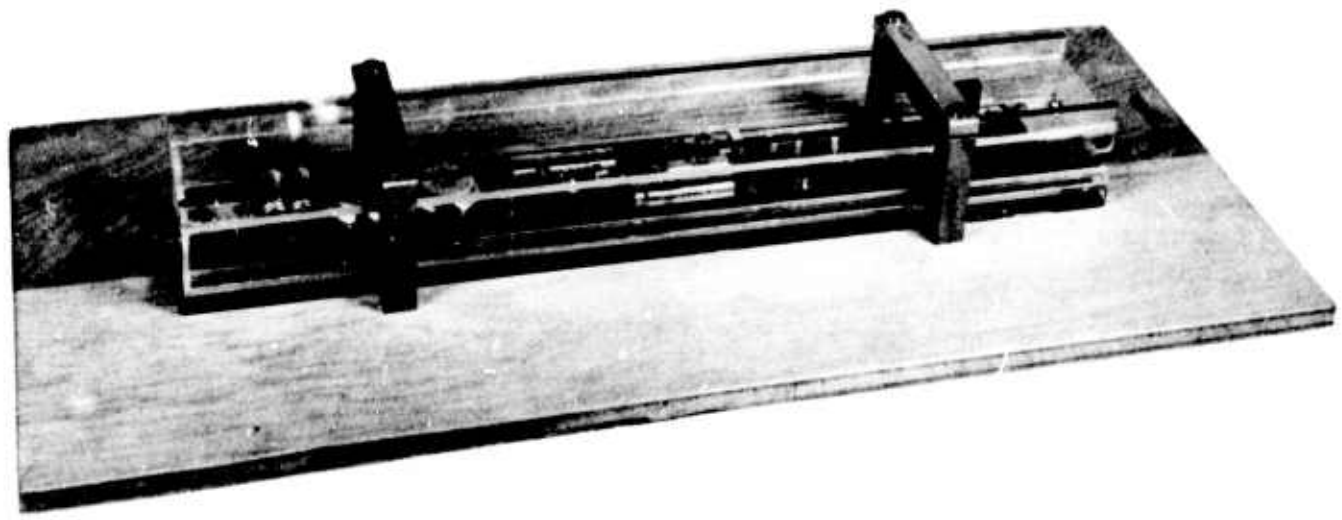

1926P

Figure 12. Mockup of Section of Array Frame with Driver in Place. Black plastic surfaces represent discontinuities of mockup section.

It should be noted that the delivered models had as a permanent part of the phase shifters the interconnecting cables. It is possible that a suitable connector can be designed as part of the phase shifter which will permit permanent installation of interconnecting cables at the time of array construction. This connector must be chosen dependent upon the space configuration chosen by the array designer.

2.4.2 Cooling

A suitable means of cooling must be provided as part of the phase shifter array. This cooling must not only control the phase shifter temperature due to variation in ambient but is of great importance in rf dissipation heat removal from the toroid cross section.

Several methods of cooling wherein the cooling structure was part of the array frame rather than part of the phase shifter were studied. In each case, thermal transfer efficiency was not adequate in an array permitting easy removal of any phase shift element.

In addition, because of the high level of power dissipation in a small volume, forced air was rejected as a suitable means of cooling.

In the models designed on this program, water cooling channels were incorporated as part of the waveguide sidewalls. A cross section in the ferrite region showing these channels is shown in Figure 13. Such ccoling channels can be incorporated into each sidewall and routed to one end of the phase shifter. Some form of quick disconnect filtering must be developed if independent removal of each phase shifter element is desired.

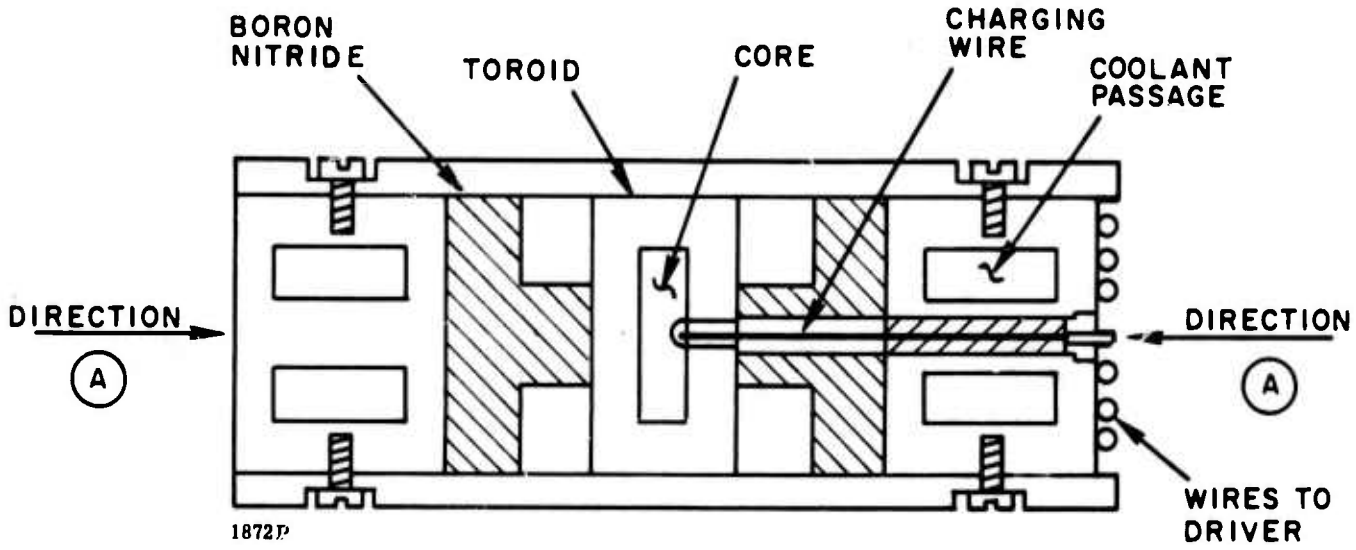

Figure 13. Cross Section of C Band Phase Shifter with Four Piece Housing

The devices developed under this program were designed to operate with a water temperature of approximately 25°C. If a different water temperature were desired or if a large range in cooling temperatures was anticipated, the phase shifter could be suitably designed for such operation. It may be necessary to sense array or water temperature and suitably compensate the drivers.

3. HIGH POWER EVALUATION

3.1 GENERAL

Difficulties arising from high peak and average power and associated pulse widths were considered to be most serious.

In particular, these difficulties revolved around:

- Limiting threshold: attainment of desired value.
- Effects of minor loop operation on limiting threshold.
- Waveguide breakdown of the microwave structure at high peak power, wide pulse operation.
- Thermal and magnetostrictive effects with average power.

3.2 LIMITING THRESHOLD

3.2.1 Choice of $4\pi M_S$

Selection of limiting threshold in phase shifters has developed into a rather exact procedure. However, it is easily seen in Figure 7 that small changes in either $4\pi M_S$ or ω_c and hence m_s will cause large changes in h_{crit} and peak power equivalent (for values of h_{crit} greater than 30 oersteds).

When material is chosen for high power operation, the maximum m_s value should be that at the lowest frequency (5.25 GHz for this program) and $4\pi M_S$ maximum should be used. This approach is necessary to compensate for variations in $4\pi M_S$ in manufacture and measurement.

Using the above limits and the cross section of Figure 8, a limiting threshold of 125 KW peak was attained. Figure 14 is a plot of limiting threshold for Sperry G-311, a 15% gadolinium doped YIG material with a typical $4\pi M_S = 620$ gauss.

3.2.2 Minor Loop Operation

Referring to Figure 14, curves have been plotted for five modes of operation, that is, saturated in +m and -m states, demagnetized and partially magnetized +m and -m.

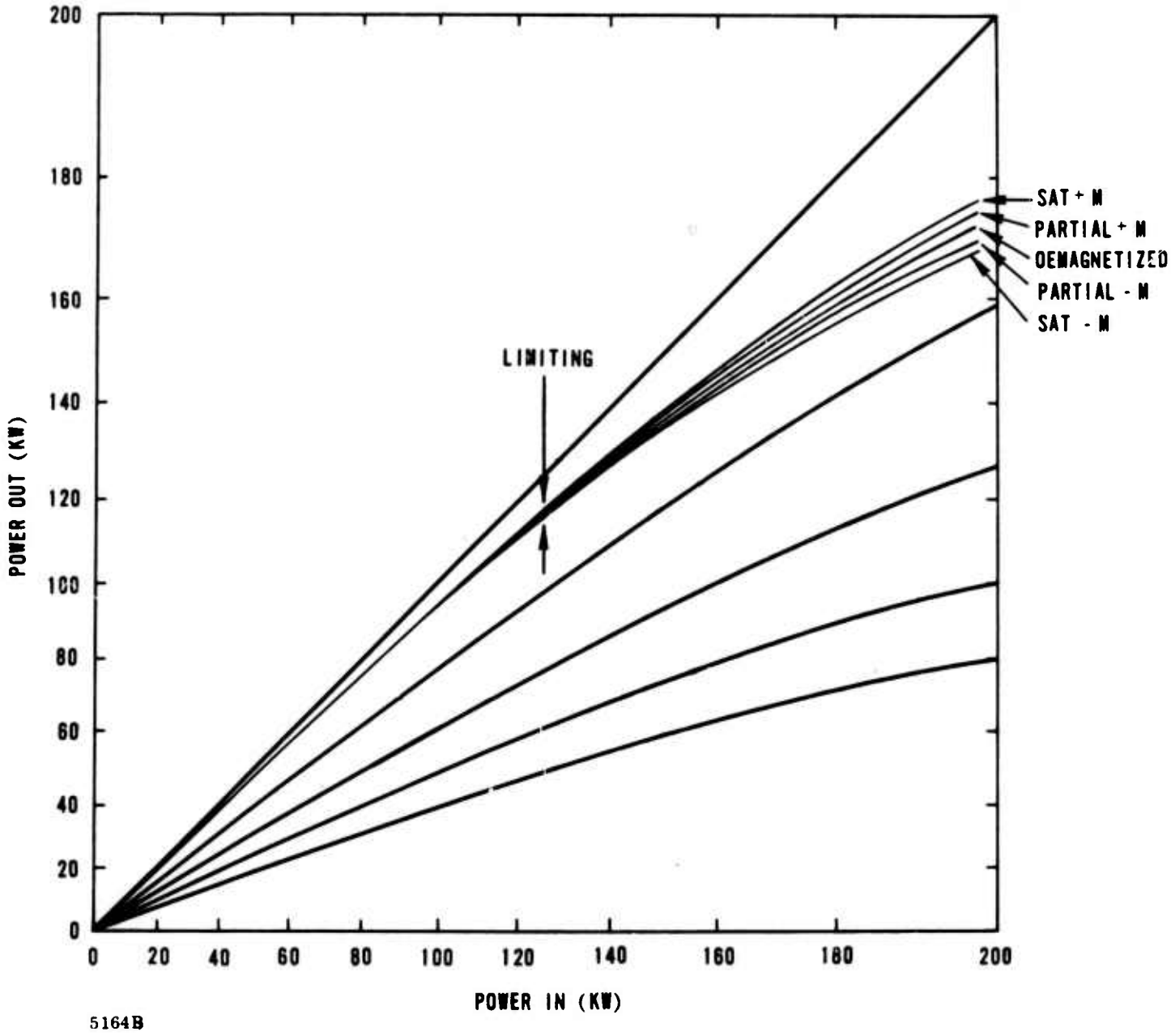

Figure 14. Limiting Threshold G-311

It can be seen that at power levels below the limiting threshold, there is essentially no difference in insertion loss between the five test states. Loss above the limiting threshold does depend upon magnetization state. The limits of variation are defined by the two saturation states with all other states uniformly distributed between these limits.

This figure clearly indicates that the limiting threshold of garnet materials used in phase shifters is not adversely effected by minor loop operation.

3.3 WAVEGUIDE BREAKDOWN

A test structure was designed to the cross-section of Figure 8 for high power evaluation. The primary purpose of this structure was high power evaluation. Therefore, although this was a test structure, careful assembly of all components was maintained.

It was generally accepted that the extensive loading employed in a phase shifter would reduce its power breakdown point below unloaded waveguide. From past experience on high peak power phase shifters, arc-over in the microwave structure occurs at a point where fit between the various loading parts is poor; that is, between the various toroids. This probability of arc-over is reduced by close control of fit but also by filling all air gaps in the assembly.

The material chosen to fill these air gaps in the C band phase shifter was Sylgard 184 (Dow-Corning), a two part plotting compond which readily penetrates into open spaces and remains flexible after curing.

Tests were run with this sealant used in varying degrees in the phase shifter structure. Following are the results and conclusions:

- Use Sylgard 184 liberally on all toroid-core-charging wire surfaces.
- Take extreme care at input (and output) junctions of toroid structures where mating with matching transformers occurs.
- Allow excess Sylgard 184 within the structure to cure normally; no wiping necessary. This excess material in no way degrades the phase shifter and does enhance high power performance.

Breakdown tests were performed at short rf pulse widths with the following results.

Test No.	Peak Power (KW)	Arc-Over	Pulse Width (μsec)	Comments
1	300	Yes	2.5	Input toroid - transformer interface; insufficient Sylgard.
2	500	Yes	2.5	Section of D16 added to input to relocate toroid relative to mode suppression. Arc-over at D16 toroid interface.
3	650	No	2.5	Toroid-transformer same as Test No. 1; generous amounts of Sylgard.
4	1050	Yes	2.5	Arcing at toroid-transformer charging wire interface; same structure as Test No. 3.

The final arc-over at 1050 KW peak, 2.5 microsecond pulse width indicated that, with liberal use of Sylgard 184 and care in attaining a good toroid-transformer interface fit, the peak power handling of the unit could be increased to values well in excess of those required on this program and approaching that of WR-137 waveguide.

An important aspect of the above data is that each time arc-over occurred, the point of breakdown was the same -- that is, the toroid-transformer interface. Changing the position of this interface relative to the position of side wall mode suppressors had no effect on the point of arc-over. It is concluded that the abrupt change in impedance at this point, coupled with heavy dielectric loading and magnetic and wire effects, creates a condition most likely to arc-over in the structure.

The above tests were performed at short pulse conditions of 2.5 microseconds. It was necessary to determine the effects of pulse length on peak power, an effect that from general microwave experience is significant.

The curve of Figure 15 was derived from arc-over information available in WR-2100 waveguide. This curve is based upon data for waveguide with no special provisions (such as rounding corners for suppressing arc-over). It is also obvious that with only three points available, the precise shape of the curve is unknown.

Taking the curve at face value, however, to attain 125 KW minimum arc-over at 100 microseconds would require 270 KW at 10 microseconds and 560 KW at 2.5 microseconds.

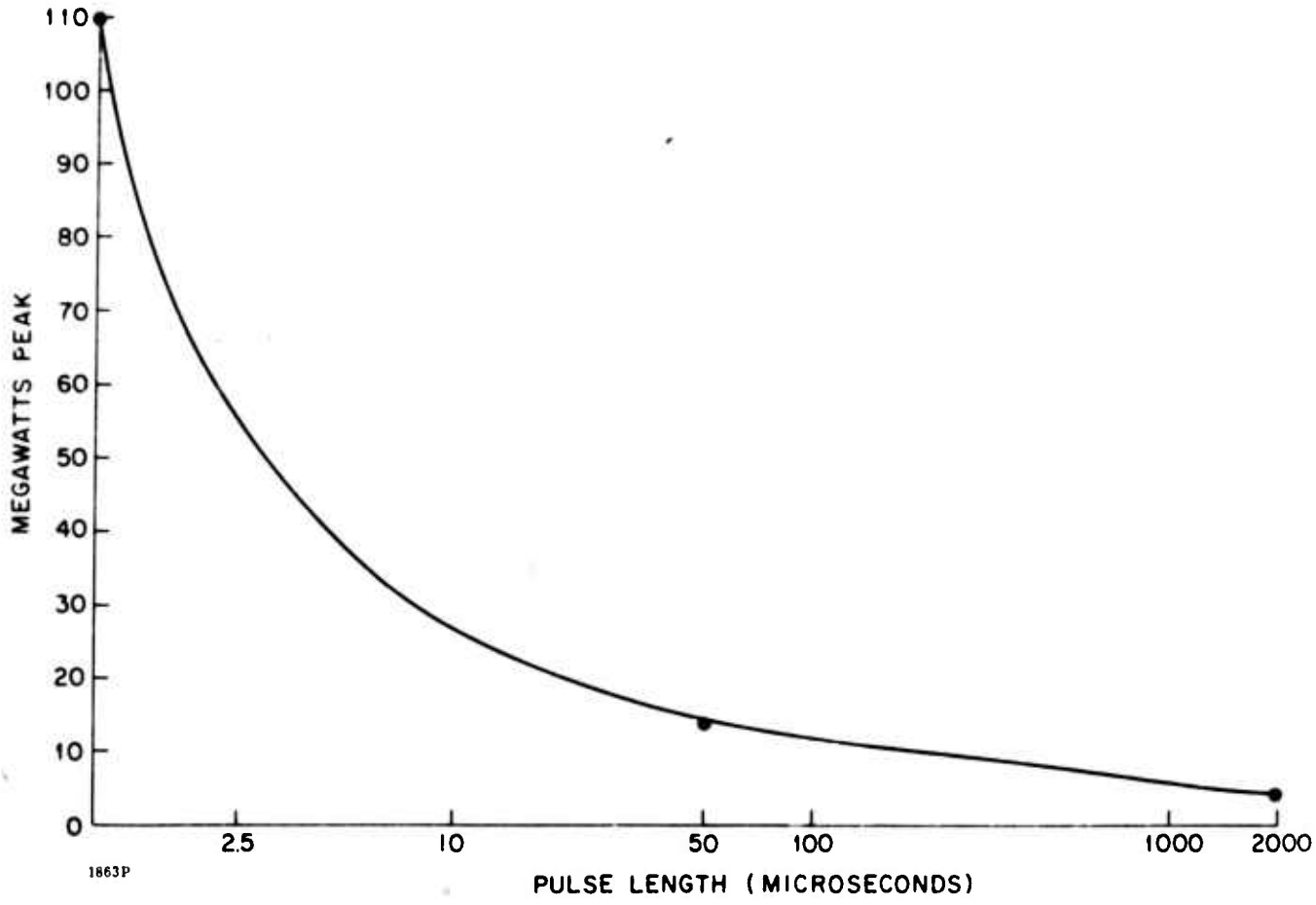

Figure 15. Arc-Over of WR-2100 Waveguide versus Pulse Width

Previous data indicated that levels in excess of this value were attainable; therefore, testing at 10 microseconds was approached with confidence.

Testing at 10 microseconds was performed at MIT-Lincoln Labs under the supervision of Mr. D. Temme, with RADC and Sperry personnel present.

The test structure was evaluated at 309 KW peak, 10 microseconds with no failure; the testing was discontinued because of the limit on available power. Conclusions could be drawn from the above data that indicate adequate safety factors in the phase shifter at 100 microseconds pulse width, assuming the curve of Figure 15.

Peak powers at the desired pulse length were not available during the time interval covered by this program. Therefore, final evaluation at rated conditions must await availiability of a test facility. Confidence in the design is high from the above data.

All units delivered under this program were assembled to the same high standards dictated by the above test results and should perform satisfactorily under rated conditions.

3.4 AVERAGE POWER PERFORMANCE

Average power performance can be resolved into two areas of study:

- Variations in $4\pi M_S$ with temperature
- Magnetostriction

Both of these effects in a high power phase shifter that employs some form of cooling for housing stabilization will resolve themselves to toroid temperature and temperature gradients.

If one were to assume uniform heating dissipation throughout the garnet material of Figure 16, then a gradient would be established in the direction of the rf E field. Because of long path length and the poor thermal conductivity of garnet materials, this increase in temperature would result in extremely poor performance with average power. This performance would primarily be a result of changes in $4\pi M_S$ as a function of temperature.

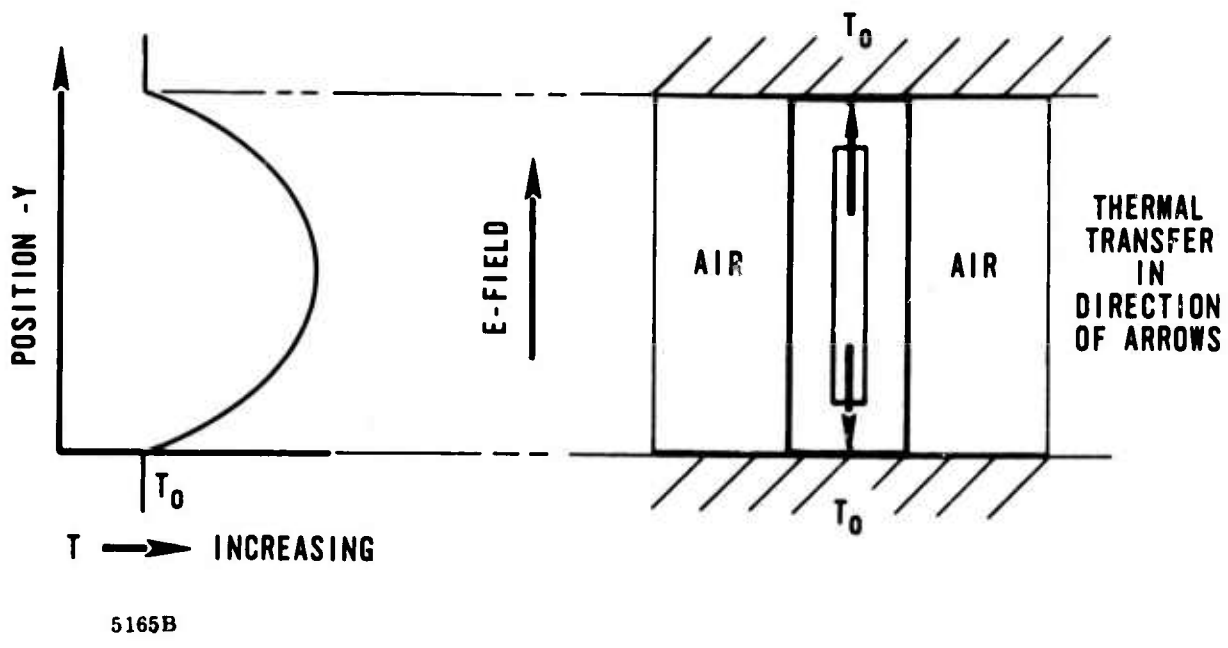

Figure 16. Temperature Gradient in Phase Shifter Toroid Assuming Uniform Dissipation and No Side Wall Cooling

If, however, an additional cooling path to the waveguide side walls can be established, the overall temperature of the garnet material can be greatly reduced. This additional cooling has been attained by the use of boron nitride cooling structures placed in the waveguide. Boron nitride is ideal for this purpose because of its low rf loss, ease of manufacture (machining), and good thermal properties.

Experimental evaluation has shown that the use of a "T" structure yields an optimum cooling/phase shift structure.

This structure removes heat from a point a maximum distance from top and bottom of the waveguide. A thermal pattern as a function of horizontal position is shown in Figure 17.

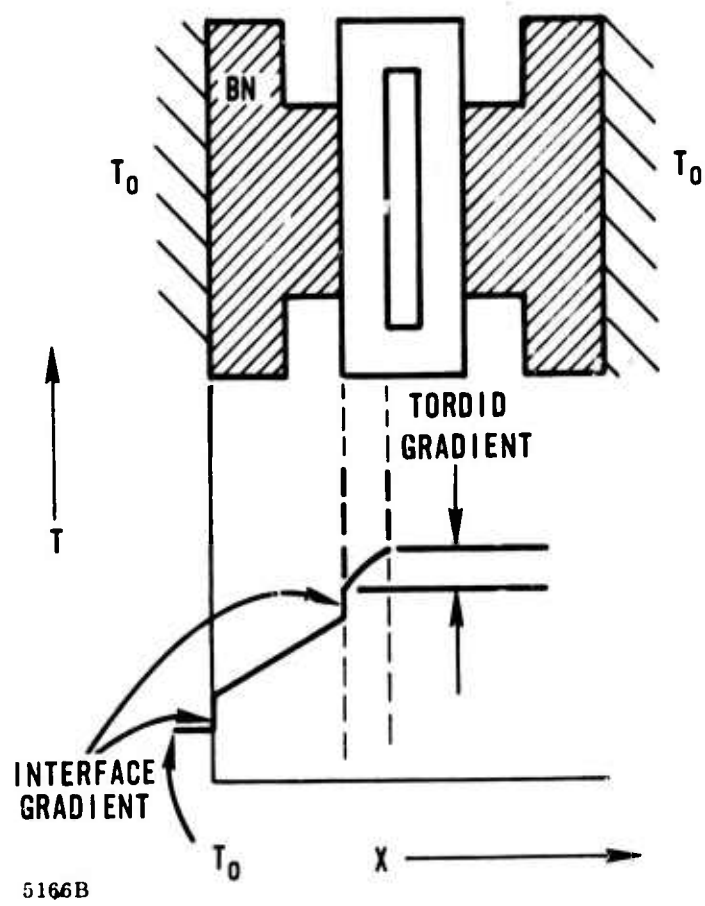

Figure 17. Temperature Gradient in Phase Shifter Assuming Toroid Dissipation only with Efficient Thermal Transfer to Side Walls

In general, a structure of this type should have a phase shift drop of 2 to 3% of low power values at 1000 watts resulting only from overall temperature increase and the appropriate drop in $4\pi M_S$ (and $4\pi M_R$). See Figure 18 for a plot of $4\pi M_S$ as a function of temperature.

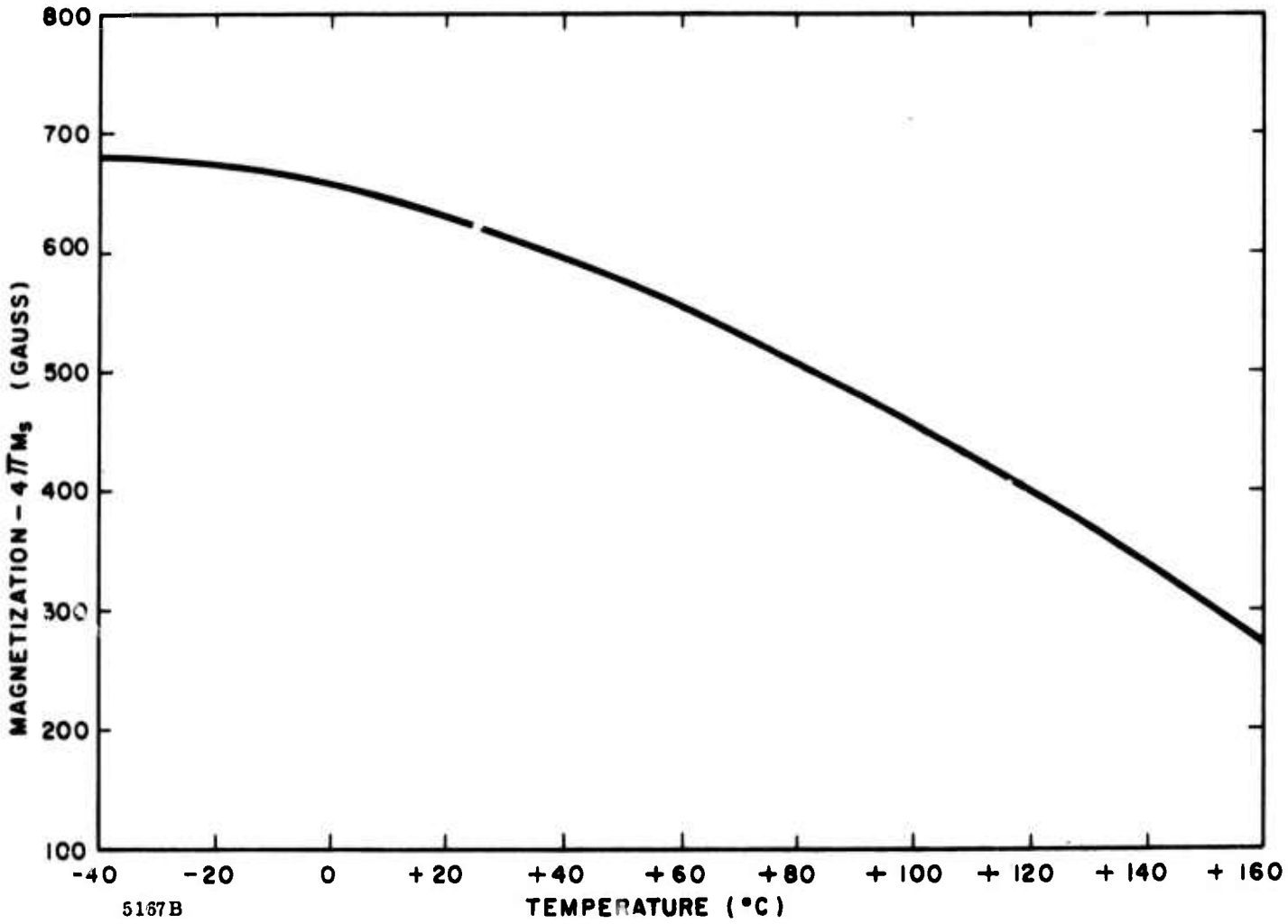

Figure 18. Magnetization ($4\pi M_S$) versus Temperature, 15% Doped YIG and Aluminum G-311

Figure 17, however, indicates a gradient across the toroid surface due to nonuniform cooling. This gradient causes a physical dimension change which, in turn, results in internal toroid stresses -- and magnetostriction.

This magnetostriction can be reduced by attaining a maximum cooling efficiency (overall reduction in temperature reduces the thermal gradient) or by other means such as a reduction in wall thickness.

An additional technique employed where extremely high power operation is required is internal core cooling. This technique however is extremely costly and has not been employed under this program.

As described in previous sections, the reduction in wall thickness from "optimum" has resulted in an improvement in high power performance. The curve of Figure 19 is typical of the performance of the units delivered under this program. Available average power at Sperry was 800 watts; therefore, testing to 1000 watts was not performed. An estimate to 1000 watts, however, can be drawn from Figure 19.

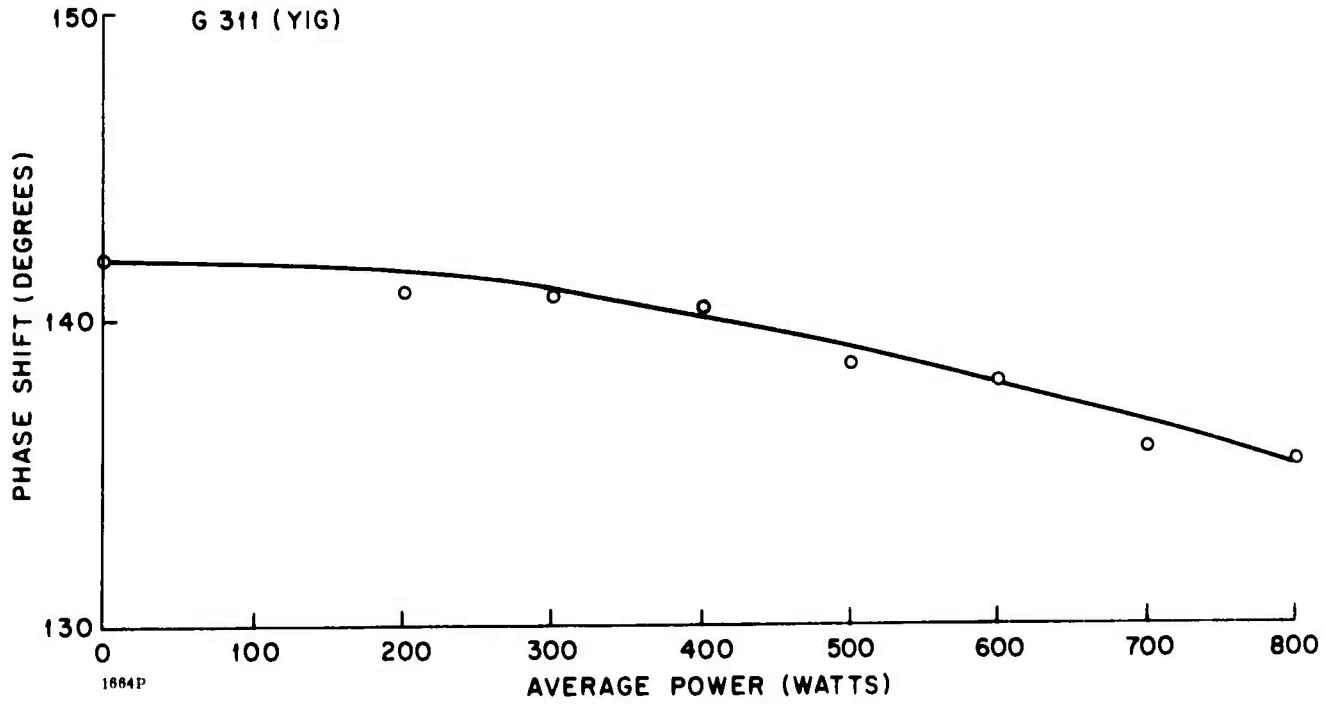

Figure 19. Phase Shift versus Average Power, G-311 (YIG)

It should be noted that variations from unit to unit can be expected due to variations in fit and thermal transfer. However, Figure 19 is typical for the units delivered under this program.

3.5 NONMAGNETOSTRICTIVE MATERIALS

As part of this program, an evaluation was undertaken of a different family of garnets -- that of the Calcium-Vanadium-Bismuth family (CVB). For high power applications, these materials offer the advantage of essentially zero magnetostrictive properties. In fact, there appears to be a slight increase in $4\pi M_R$ when the material is placed under stress. A summary of properties is given below for reference:

$4\pi M_S$	200 to 700 gauss
R_R	0.3 to 0.4
$\tan\delta$	0.0005
$\Delta H_{effective}$	≈25 oersteds (not polycrystalline linewidth)
H_c	1.0 to 4.0 oersteds

Because of the limited range of $4\pi M_S$ available, these materials are suitable for S and C bands only. In addition, the low $4\pi M_S$ materials possess the highest values of coercive field, H_c, and are therefore quite difficult to switch by conventional driver techniques. The low value of remanence ratio, R_R, also requires an increase in length (and resulting loss) over the YIG family.

For the above reasons, the CVB material was not chosen for deliverable hardware under this program. However, test data was derived on a test sample of G-444 having the following characteristics:

$$4\pi M_S = 590 \text{ gauss}$$
$$4\pi M_R = 180 \text{ gauss}$$
$$H_c = 2.5 \text{ oersteds}$$
$$\tan \delta = 0.0006$$
$$\Delta H = 85 \text{ oersteds (polycrystalline linewidth)}$$
$$\epsilon' = 15.3$$

Figure 20 is a plot of phase shift as a function of average power. Referring back to Figure 19, the difference in total phase shift should be noted and is partially a result of reduced remanence ratio, R_R. This unit with G-444 required a 90 V capacitor discharge to drive it into approximate saturation -- this as a result of higher H_c over that of YIG. Comparison of Figures 19 and 20 does yields improved performance with average power.

Because of the lower value of $4\pi M_S$ for G-444 (CVB) compared to G-311 (YIG), it is not suprising that the limiting threshold for this material was higher than that for G-311. The limiting threshold was in fact greater than 200 KW, the maximum peak power available for evaluation.

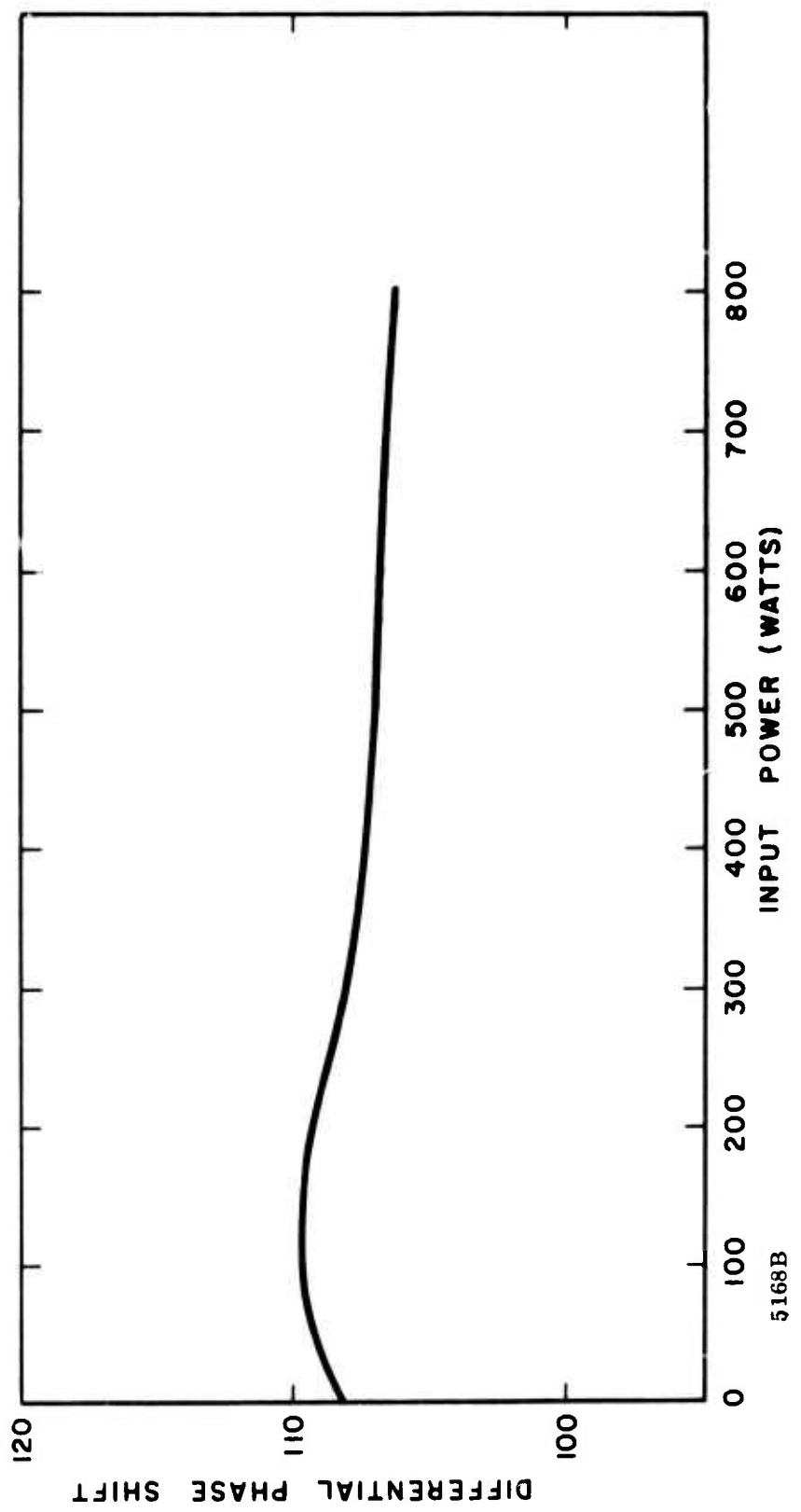

Figure 20. Differential Phase versus Average Power, Material G-444

4. DRIVING OF MATERIALS

4.1 GENERAL

This section is devoted to the development of a sound understanding and a basis for design of phase shifters employing flux drive principles. Theoretical considerations and experimental data developed under this program have yielded a better understanding of the limits of the basic flux drive theories now commonly accepted.

4.2 BASIC HYSTERESIS LOOP (B-H CURVE)

Figure 21 is a typical plot of B versus H for G-311, the material used in the phase shifters developed under this program. Note that I has replaced H on the plot. The toroid tested was ground to finished dimensions and driven by a single turn of wire.

Table I lists important material parameters at different drive levels for G-311.

Note that the B-H curve has a distinctly rounded shape. This is typical for the heavily doped garnets commonly used in high power phase shifters.

Figure 22 is a typical plot for Sperry F-167, a magnesium-manganese ferrite with $4\pi M_S$ = 1260 gauss while Table II lists important parameters at various drive levels.

The cross section of F-167 used above is given in Figure 23. Note the squareness of this plot as compared to that of Figure 21. It should be noted that each of these figures was produced with a symmetrical drive current. In practice it is difficult to attain precise drive symmetry in pulsing a phase shifter so that the result is a loop which is offset from the B-H axis.

Figure 24 shows two possible plots for a theoretical material similar to F-167 with the same values of $4\pi M_S$, $4\pi M_R$, and H_C. The B-H curves are distinctly different, indicating the need for specifying additional parameters to define a microwave magnetic material.

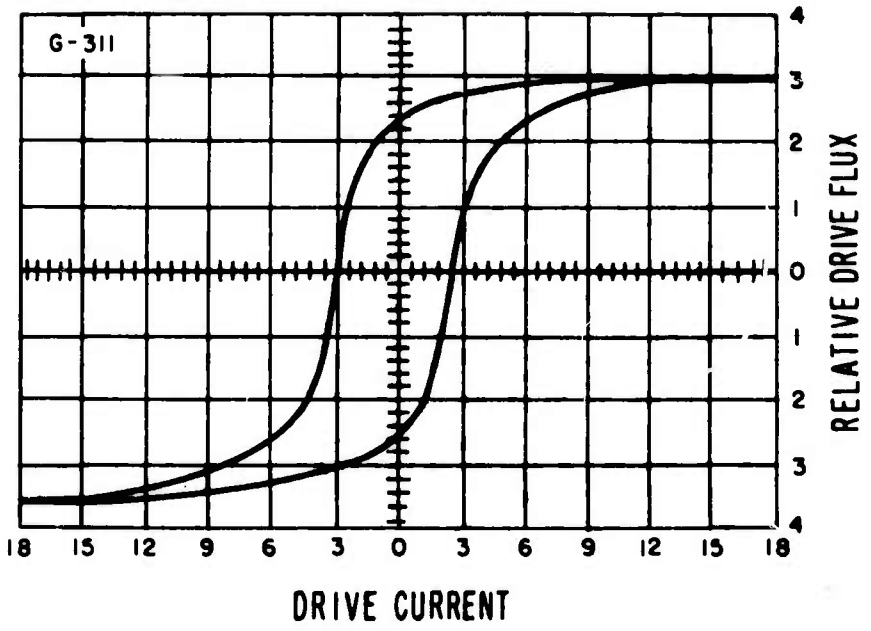

Figure 21. Typical Hysteresis Loop for G-311

TABLE I

Drive (I_{rms}) (amp)	B_R/B_D	$4\pi M_r$ (gauss)	H_c (oe.)
3.0	0.674	146	0.19
4.0	0.729	241	0.25
5.0	0.736	288	0.32
6.0	0.730	308	0.38
7.0	0.729	328	0.44
18.0	0.651	351	1.14

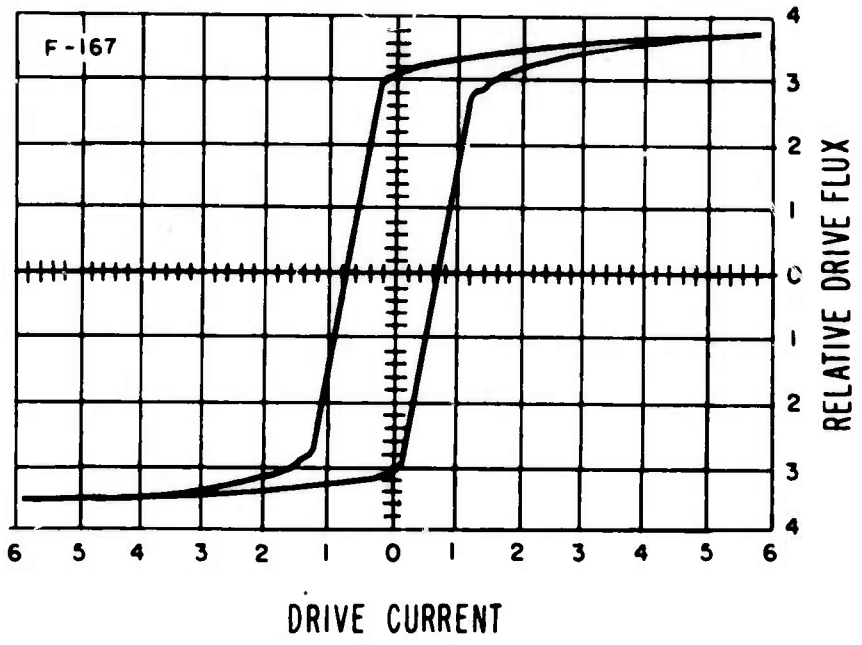

Figure 22. Typical Hysteresis Loop for F-167

TABLE II

Drive (I_{rms}) (amp)	B_R/B_D	$4\pi M_r$ (gauss)	H_c (oe.)
1.0	0.857	508	0.11
1.25	0.878	680	0.14
1.5	0.882	737	0.17
1.75	0.879	775	0.20
2.5	0.871	832	0.29
5.95	0.816	880	0.68

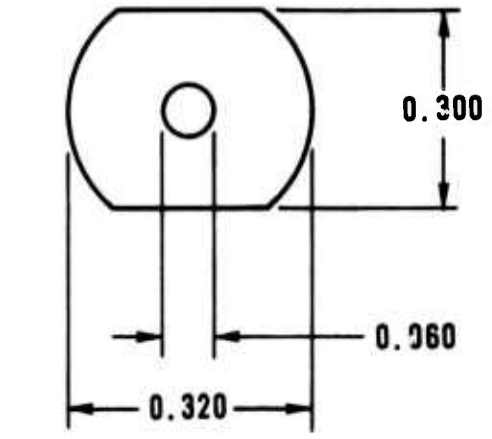

Figure 23. Cross Section of F-167

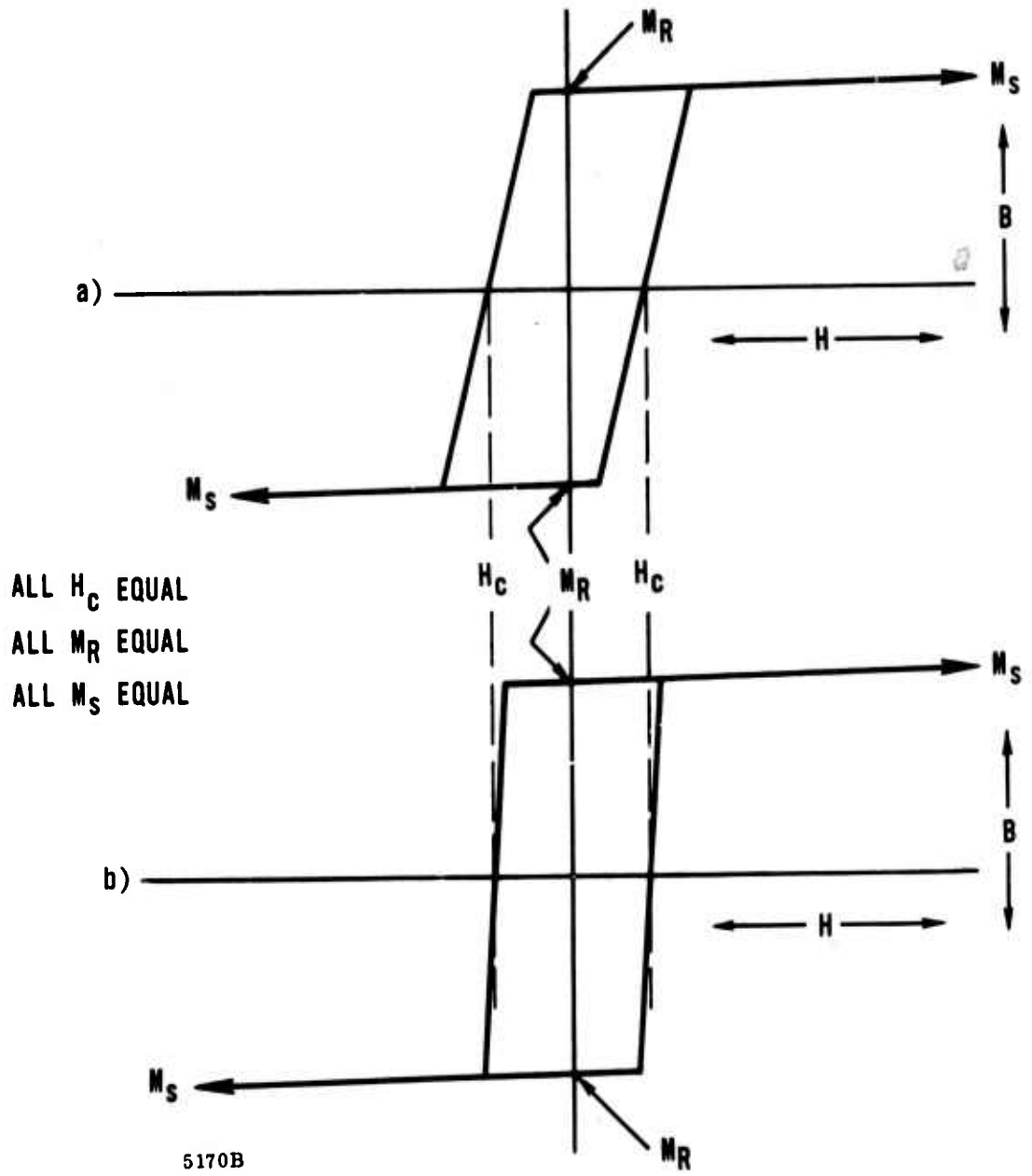

Figure 24. Typical Ferrite B-H Curves

Referring to Figure 25, one sees a typical cross section as encountered in phase shifters - that is, a rectangular toroid with chargine wire.

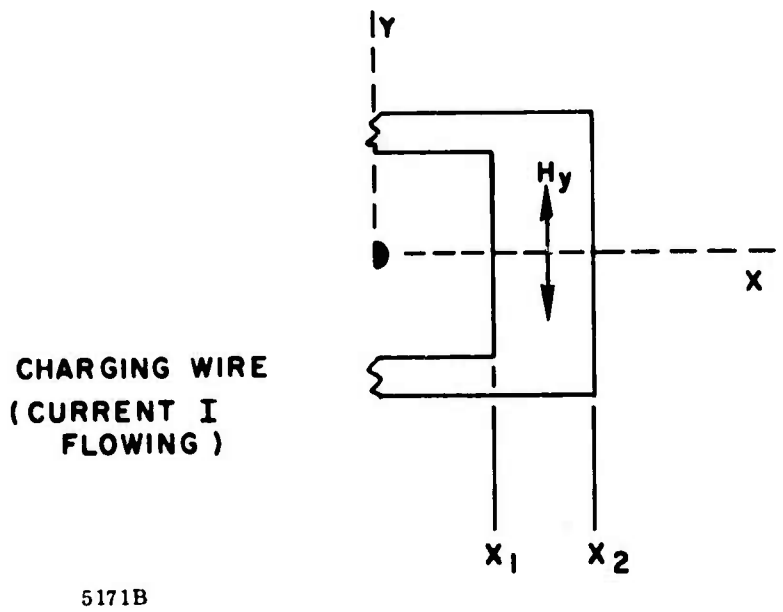

Figure 25. Phase Shifter Cross Section

If one considers the field generated at any point along X in the Y direction by a current I flowing in the charging wire given by

$$H = \frac{I}{2\pi X}$$

then the field at X_1 and X_2 is

$$H_{(X_1)} = \frac{I}{2\pi X_1}$$

$$H_{(X_2)} = \frac{I}{2\pi X_2}$$

Given the above information, it is now possible to relate B to X for any given charging current I.

Figure 26 shows two typical B vs X curves for the B-H curves of Figure 24.

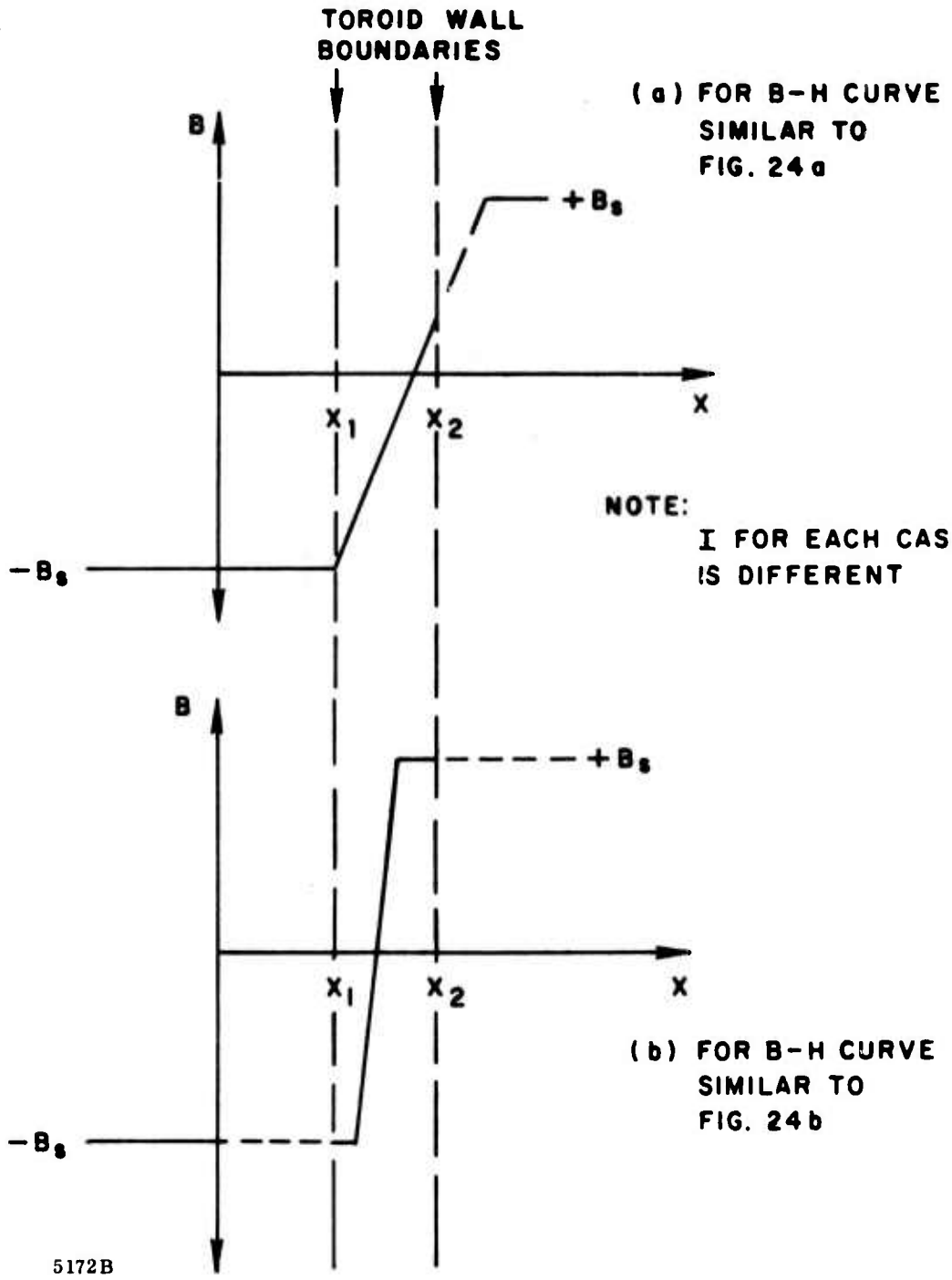

Figure 26. B Across Toroid Wall

If one averages the magnetization B from X_1 to X_2 and locates the point at which this average value occurs, it is obvious that the average magnetization level is dependent on the magnitude of the charging current. Further, the X position of this average value changes with I.

In addition, the shape of the B-X curve over X_1 to X_2 is dependent upon the shape of the original B-H curve.

Not only is the average value of B and its position important to microwave phase shifters but the variation with X is also vitally important.

When one considers a phase shifter design, it is common practice to define the cross section and a value of $4\pi M_r$. It is assumed that the value of $4\pi M_r$ is constant over the cross section chosen. It is necessary, however, for a rigorous study to determine the value of $4\pi M_r$ at each value of X.

A similar phenomenon occurs as a function of temperature. If drive current (therefore $H_{(X)}$) is held constant at a level below that for saturation, the resultant $4\pi M_r$ at any point X from the charging wire will vary as a function of temperature. It is therefore necessary to consider the effects of toroid wall thickness and the associated variation in B when considering flux drive for temperature variation.

4.3 FLUX DRIVE

Consider the circuit for Figure 27.

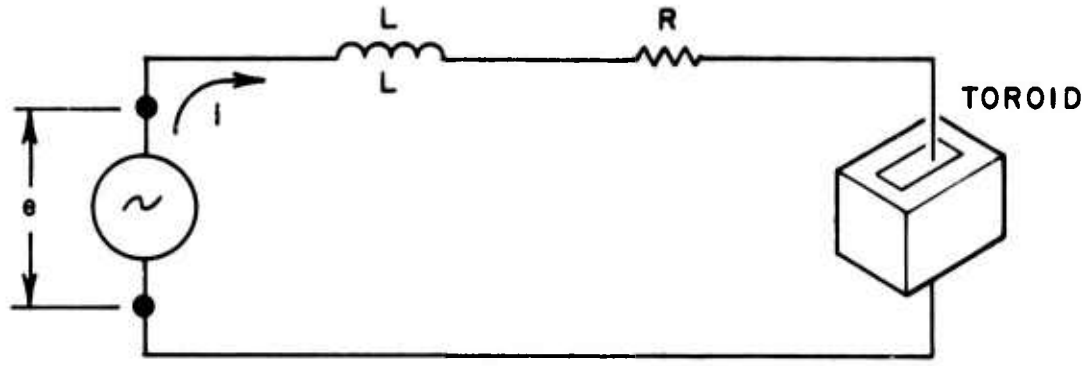

Figure 27. Equivalent Phase Shifter Driver-Load Circuit

Then:

$$e = iR + L\frac{di}{dt} + \frac{d\psi}{dt}$$

where R is the series resistance of charging wire and drive circuit, L the inductance and ψ the flux in the toroid.

If one assumes that $R \longrightarrow 0$ and $L \longrightarrow 0$, then the equation becomes

$$e = \frac{d\psi}{dt}$$

or

$$\psi = \int e\,dt$$

where

$$e = e(t)$$

Since e is a driving function, then the flux, ψ, becomes drive flux ψ_D. If one assumes that the remanence of the toroid material is a constant with temperature and that the toroid is not driven to saturation, then

$$\frac{\psi R}{\psi D} = \text{constant}$$

and

$$\psi R = C\int e(t)dt$$

In addition, the insertion phase of a microwave phase device is directly related to remanent flux such that

$$\Delta\phi = \psi R_+ - \psi R_- = \int e_+(t)dt_+ - \int e_-(t)dt_-$$

when $\Delta\phi$ is differential phase obtained by switching the material between two remanent states (+ and -).

It can be seen from the above discussion that many assumptions have been made. In practice, R is not zero and although small (0.1Ω to 0.5Ω), it can become appreciable - especially if the toroid load impedance is low, which occurs as the permeability approaches zero. The inductance of the charging circuit is likewise not zero but is in practice usually negligible. However, for remote driver applications where the charging wire is up to three feet long, the inductance must not be arbitrarily neglected.

As stated earlier, R also includes the internal impedance of the driving circuit. A driver operating in saturation presents a variable source R as a function of current, with R becoming noticeably large if an excessive current is drawn from the circuit (transistor pulls out of saturation).

Remanence ratio is normally a constant with temperature to a first order approximation, but slight variations may occur depending upon material composition and temperature excursion.

The final assumption, that insertion phase of the microwave device is directly related to ψ_R or $4\pi M_r$, is correct but must be conditioned by discussions in Section 4.2; that is, that ψ_R is dependent upon distance from the charging wire and shape of the charging loop.

4.3.1 Experimental Verification

Attempts were made to experimentally verify the theory that constant phase shift could be attained over a temperature range if drive flux, ψ_D, were maintained constant.

The units developed under this program were intended to be used with water cooling, thus limiting housing and toroid temperature excursion. Attempts at low power without water cooling to measure flux as a function of temperature were frustrated by magnetostriction resulting from waveguide dimensional changes which caused pressures to be applied to the toroids. Magnetostrictive effects completely overshadowed the effects of flux drive.

It was possible to evaluate this flux -$\Delta\phi$ relationship in two other structures, one at X band using a garnet and one at C band using a ferrite.

Figures 28 and 29 are plots of drive flux vs temperature for constant phase shift for each of these structures with cross sectional dimensions given.

Although the ferrite structure employed a round toroid which hinders direct and clear comparison, it is evident that a material which possesses a rapid change in B for small changes in H (or X for a given cross section) and which has a large wall thickness (thus large change in H over its cross section) is subject to changes in flux required with temperature for constant phase shift.

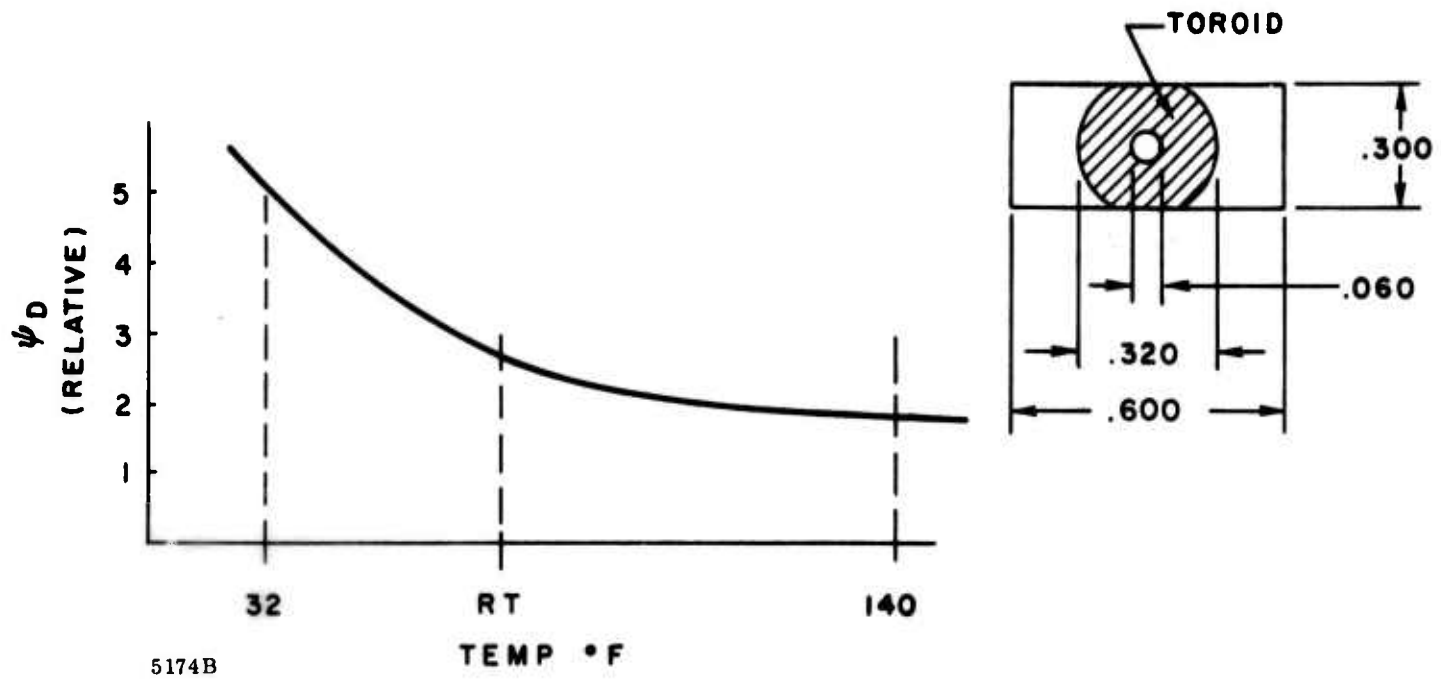

Figure 28. Drive Flux versus Temperature, C Band

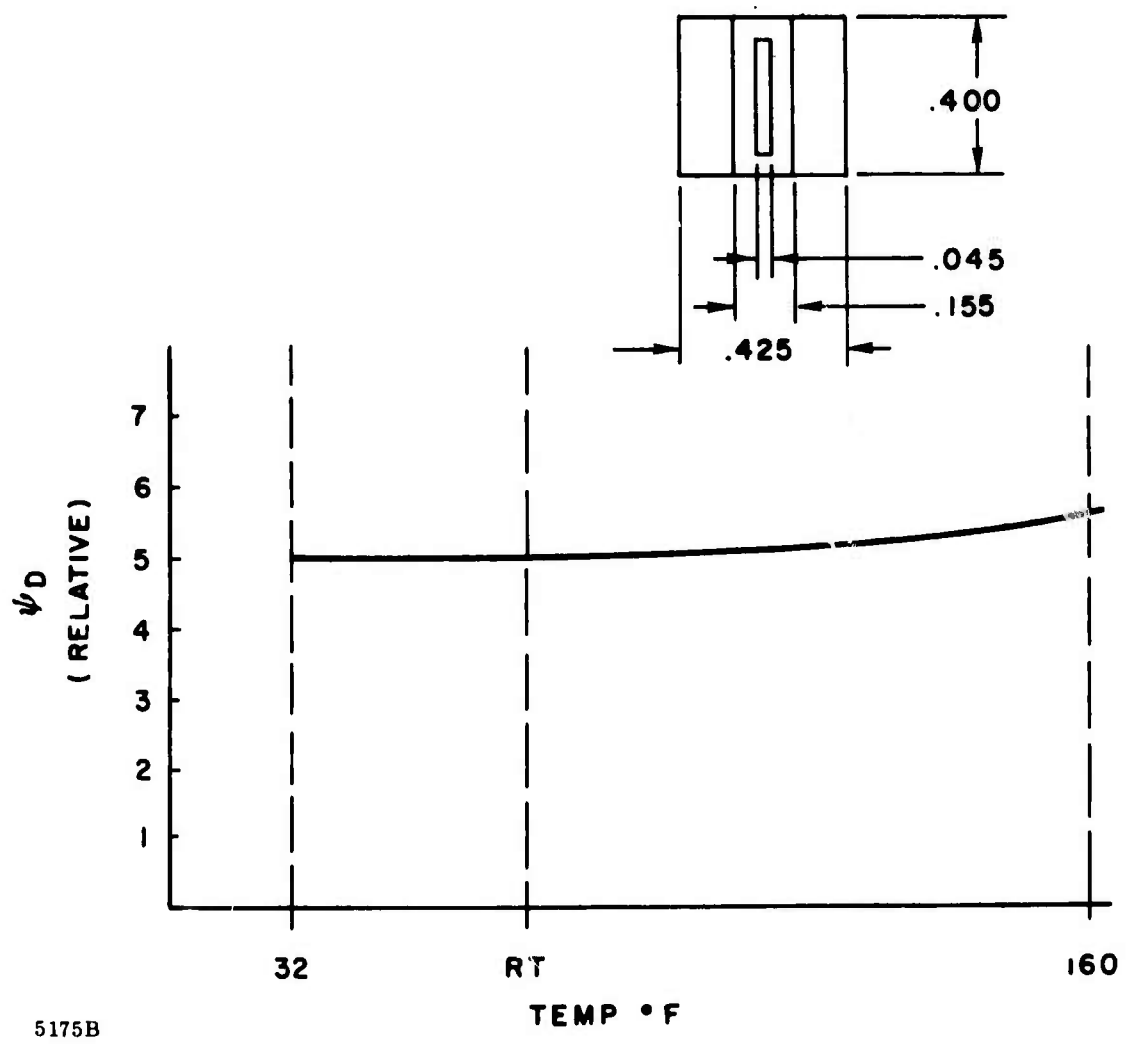

Figure 29. Drive Flux versus Temperature, X Band

The shape of the curve for the ferrite material, however, was unexpected. After analysis this variation became reasonable since H_c, coersive field, decreases significantly with increase in temperature.

4.4 SYMMETRICAL DRIVE

If one were to measure insertion phase as a function of magntization, including the demagnetized state, a plot similar to Figure 30 would be obtained. Note that the change in insertion phase is not symmetrical about the demagnetized state. The degree of nonsymmetry about the demagnetized state is dependent upon the microwave cross section. (Computer results indicate that symmetry can be obtained for special but not necessarily "optimum" cross sections.)

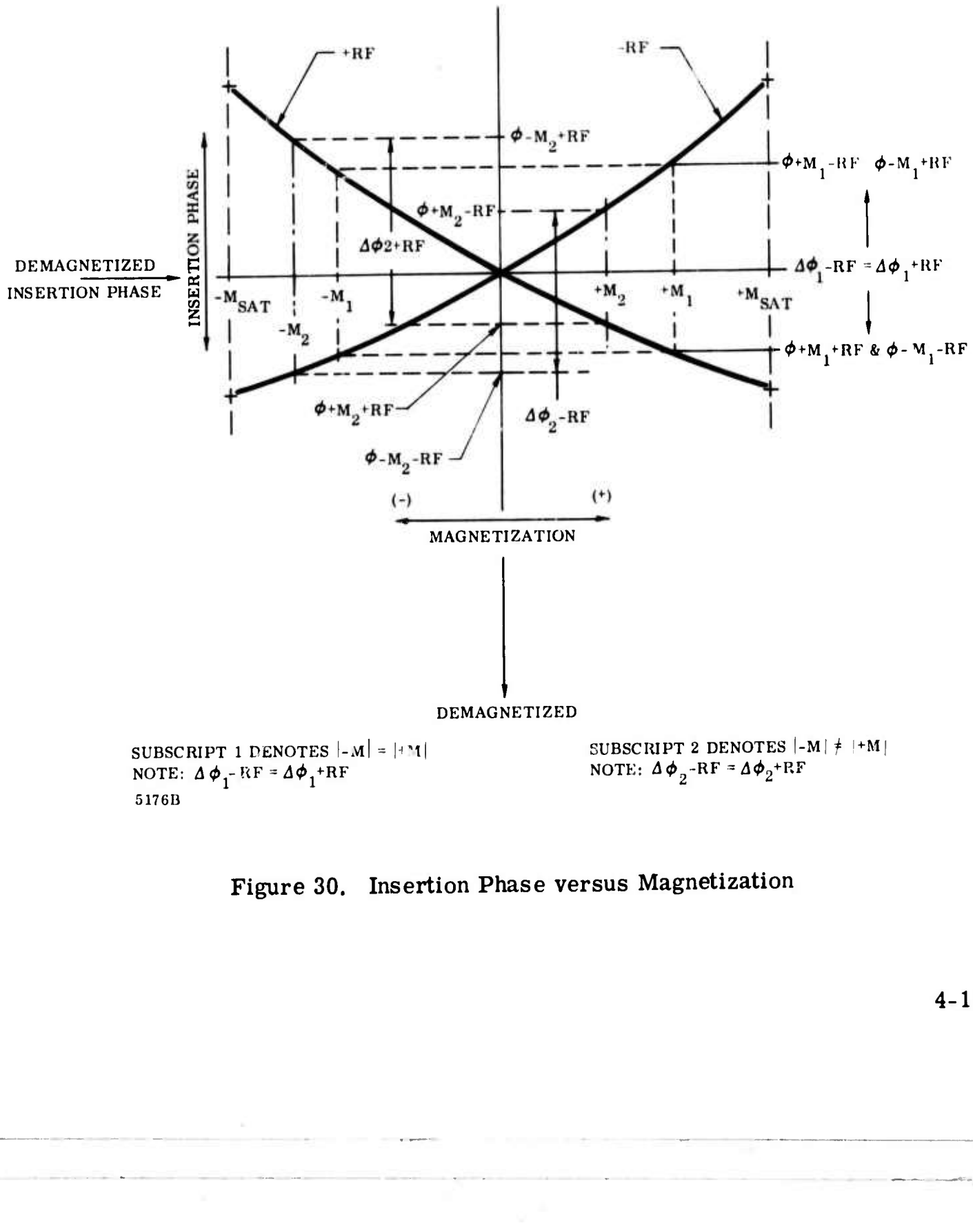

SUBSCRIPT 1 DENOTES |-M| = |+M|
NOTE: $\Delta\phi_1$-RF = $\Delta\phi_1$+RF

SUBSCRIPT 2 DENOTES |-M| ≠ |+M|
NOTE: $\Delta\phi_2$-RF = $\Delta\phi_2$+RF

5176B

Figure 30. Insertion Phase versus Magnetization

The plot has been made for a specific direction of rf relative to the +m and -m states. If the direction of rf propagation is reversed then the effect of a given magnetization is reversed and the second curve is obtained. For simplicity, rather than speak of reversal in +m and -m, the nomenclature +rf and -rf have been employed.

If one were to operate between any two states where

$$\left|-m\right| = \left| +m\right|$$

then the differential phase shift would be the difference between two values of insertion phase and the magnitude

$$\Delta\phi_{rf+} = \Delta\phi_{rf-}$$

As can be seen also from Figure 30, if one were to operate with the magnetization states at different levels, then the differential phase for the two directions of propagation is not equal, that is:

$$\left|-m\right| \neq \left| +m\right|$$

and

$$\Delta\phi_{rf+} \neq \Delta\phi_{rf-}$$

The degree of error obtained as a result of nonsymmetrical drive is highly dependent upon the phase shifter cross section. For the cross section of the phase shifters designed under this program, it was experimentally found that a current unbalance of 0.3 ampere typically produced a differential phase error between the two directions of propagation of less than 2%.

Symmetrical drive of a phase shifter is thus important if an array of high accuracy is to be used for both transmit and receive modes. Difficulties do arise, however, with the use of a symmetrical minor loop drive in that there is no truly fixed point on the B-H curve from which to reference drive. It is, therefore, necessary not only to balance drive currents for the two drive conditions but to control this balance over any temperature range encountered. The need for balance control with temperature arises from relative insertion phase requirements placed upon each unit of the array.

5. MULTIBIT PHASE SHIFTER

5.1 GENERAL

Section 5 of this report has been reserved specifically for a detailed description of the multibit phase shifter delivered as part of this program. Emphasis is placed upon the actual hardware rather than its theoretical design.

5.2 DRIVER

The driver employed on the multibit unit is shown in the functional block diagram of Figure 31.

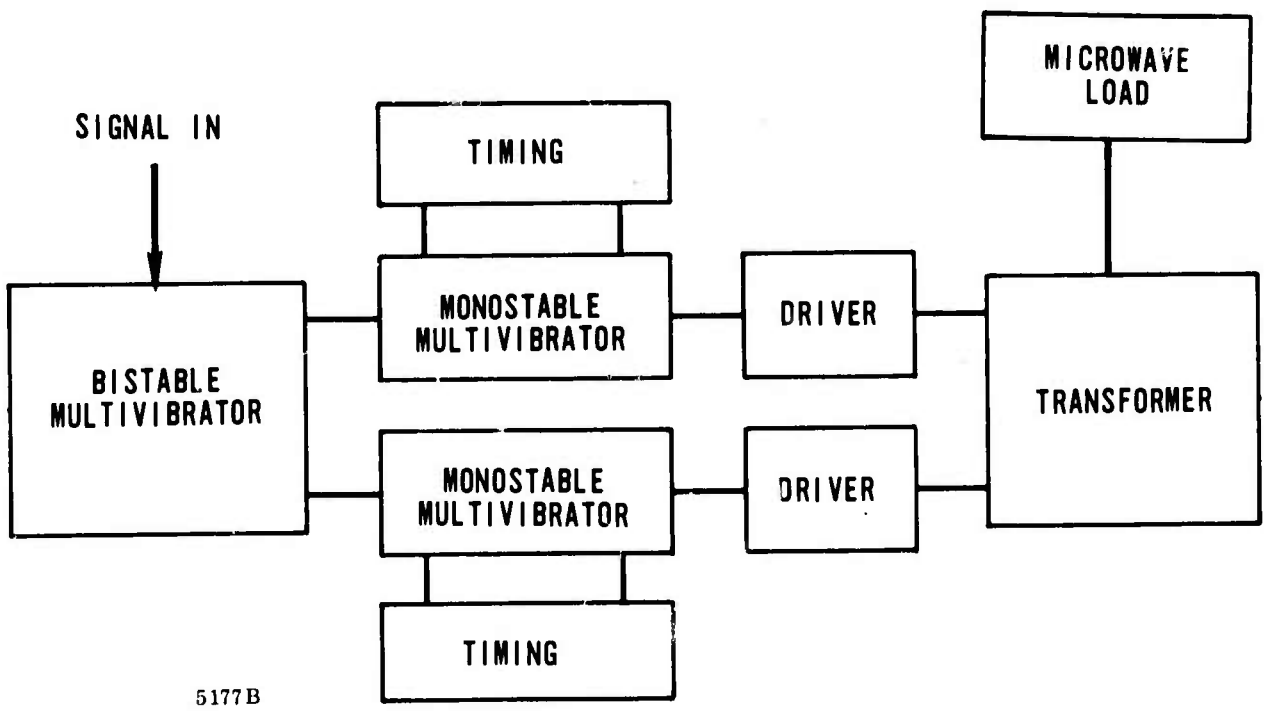

Figure 31. Functional Block Diagram - Multibit Driver

Signals of dual polarity are injected into each bit of the phase shifter. These signals trigger a bistable multivibrator used to prevent multitriggering of the driver in one direction. If multitriggering of the bit in any one direction were permitted on a unit employing symmetrical minor loop drive, errors would be introduced into the rf system due to creeping of the loop to new insertion and differential phases.

The outputs of the bistable multivibrator are fed to two monostable multivibrators. The lengths of the pulses generated are adjustable for proper balance in output current to the microwave load.

The outputs are fed through driver stages to a matching transformer for the microwave load. The transformer also permits the use of similar driver stages by inverting the polarity of one side of the driver and permits the use of one drive wire to the microwave load.

The driver used specifically for this program employed a saturable reactor in series with the microwave load as shown in Figure 32.

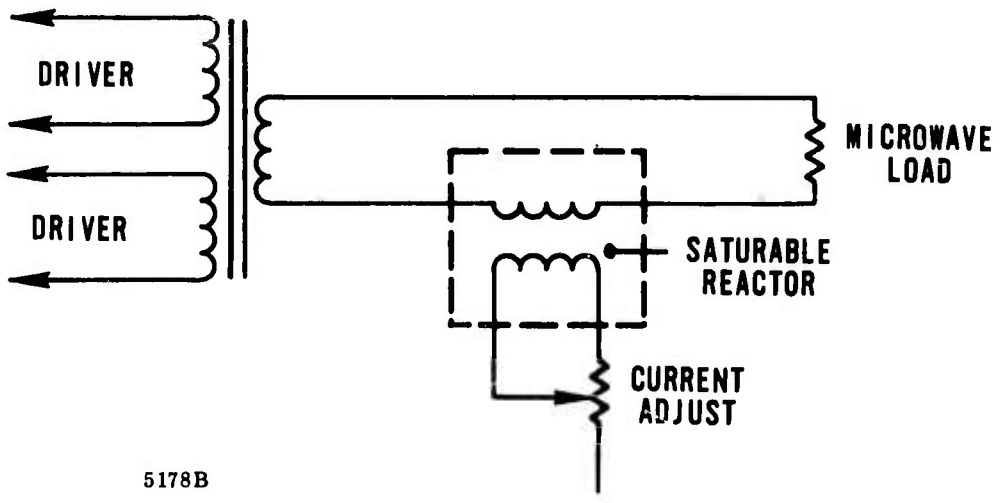

Figure 32. Output Circuit of Multibit Driver

The intent of this circuit was to provide a single control which would fine-trim both positive and negative pulses to the microwave load. Coarse adjustment to attain initial current balance is performed in the timing circuits of each section.

Depending upon the load resistance of the saturable reactor, a voltage drop across the primary of this reactor could be accomplished.

The circuit performed in a satisfactory manner but has the following limitations:

- Efficiency of the circuit is degraded since drive to the load is always set for maximum and is reduced by dissipation in the reactor circuit.
- Due to variations in microwave load parameters with temperature (when microwave component temperature control is not employed), there is difficulty in properly damping the circuit, especially at cold temperatures.

The circuit offers the advantage of a single adjustment for both polarity pulses after initial balance is attained in the timing circuit.

Figure 33 shows the completed 4-bit driver delivered as part of this program. Note that this driver is used for remote applications and employs a cross-section similar to that of the phase shifter. Connectors are provided at each end, one for input signals and one for connection to the microwave hardware. In addition, clips are provided for locking the driver into an array frame.

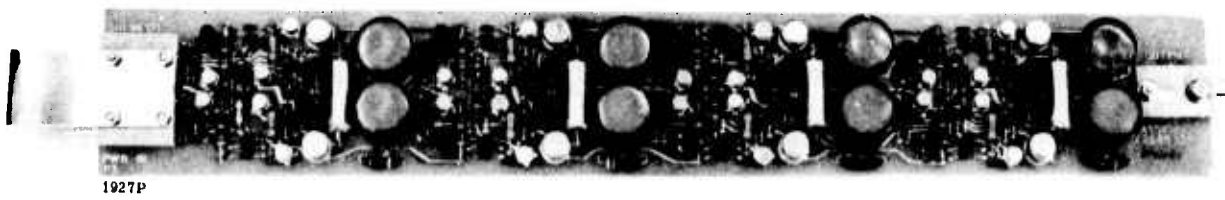

1927P

Figure 33. Multibit Driver

Following is a list of power and signal requirements for the multibit driver:

Signal Input	One line per bit, plus and minus pulses, 2 μsec at 10 V
B+	28 V
Switching Rate	5000 switching operations per sec. max.
Switching Time	$\approx$3.0 μsec

5.3 PHASE SHIFTER

Figure 34 shows the microwave phase shifter as delivered, and Figure 35 shows the driver and phase shifter with interconnecting cable.

Figure 34. Multibit Microwave Phase Shifter

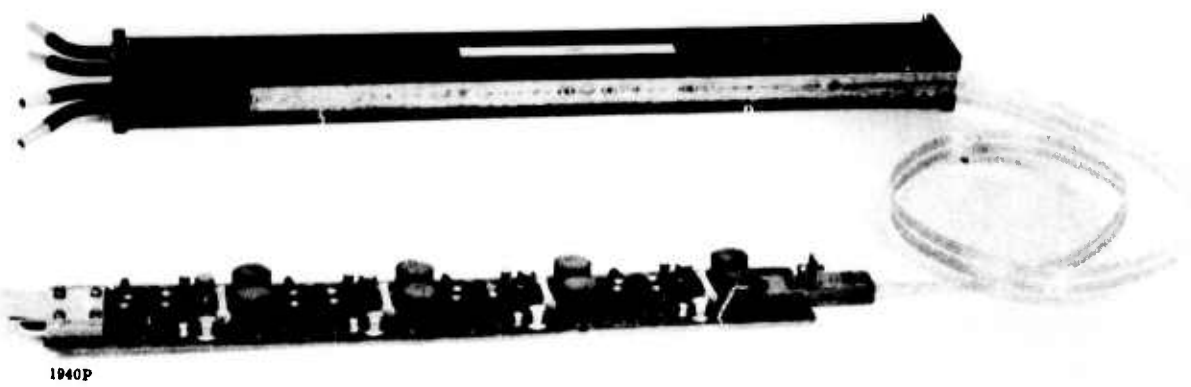

Figure 35. Phase Shifter with Driver and Interconnecting Cable

A plot of differential phase as a function of frequency for two units is shown in Figure 36. Note that a slight phase slope is indicated from this plot, as was predicted from the computer data described in previous sections.

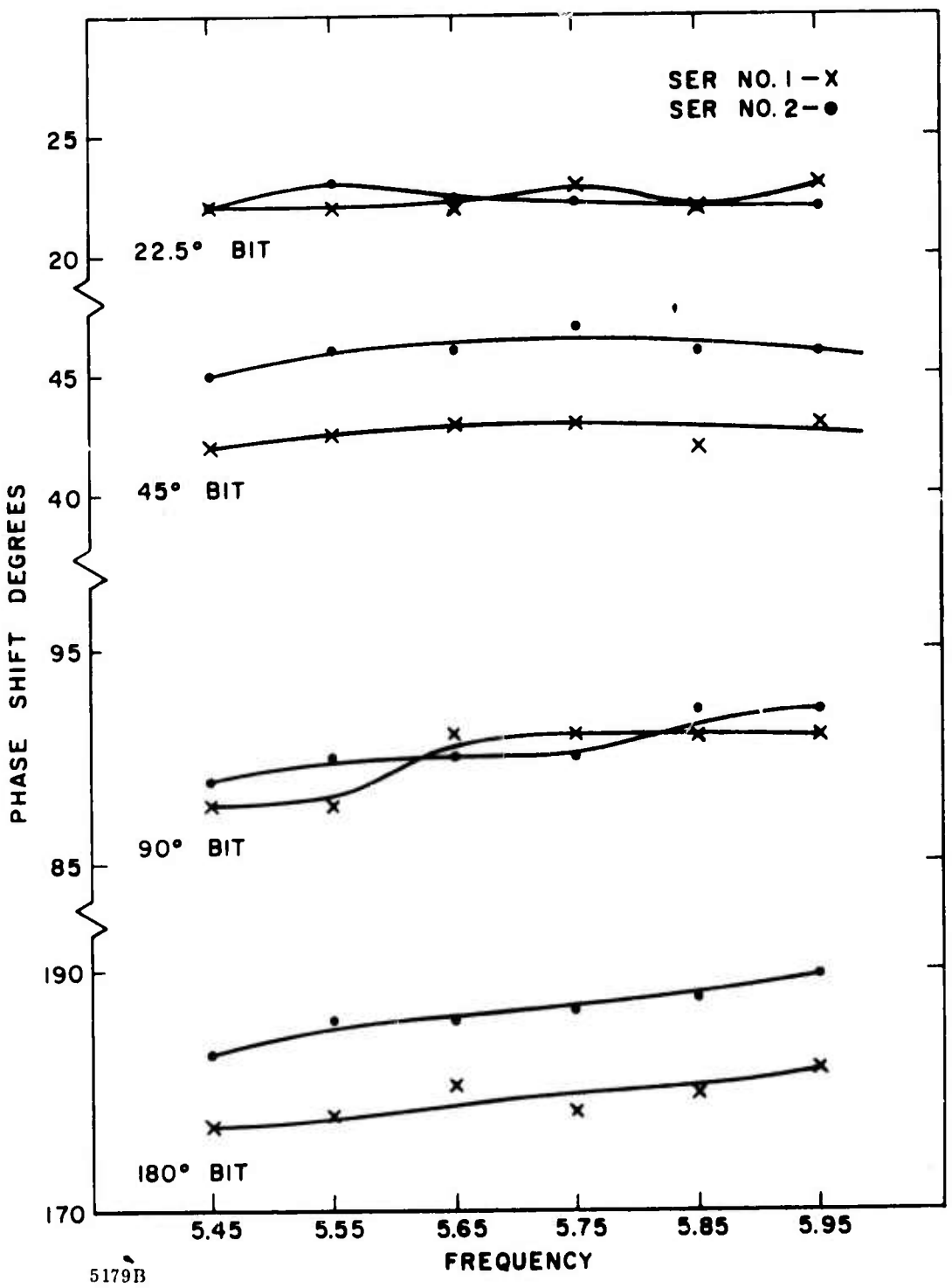

Figure 36. Differential Phase versus Frequency for Multibit Phase Shifter

Figures 37 and 38 illustrate VSWR and insertion loss of the multibit phase shifter. Spikes in the insertion loss curve are caused by imperfect fit of core and toroid in the overall structure and are emphasized by the height dimension (0.622 inches) of the unit. This height was required to reduce potential arc-over to a minimum.

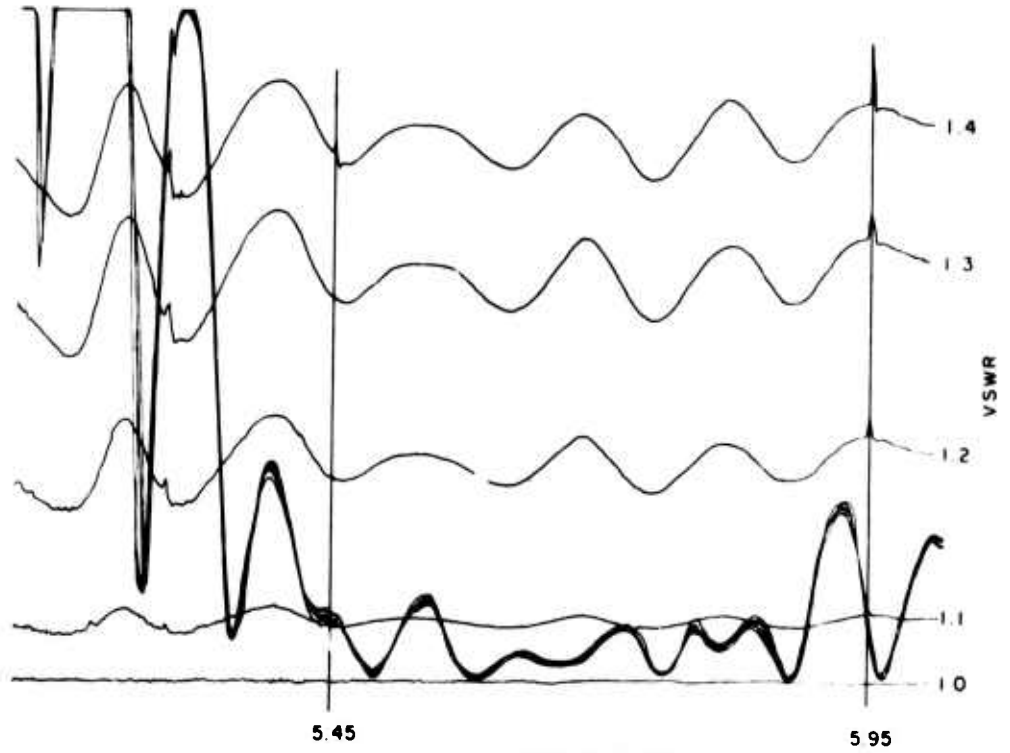

5180B

Figure 37. VSWR versus Frequency, Multibit Phase Shifter

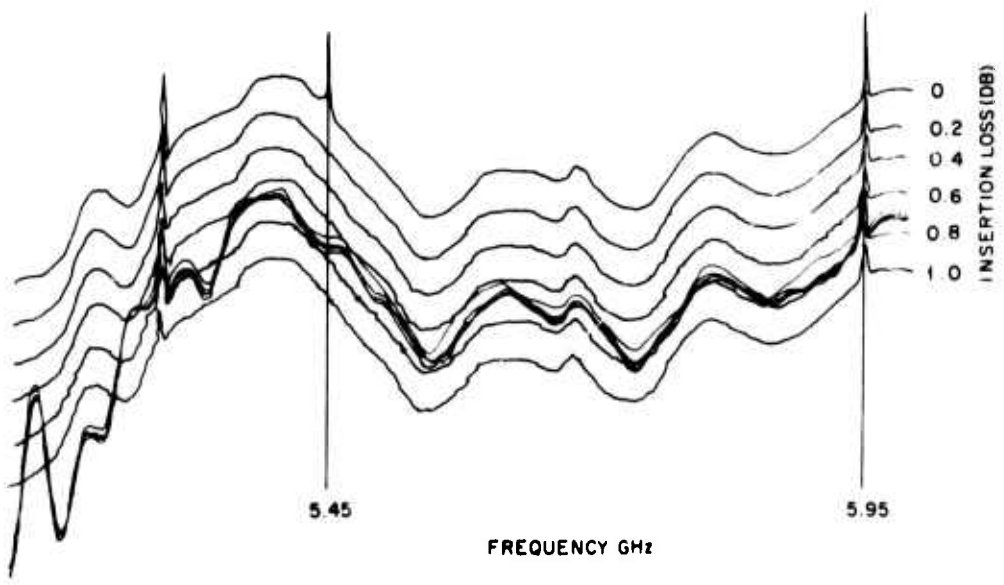

5181B

Figure 38. Insertion Loss versus Frequency, Multibit Phase Shifter

6. SINGLE BIT PHASE SHIFTER

6.1 GENERAL

The single bit phase shifter employs a microwave structure with the same cross section as that employed in the multibit unit. The length of the unit has been increased to assure minimum error when employing flux drive. A single bit is driven into saturation and then to the desired phase shift value each time a change in phase shift is desired. The increased length is required to maintain linear operation.

Flux drive is employed to assure an accurate phase-time relationship, thus allowing a set of discrete differential phase increments proportional to input timing sequence.

Figure 39 shows the single bit phase shifter with remote driver. Note the similarity in construction to the multibit unit.

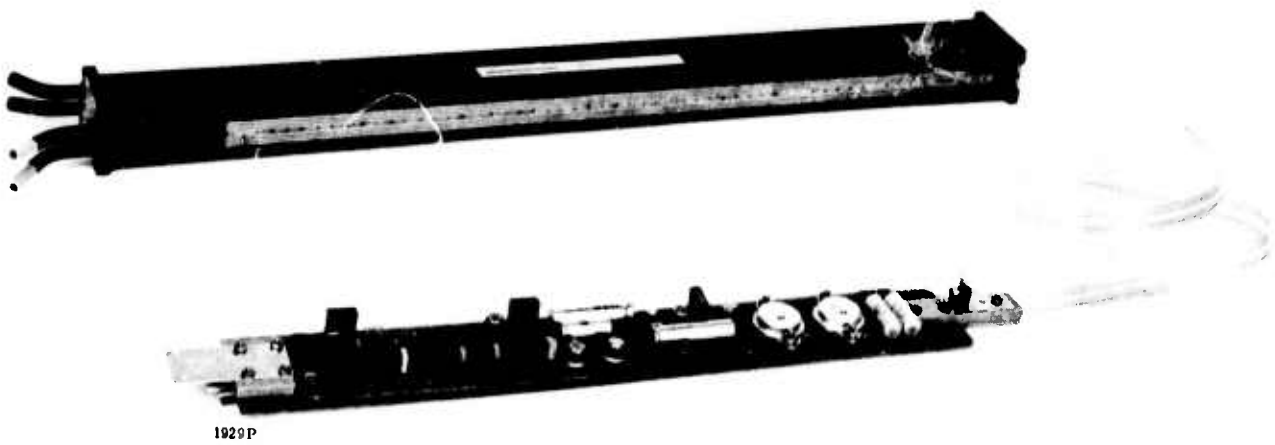

Figure 39. Single Bit Phase Shifter with Remote Driver and Interconnecting Cable

6.2 MAGNETIZATION ANALYSIS

A suitable set of specifications can be derived for a single bit unit from those normally considered for a multibit unit, but with variations.

Each bit of the multibit unit operates in only two states which can be called, for convenience, 0 and 1 states.

The single bit unit will operate in the conventional 0 state but the 1 state is divided into many substates. For equivalency to a four bit phase shifter, it is necessary to establish 15 sublevels of the 1 state. It is, therefore, necessary to establish not only the end points of the magnetization loop but the shape of the loop at intermediate points (see Figure 40).

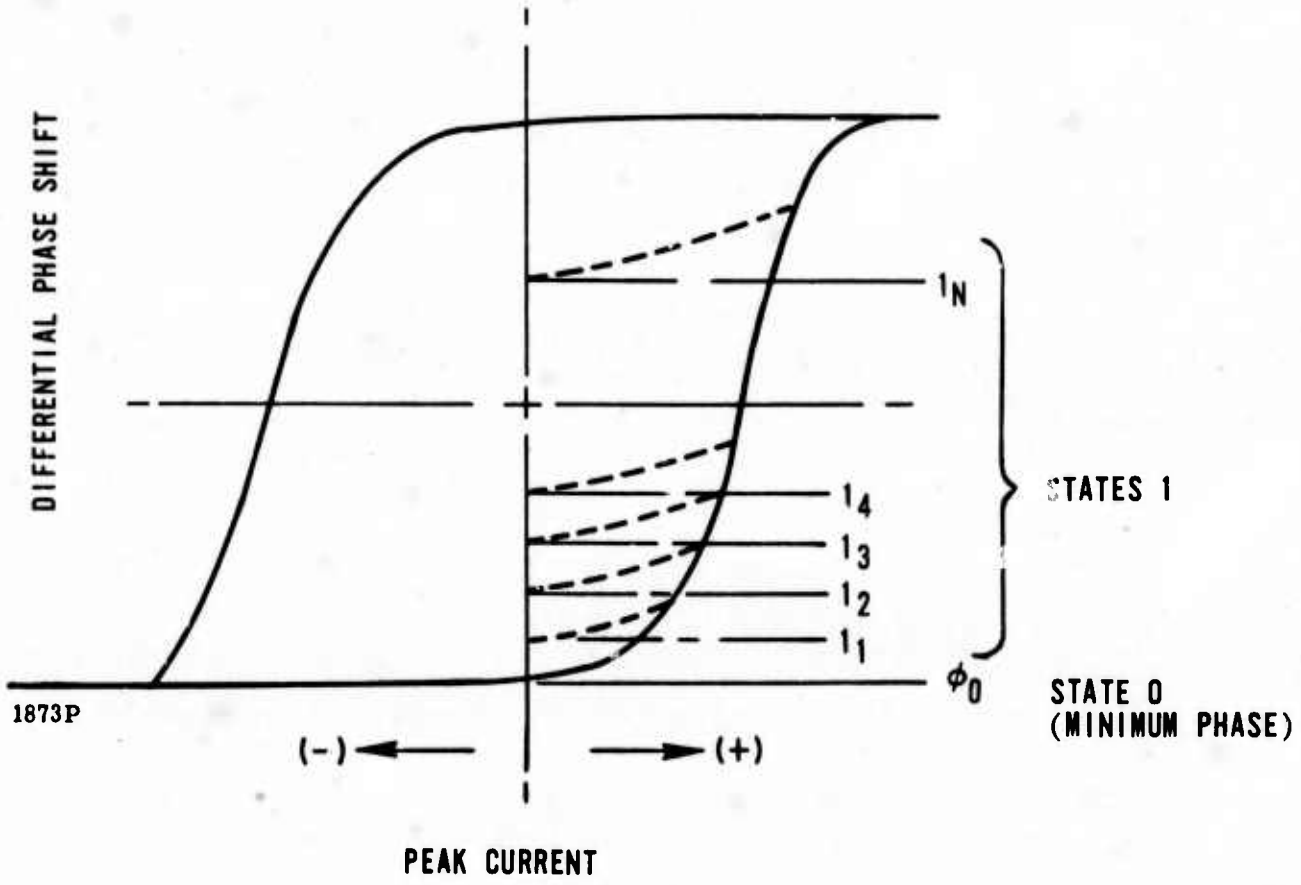

Figure 40. Magnetization Loop with Intermediate Phase Points

Position of intermediate points can best be controlled in a useful manner if one assumes that discrete amounts of flux are used to drive the phase shifter. A plot of differential phase versus flux is given in Figure 41.

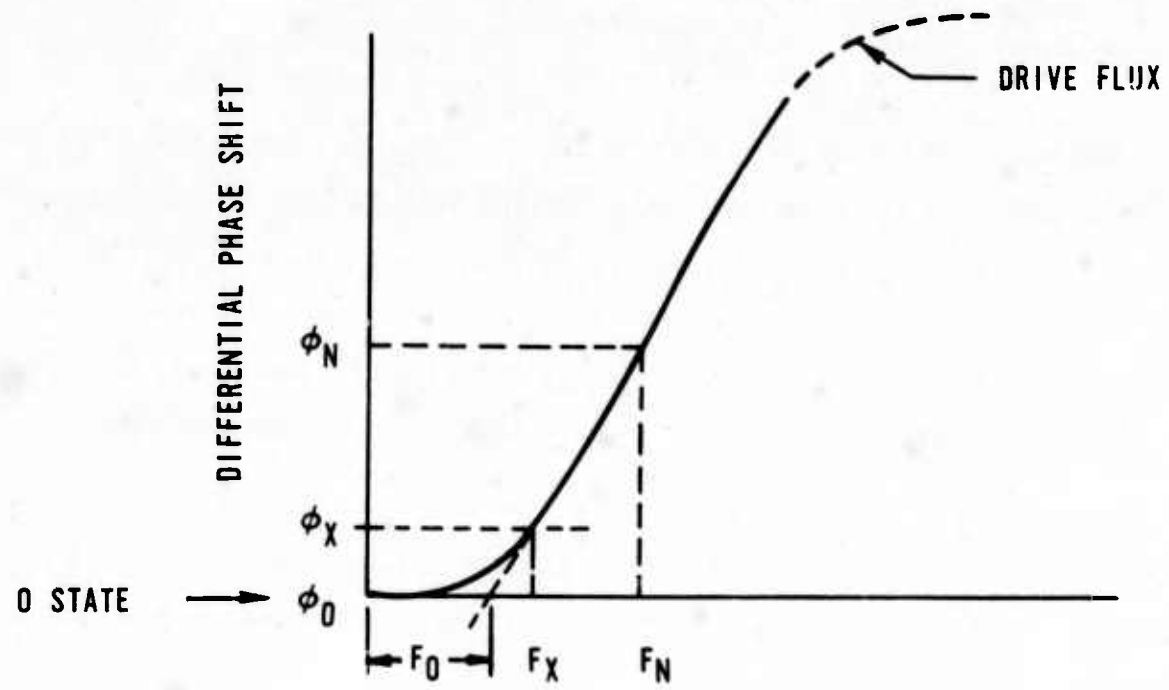

1874P

Figure 41. Flux versus Differential Phase Shift

To a first approximation, the plot of phase shift versus flux for most garnet materials approaches a straight line over a large portion of its useful range. If one assumes that material parameters are constant, then it is possible to supply a predetermined amount of flux to the phase shifter and obtain a known amount of phase shift. This is definitely a superior method of drive to programming current, since current is heavily dependent upon material and ambient parameters, and phase shift is not linear with current.

Over the linear portion of the flux-phase shift curve, one may write some simple approximate expressions:

$$\text{Flux} = \int E(t)dt$$

assuming

E = constant

Flux = $E\Delta T$

If one considers the curve of Figure 15 as composed of two straight lines then

$$\Delta\phi = \phi_n - \phi_o = F_o + E\Delta T = (ET_o + E\Delta T)$$
$$\Delta\phi = E(T_o + \Delta T)$$

This equation states that there is a flux F_o which accounts for the nonlinear effects of the material and if the applied charging voltage remains constant with time, then phase shift can be directly related to charging time plus a fixed time T_o. In practice, this curve is essentially true. However, the approximation of the curve to two straight lines is only true if one applies a total flux F_x minimum (see Figure 15). This is a limiting case of the smallest allowable bit for the phase shifter.

One may also allow E to vary with time in the above analysis. It should be noted also that peak current does not enter the above analysis. If the voltage E is maintained, the current I will reach the value required to satisfy the loop parameters in a specified amount of time.

The single bit phase shifter can now be conveniently programmed:

- A reset pulse drives the unit to saturation, and return to remanence results in the 0 state phase shift.
- A variable length pulse drives the phase shifter to the desired 1_n state.
- Because of material parameter variations (variations in H_c, coercive field, remance ratio, and $4\pi M_s$) the programming time pulse will be extended by a time T_o internally to the driver, and the voltage E will be adjusted to produce a value in a time interval specified by the customer.

All phase shifters in an array, therefore, can be programmed in a similar manner.

6.3 SPECIAL COMMAND PROVISIONS

As an extension of the above analysis, the phase shifter/driver being developed under this program was designed to incorporate Alpha-Beta set triggers.

Referring to Figure 42, each column and row of an array or sub-array requires an equal value of phase shift. If an array were steered only in the α direction, then each α column would have a fixed value of phase shift which can be related to a time interval when using the driving method described in Section 6.2, alpha values become timing intervals. Beta steering follows a similar method. If simultaneous alpha-beta steering is desired, then the phase/time of any element is the sum of alpha and beta times.

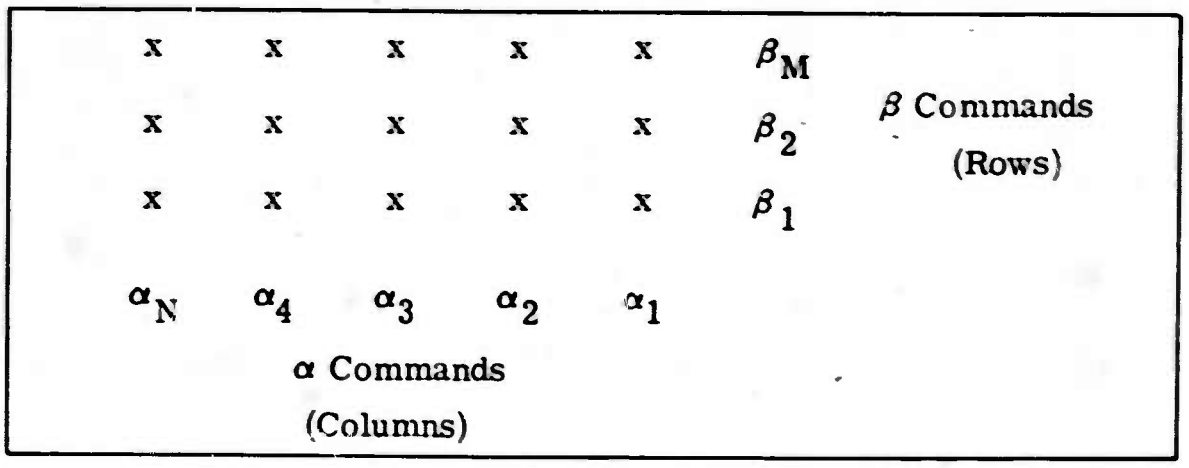

Figure 42. Alpha-Beta Array Steering

In practice, alpha and beta pulses are generated by proper electronics-computer circuitry: one as a start pulse and one as a stop pulse for the set timing of the phase shifter.

A typical timing sequence is shown in Figure 43 where every element in the array receives a reset trigger simultaneously at time t_1. This pulse t_1 drives all phase shifters into a reset condition which corresponds to a phase shift reference of zero degrees if α and β arrive simulatneously at time t_4. α_N and β_N pulses arrive at each phase element (on a row-column basis) about the time element t_4.

The total switching sequence was selected at 10 microseconds to assure a minimum of 5 microseconds for $(\alpha + \beta)$ maximum thus permitting reasonable resolution of times for the 16 possible values of $(\alpha + \beta)$.

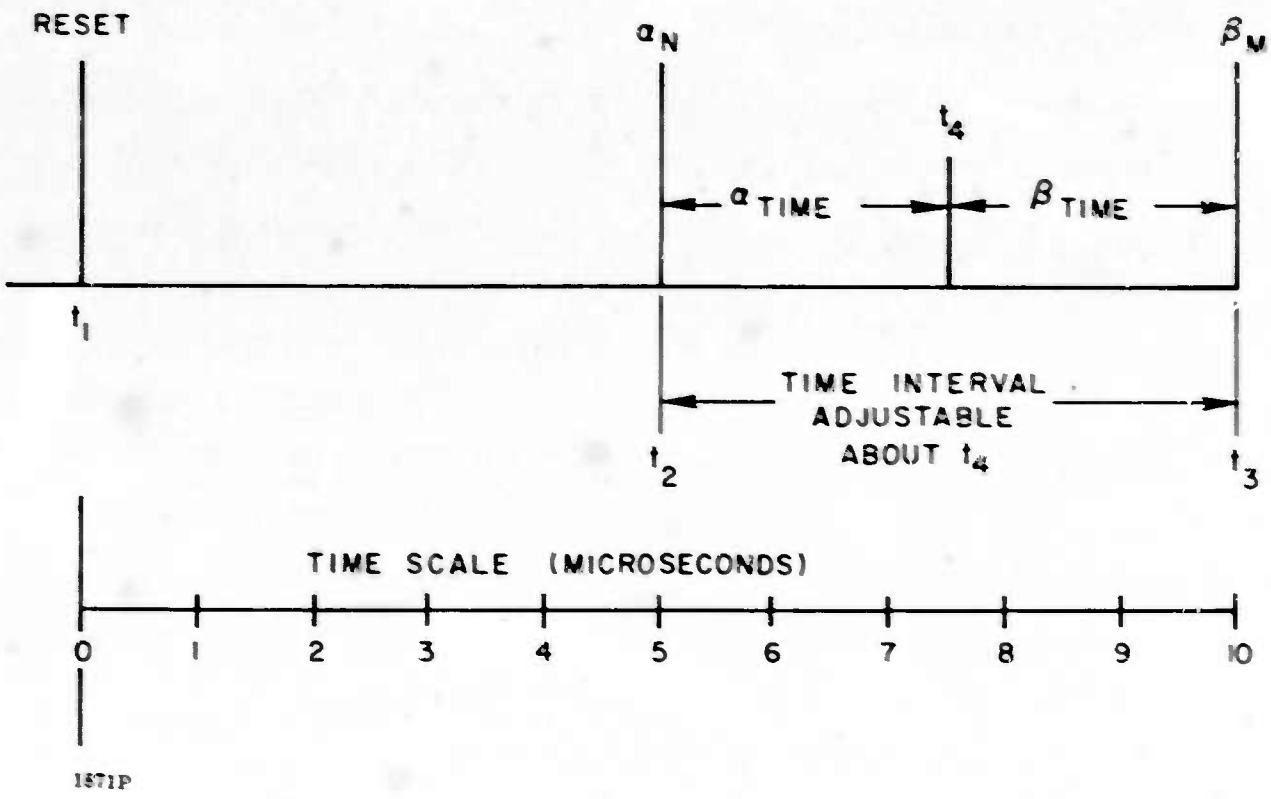

Figure 43. Typical Alpha-Beta Timing Sequence

The first 5 microseconds have been alloted to reset, 3 microseconds for the charging current to drive the toroid to saturation, 2 microseconds to permit all currents to return to zero (the microwave element returns to remanent magnetization).

For such a 10 microsecond timing sequence, the maximum switching time of the rf signal will be approximately 11 microseconds, allowing for an increased T_O (see F_O of Figure 41) and time for the set current to return to zero.

Such a triggering scheme does require 3 separate inputs to each array element but these can be connected on a two-column basis, which is much reduced in complexity to the input signal circuitry in multibit element methods.

For equivalent steering on transmit and receive, each element is set to its complementary time. An example would be:

For element $_{MN}$

$$\text{Transmit Set Time} = \alpha_M + \beta_N$$

$$\text{Receive Set Time} = (\alpha + \beta)\ \text{Maximum} - (\alpha_M + \beta_N)$$

Again as for the multibit phase shifter, accuracy between individual phase elements of an array will be dependent upon original insertion phase of each element and tolerances in setting the desired phase of each element.

6.4 DRIVER

A driver capable of producing the characteristics given in Section 6.2 and 6.3 was designed and used on single bit phase shifters. A basic block diagram is given in Figure 44.

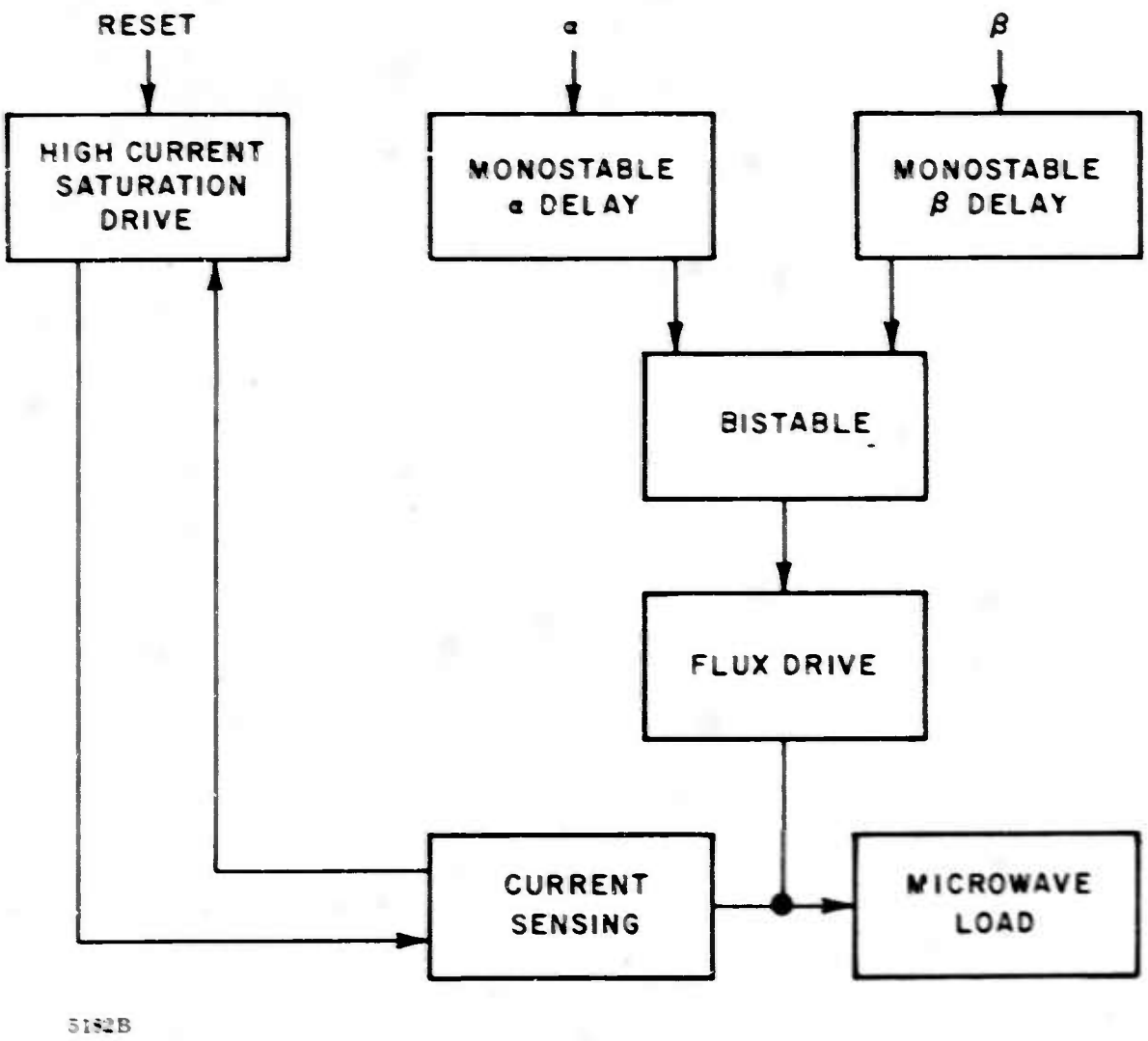

Figure 44. Single Bit Driver, Block Diagram

The driver can be divided into two parts. The reset portion of the driver is capable of delivering large currents (in excess of 10 amperes) to drive the microwave load material into saturation. A current feedback loop has been provided to yield maximum efficiency. The time required for the reset pulse to reach a desired current level is dependent upon the level of magnetization attained during the set phase of driver sequence. To attain a current of 10 amperes reset from set state 15 takes longer than that required for set state 1.

The current feedback loop senses the reset drive current and turns off the reset pulse when this current is attained. It is thus possible to reduce reset power consumed to a minimum.

The alpha or start pulse turns on the flux drive set portion of the driver and the beta pulse stops flux drive. Incorporated into this circuit are delay provisions to correct for transistor storage time, shape of the hysteresis loop (F_0 of Figure 41) and rise and fall times of the flux driver.

The driver is designed such that simulatneous receipt of α and β pulses yields no output; thus the reset pulse yields the zero or insertion phase state. Appendix A of this report gives details on the driver and special signal pulse generator used with the single bit phase shifter.

6.4.1 Limitations

The driver design assumes the following:

- Over the range of phase shift desired, the flux is proportional to time.
- The reset pulse drives the microwave load into saturation or to such a point as to eliminate "memory."

The first of the above statements is approximately true. However, when one considers that over a large range of flux, phase shift is only approximately linear with flux, an error is automatically introduced. In addition, a set time of 5 microseconds is designed to yield 337.5 degrees with an increment of 22.5 degrees corresponding to approximately 0.35 microseconds. The accuracy of α and β timing pulses and the point of trigger become extremely important. Likewise, any variation in voltage over the duration of the pulse causes a nonlinear flux for equal timing increments.

The errors in some instances are cumulative and imply that an accuracy of any bit position of ±2 degrees of desired value is extremely difficult to attain and control.

The second of the above statements has proved extremely difficult to attain. Reset drive currents as high as 60 amperes peak were used to assure saturation; even at this level it was not possible to completely eliminate the load "memory."

Further discussion of this effect will be covered in following sections which present data.

6.5 DATA

Since most parameters of this unit are similar to those attained on the multibit unit described in Section 5, only those parameters that are different will be presented here.

6.5.1 Phase Shift

Because of the method of attaining differential phase shift, phase shift will be given in terms of differential phase relative to the condition of reset pulse only; the reader is reminded that for each phase cycle a reset pulse is required.

Figure 45 is a plot of repeated cycling of the phase shifter to a given phase position. Each step in phase position corresponds to 22.5 degrees relative to the previous position. The differential phase recorded is referenced to the insertion phase value obtained for the zero phase position. The desired phase curve is also plotted for reference.

Figure 46 shows typical waveforms as the phase shifter was cycled through the zero and 15 phase positions. Note that no attempt was made to cycle the phase shifter alternately between two different phase positions.

Figure 47 displays the results of alternate cycling between pulse A, which was maintained in pulse position 1, and pulse B, which was stepped from position zero to 15. Note that an error occurs in the actual null of pulse B from the theoretical. Also the null position of pulse A, which theoretically should have remained fixed, varied as a function of pulse B.

Figure 48 shows current waveforms for alternate pulsing between set positions 1 and 15 and set positions 1 and 7.

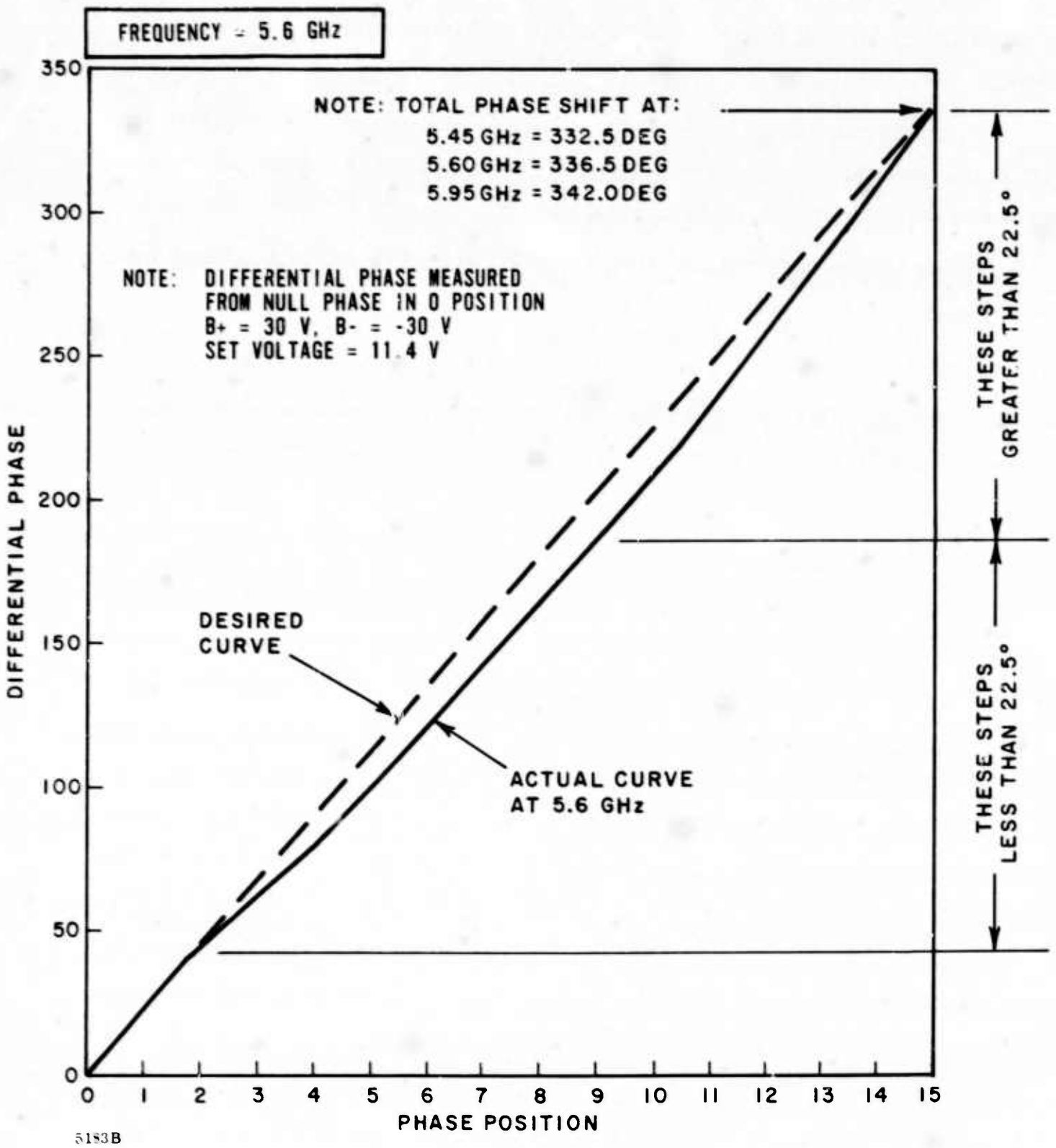

Figure 45. Differential Phase versus Set Pulse Position of Single Bit Phase Shifter

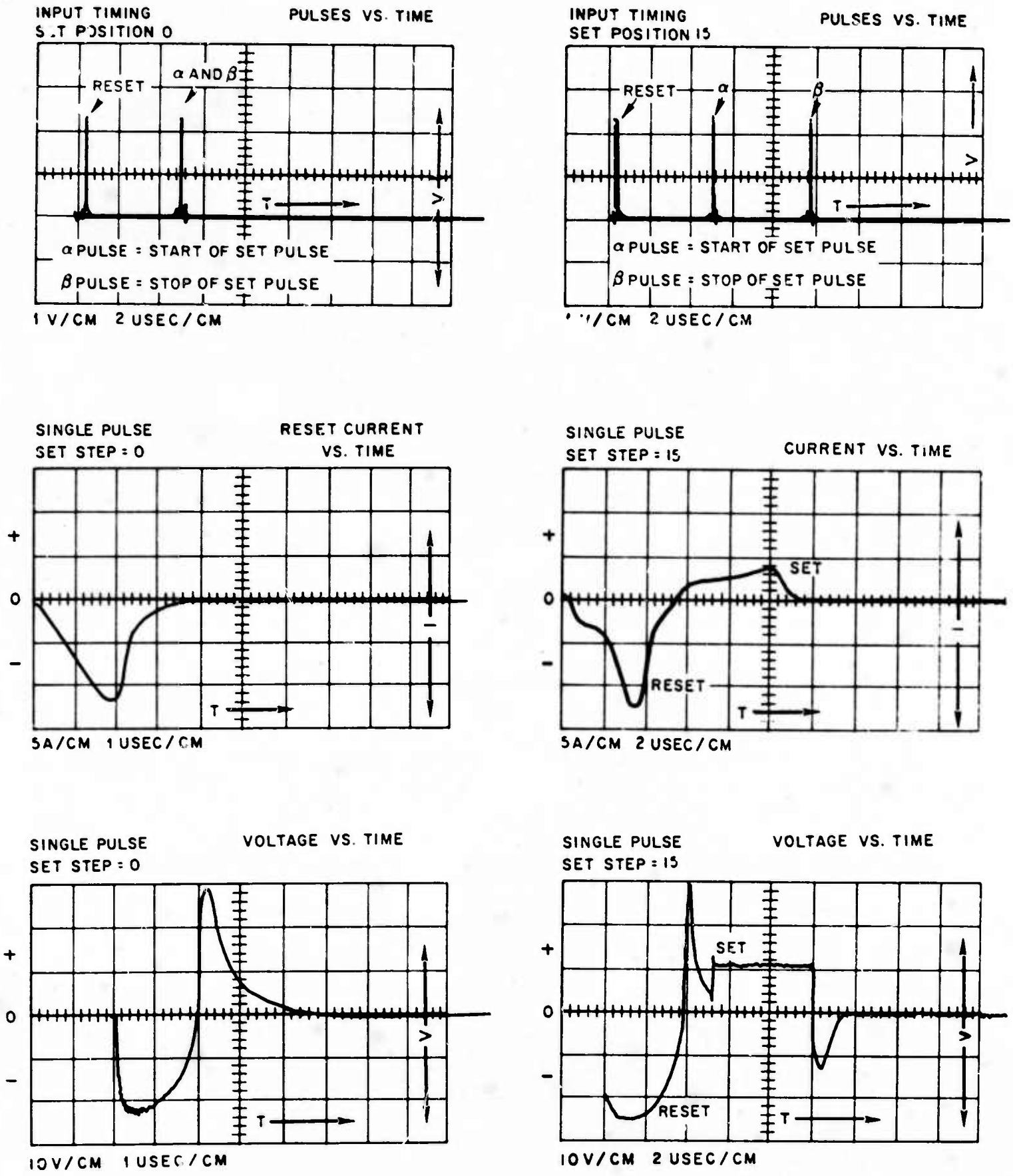

Figure 46. Typical Input Waveforms for Single Bit Phase Shifter

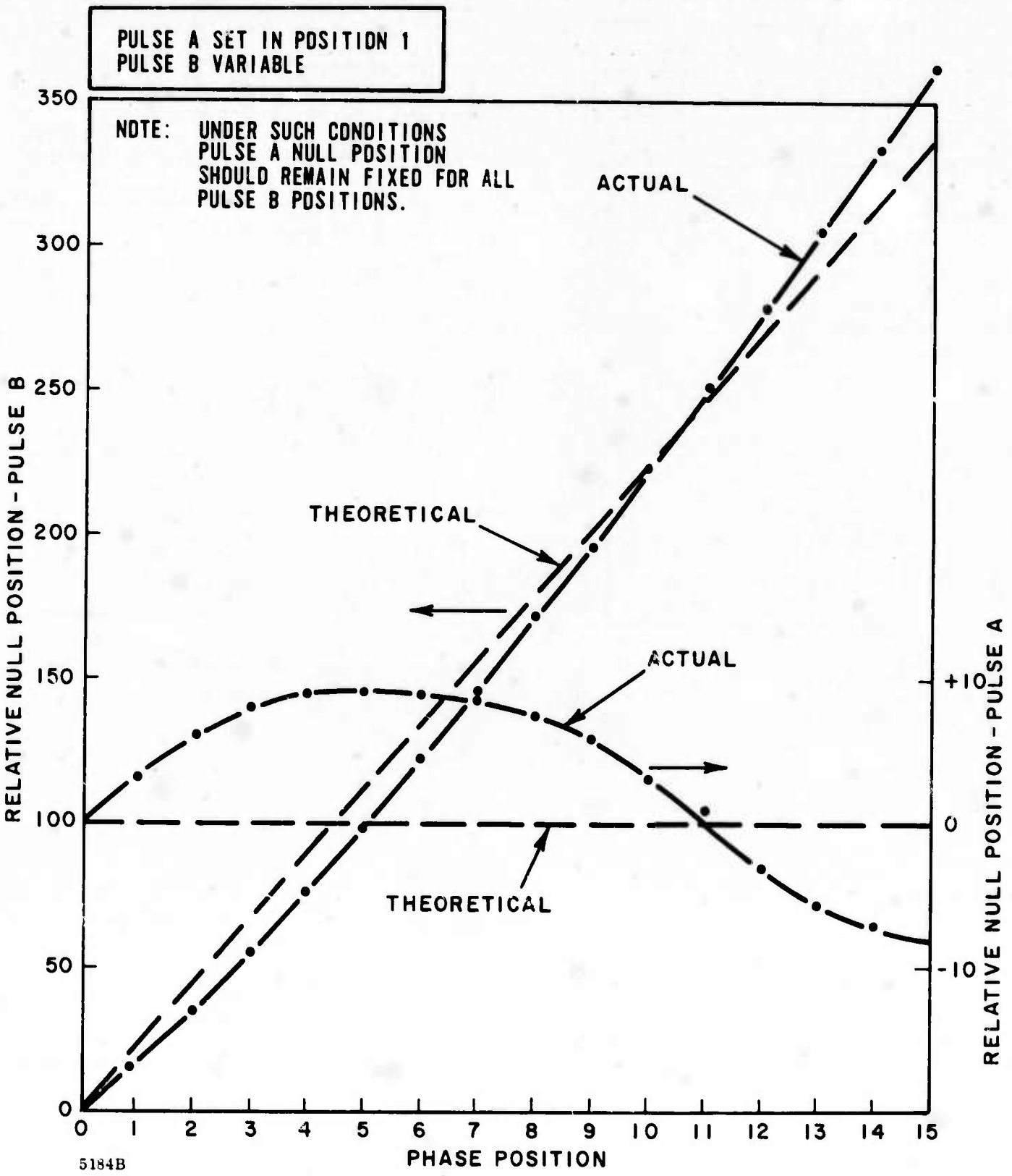

Figure 47. Relative Phase Null Position of Single Bit Phase Shifter

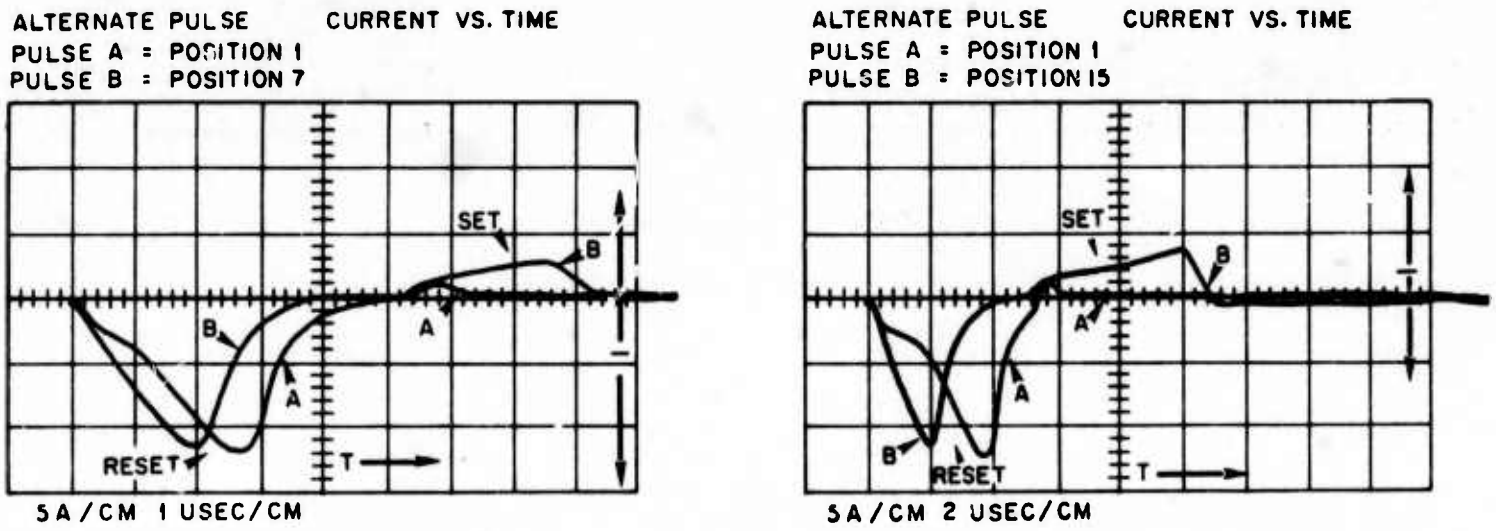

Figure 48. Typical Input Waveforms for Single Bit Phase Shifter when Cycling Between Phase Set Positions 1-7 and 1-15

Figures 49 and 50 are similar to Figures 47 and 48 except that pulse A is fixed at position 15 while B is cycled from zero to 15. Note that the error in both positions A and B becomes quite large.

The only reasonable conclusion that can be reached from the above data is that a reset current of 10 to 15 amperes peak is insufficient to remove the microwave load "memory" of its last phase position. Larger reset currents up to 60 amperes peak were used for the reset pulse and although the degree of error was reduced, the results were not satisfactory.

It can only be concluded that for typical high power garnet materials, the necessary reset current for "memory" erasure is excessive both from power consumption and switching time considerations.

6.5.2 Insertion Loss

Figure 51 illustrates insertion loss as a function of frequency for the single bit phase shifter. The loss curve is interesting for several reasons:

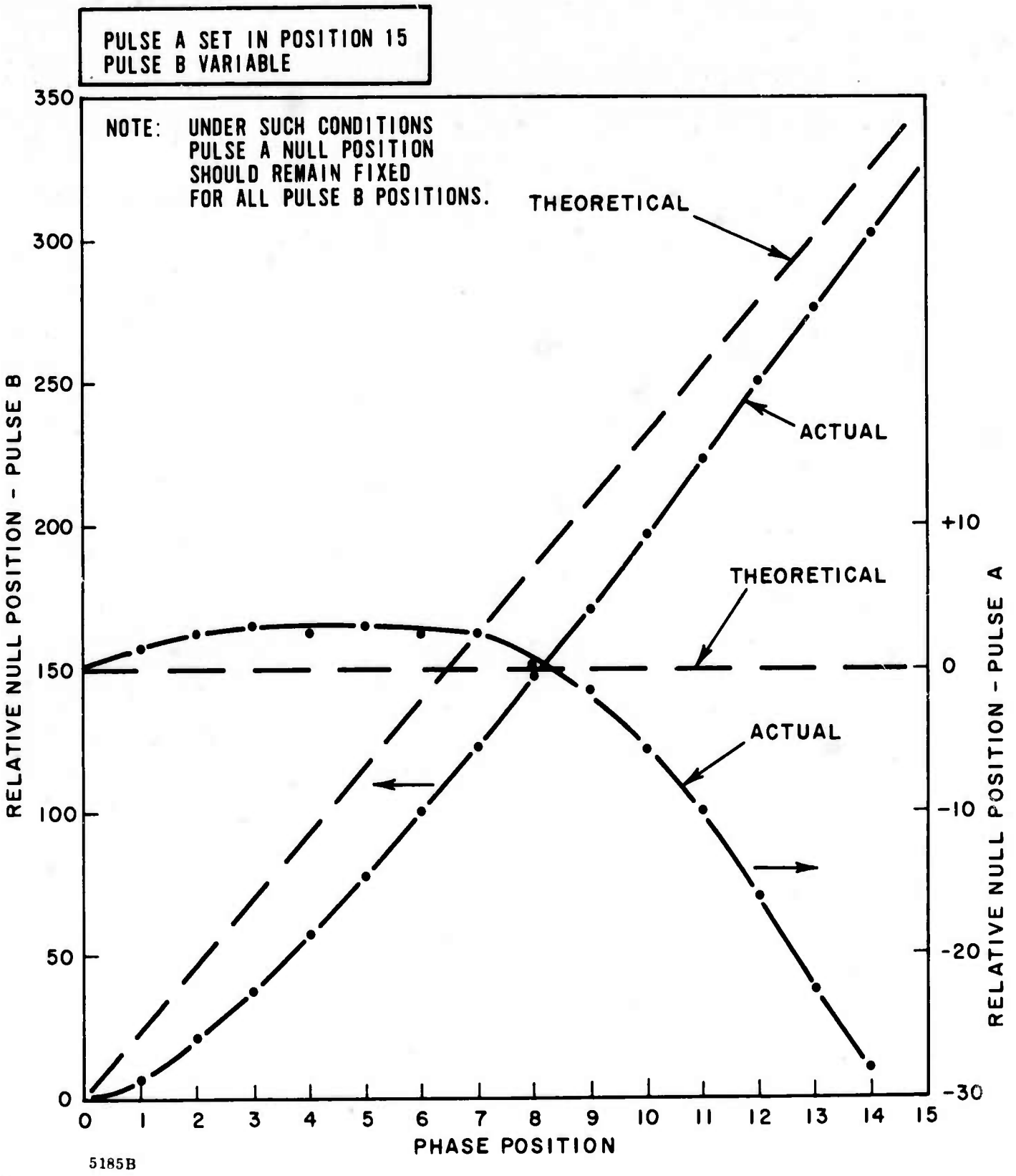

Figure 49. Relative Null Position of Single Bit Phase Shifter

ALTERNATE PULSE CURRENT VS. TIME
PULSE A = POSITION 15
PULSE B = POSITION 0

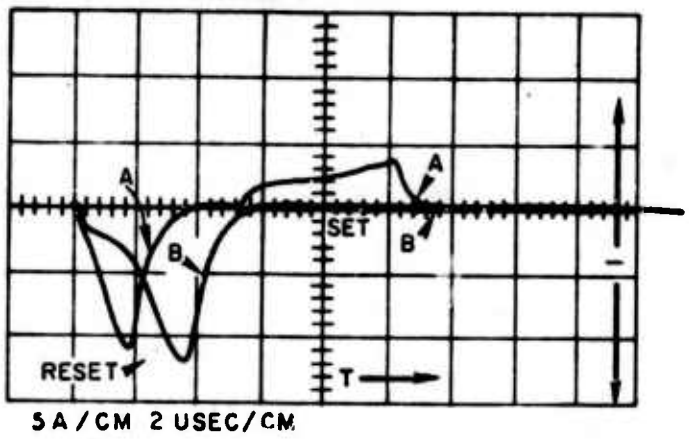

ALTERNATE PULSE CURRENT VS. TIME
PULSE A = POSITION 15
PULSE B = POSITION 6

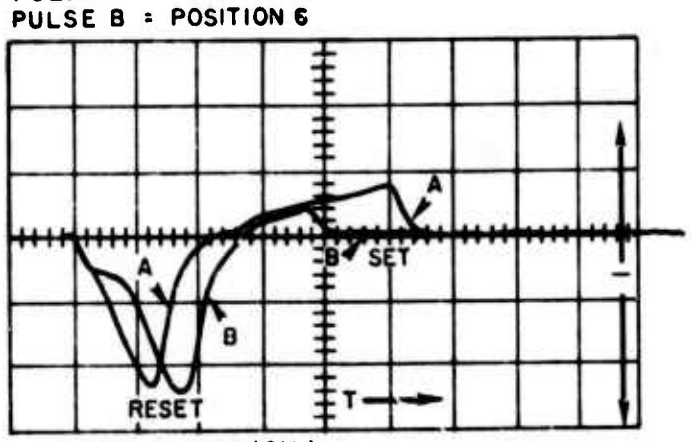

ALTERNATE PULSE CURRENT VS. TIME
PULSE A = POSITION 15
PULSE B = POSITION 14

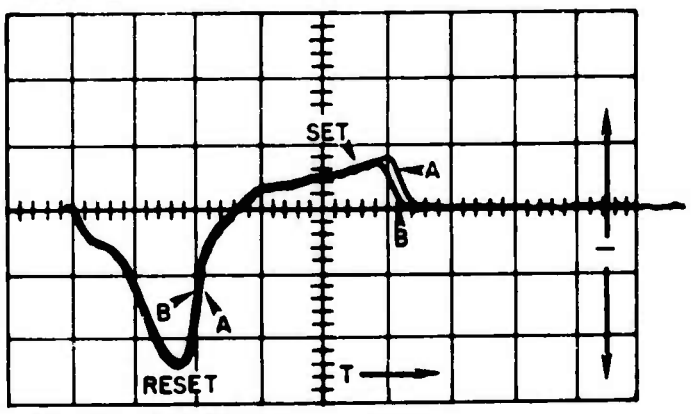

Figure 50. Typical Input Waveforms for Single Bit Phase Shifter when Cycling Between Phase Set Positions 15-0, 15-6, and 15-14

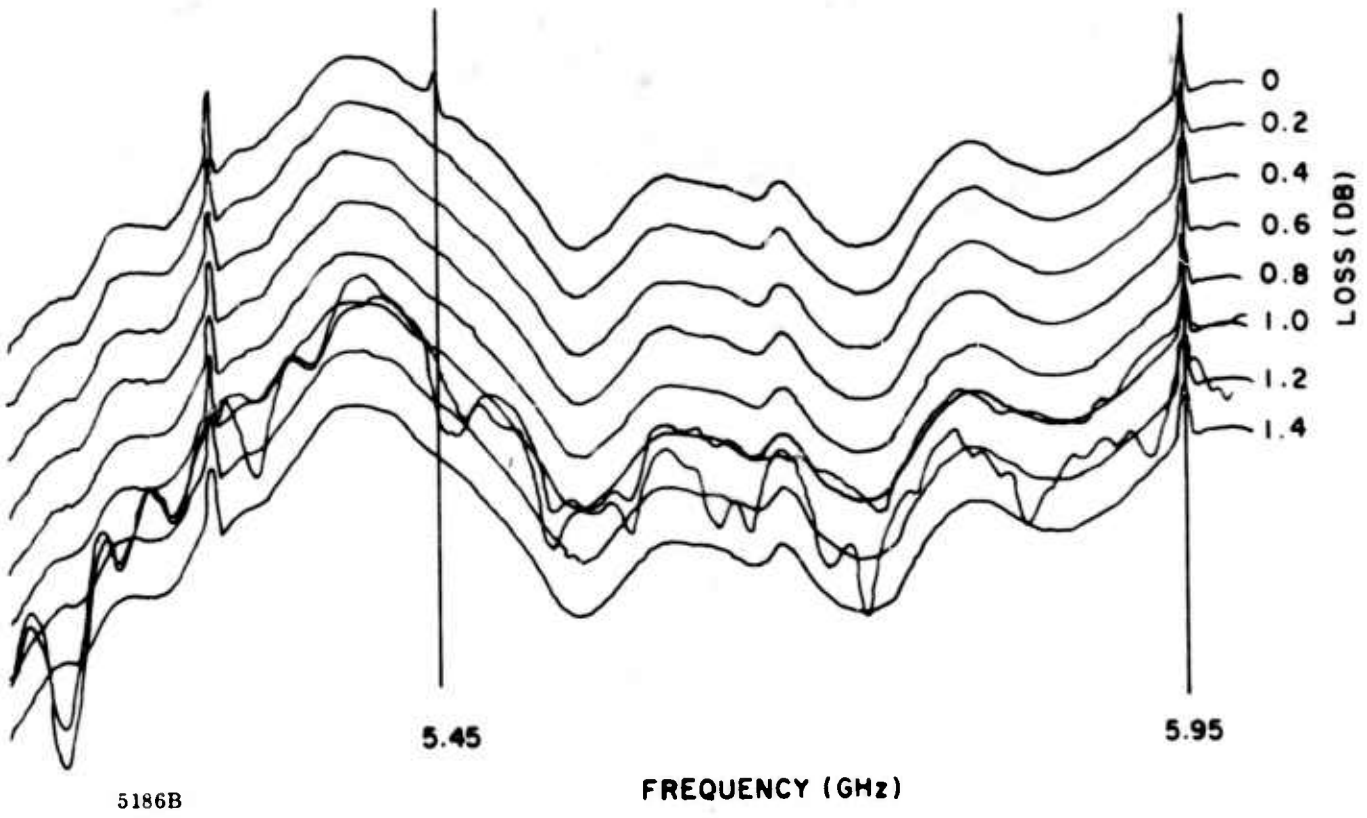

Figure 51. Loss versus Frequency - Single Bit Phase Shifter

- Average insertion loss is greater than that for the multibit unit (see Figure 38). This is a result of the increased length of toroid material required to assure adequate linearity in the $\Delta\phi$-flux response.

- There is a noticeable increase in the number of insertion loss spikes. A possible explanation for this occurrence is the charging wire. In the multibit unit, the charging wire is broken into moderate lengths for each bit whereas in the single bit unit this wire is continuous through the entire length of toroid material. This wire, along with the waveguide structure, forms a TEM structure of peculiar cross section and loading but nevertheless a TEM structure. This length coupled with the waveguide height and high loading factor yields a structure subject to moding.

7. COMPARISON OF SINGLE AND MULTIBIT PHASE SHIFTERS

7.1 GENERAL

This program has provided an excellent opportunity for direct comparison of the single and multiple bit phase shifters. Both designs developed under this program employ the same garnet material and have the same cross section. In addition, their purpose is common; that is, phase shifting at high power.

The results are not what were expected at the start of this program; in particular, the errors and difficulties encountered in attaining single bit phase shifter stability were not anticipated.

The basis for comparison is:

- Microwave performance (loss, VSWR, etc.)
- Accuracy ($\Delta\phi$, pulse control, etc.)
- Complexity
- Cost

7.2 MICROWAVE PERFORMANCE

Because of the need to assure a linear phase-flux response on the single bit phase shifter, it is in general necessary to provide a unit that possesses a saturated differential phase shift of 150% of final value. Such phase length is in excess of that necessary for a multibit unit. This increase in phase length requires an increase in physical length and an appropriate increase in insertion loss. It should be pointed out that this factor of 150% is not absolute and will depend upon the squareness of the material (β - H curve). Since low power materials with little doping usually possess square β-H loops, it can be generally concluded that this length-loss increase will be less for low power phase shifters.

The increase in loss spikes in the single bit phase shifter should not necessarily be a controlling factor. If these spikes are truly more predominant in single bit units, design changes can be incorporated into the unit to reduce their occurrence. These changes, however, may increase complexity such that the cost of each unit is essentially equal.

7.3 ACCURACY

Accuracy of the single bit phase shifter will ultimately evolve into:

- Complete material "memory" erasure after each cycle
- Trigger accuracy

7.3.1 Memory Erasure

Flux drive, when properly applied to phase shifter development, provides differential phase accuracy. It is necessary, however, to produce a fixed reference point from which to flux drive, especially since this fixed point also represents the zero phase position.

Unfortunately, there are only three stable magnetization points: the two saturation points and the demagnetized condition. Since demagnetization usually requires a time longer than 5 microseconds and also requires set drive of two polarities, it has been discarded as impractical.

Saturation implies no change in B for an increase in H, which is a point that can be only approached in practice. This is especially true for typical high power materials where it may be possible to reach 0.9 B_{sat} with a drive current of 5 amps, but 0.99 B_{sat} requires 50 amps drive.

Satisfactory "memory" erasure for high power phase shifters must therefore await the development of square B-H materials.

7.3.2 Trigger Accuracy

The method of pulse generation used on the units developed under this program and described in previous sections provides a method of individual phase shifter drive with a minimum of array interconnection. This method, however, requires extreme pulse time stabilization. Five microseconds has been divided into 337 degrees, yielding approximately 15 nanoseconds per degree. If an accuracy of ±3 degrees is desired, then it is necessary to generate a trigger pulse and produce phase shifter triggering with an accuracy of ±45 nanoseconds.

When pulse shape and amplitude along the lines of an array are considered, this accuracy is beyond practical feasibility.

It will be necessary to generate a new method of triggering a single bit phase shifter that is compatible with present technology.

It should be mentioned that a similar trigger difficulty is associated with the multibit phase shifter. At first it would appear to be four times as severe since there are four times as many bits. However, with the addition of internal (to the

driver) generation of timing pulses, input signal amplitude and shape becomes less critical. In addition, if logic is added to the driver circuit, including an I.C. counter, then the driver logic can be driven by a series of pulses the number of which determines the bit to be switched. α-β steering is then practical for a multibit phase shifter.

7.4 COMPLEXITY

By way of over-simplification, it is often assumed that the single bit phase shifter driver is only one-fourth of a four-bit multibit driver. This is not true in practice. Current levels in a single bit unit are greater for reset, and voltage stability for the set portion of the driver is of extreme importance. In addition, some form of input logic is required. It has been found that the single bit phase shifter designed under this program is only slightly less complex than its multibit counterpart. It is therfore estimated that the single bit driver is 90% as complex as an equivalent four bit driver.

The microwave structure of the single bit phase shifter could likewise be considered of reduced complexity since there are less charging wires and associated hardware. The increased length, however, requires close control of tolerances over this length. Thus, in actual practice, housing complexity is approximately equal to 90% of the multibit unit

When large quantities of phase elements are required, this overall reduction in complexity would become an important factor. However, performance must be likewise considered; as previously discussed, the microwave performance of the single bit phase shifter was definitely inferior to its multibit counterpart.

7.5 COST

Cost in general is related to complexity. However, comparison of these two designs must include further analysis.

The reduction in number of charging wires in the single bit unit is offset by the increase in length and therefore an increase in machining surfaces. In addition, the length increase is confined to the toroid area which creates an increase in grinding and new ferrite (garnet) material costs.

If one were to consider overall costs including grinding and toroid material, the cost of the single bit phase shifter is greater than that for the multibit equivalent. Again, applying relative numbers, the single unit is approximately 10% more costly

than its single bit equivalent.

A similar experience is found in relative driver cost. Although the multibit unit is more complex, the cost of individual parts is less (lower currents, etc. are required). When one includes cost of component installation, overall driver cost is essentially equivalent, especially if similar driver-array mounting techniques are employed.

Again, microwave performance appears to be the controlling factor.

7.6 SUMMARY

For convenience, a table is given below summarizing the above discussions

Category	Single Bit	Multibit
Microwave Performance	1.2 db loss	0.9 db loss
	Other parameters essentially equal	Other parameters essentially equal
Accuracy	Poor phase accuracy	Moderate to excellent phase accuracy
	Requires accurate input pulse control or more complex logic circuitry	Simple array wiring if logic is employed
Complexity	Approximately 10% less complex than multibit	- - -
Cost	Approximately equivalent	Approximately equivalent

It can be seen that the limiting item is phase accuracy which was poor on the single bit unit. This comment does not imply that future development will not improve this characteristic, but at present it is definitely inferior to its multibit counterpart.

8. CONCLUSIONS AND RECOMMENDATIONS

8.1 CONCLUSIONS

The following conclusions can be drawn from the results of this program:

- A practical phase shifter can be constructed that will handle 100 KW peak, 1000 watts average, 100 microseconds pulse width.
- Such a unit requires precision machining with careful assembly and is, therefore, a moderately expensive device.
- For reasons of electronic drive, a YIG material is practical whereas a CVB material is not.
- The YIG material, however, requires close temperature stabilization to prevent excessive effects due to magnetostriction.
- The multibit phase shifter is a practical device that can be adapted to array requirements.
- At its present state of development, the single bit device does not possess sufficient accuracy to be employed in array systems.

8.2 RECOMMENDATIONS

- Further development of a practical single bit phase shifter with emphasis on phase accuracy and input signal accuracy is indicated.
- The multibit phase shifter developed under this program should be adapted to a specific array configuration. This adaptation requires studies in related areas, including methods of feed, water cooling, array spacing and drive mounting.
- Further development of CVB materials is indicated with emphasis on reduction in coercive field, H_c.
- Improvement in the square loop properties of YIG materials for single bit phase shifters indicates a need for further development of such materials.

APPENDIX

SCHEMATIC DIAGRAM, SINGLE BIT
PHASE SHIFT DRIVER

LOGIC DIAGRAM, PULSE GENERATOR
SINGLE BIT PHASE SHIFTER

A

P1

αIN 6

3

4

5

6

A1A

1

C1
33

-5V

R1
10K

βIN 5

9

10

11

12

A1B

13

C8
33

-5V

R15
10K

A5A

9

10

11

12

13

RESET IN 1

2

3

4

5

6

A5B

1

C12
33

-5V

R22
10K

B

R2
1.5K

R1
10K

A2A

C2
33

-5V

R3
10K

R4
1.5K

A3A

C3
22

R6
5K

R5
1K

R7
3K

R16
1.5K

R15
10K

A2B

C9
33

-5V

R17
10K

R18
1.5K

A3B

C10
22

R20
5K

R19
1K

R21
3.9K

R23
1.5K

R22
10K

A7A

C13
680

R24
3K

+5V

A4

9

1
2
3
4
5

6

10

C4
200

11
12
13

8

7

Q1
2N2222

+30V

C5
100UF

R8
1K

C6
100

R9
150

R12
200

CR1
IN3064

C11
200

+5V

A8

9

1
2
3
4

5

8

C14
.1UF

C15
560

R25
470

Q5
2N1132

R26
470

R2
1.3

D

R10
10

C7
100UF
+

R9
150

R8
K

Q2
2N132

C6
00

R11
120

Q3
2N1613

R12
00

Q4
2N3445

R13
1K

R14
220

P2
1
2
5
6
TO MICROWAVE LOAD

CR1
IN3064

R36
.27

Q5
2N1132

R27
1.3K

Q6
2N1613

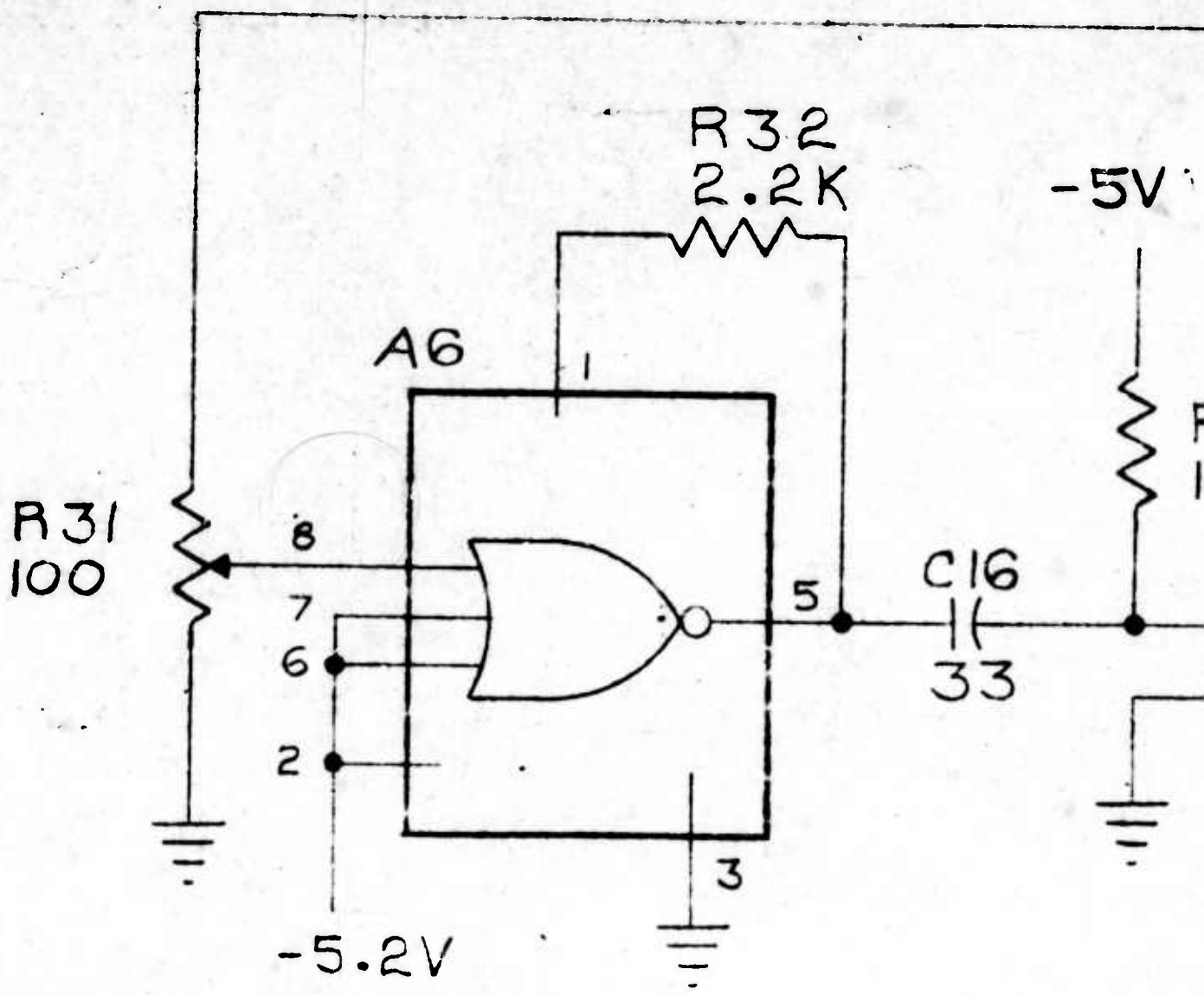
R32
2.2K
-5V
A6
1
R31
100
8
7
6
2
5
C16
33
3
-5.2V

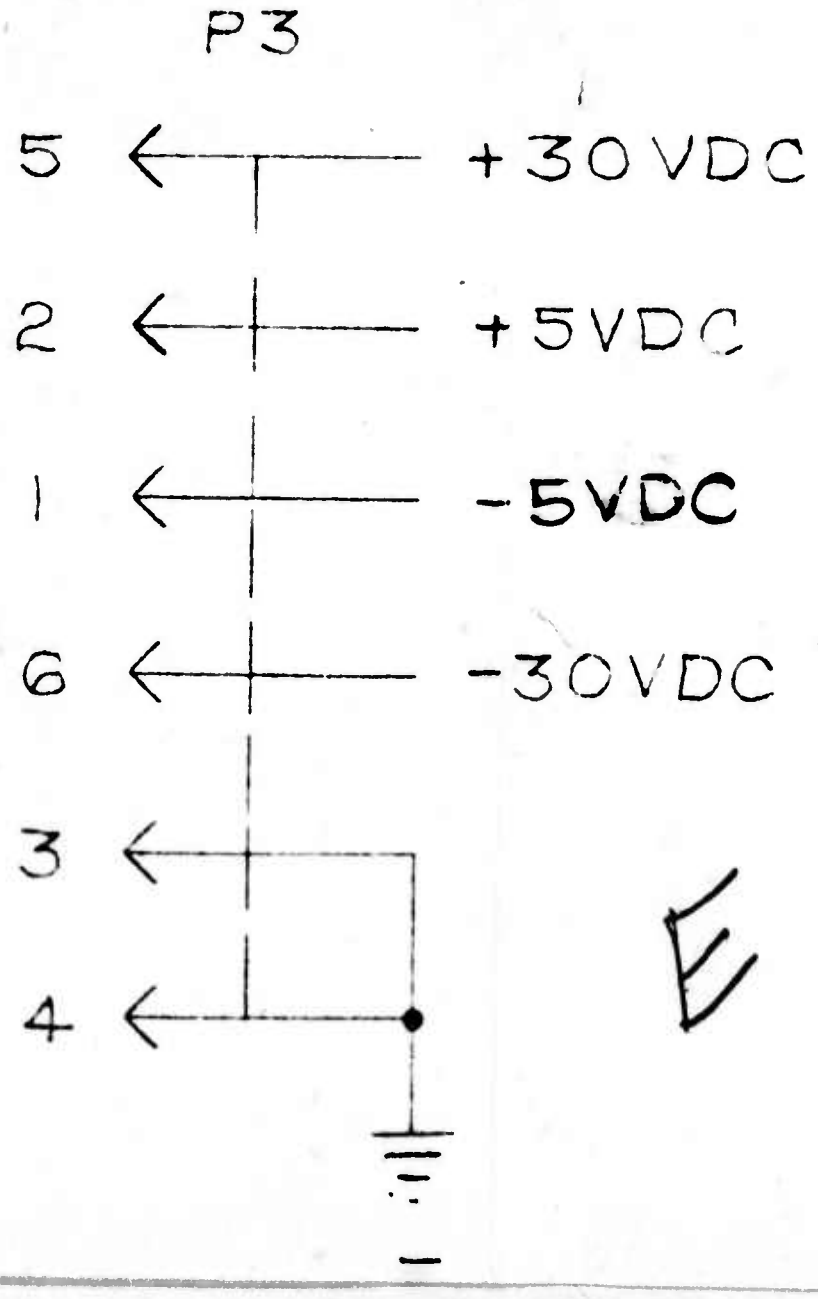
P3
5
+30VDC
2
+5VDC
1
-5VDC
6
-30VDC
3
4

E

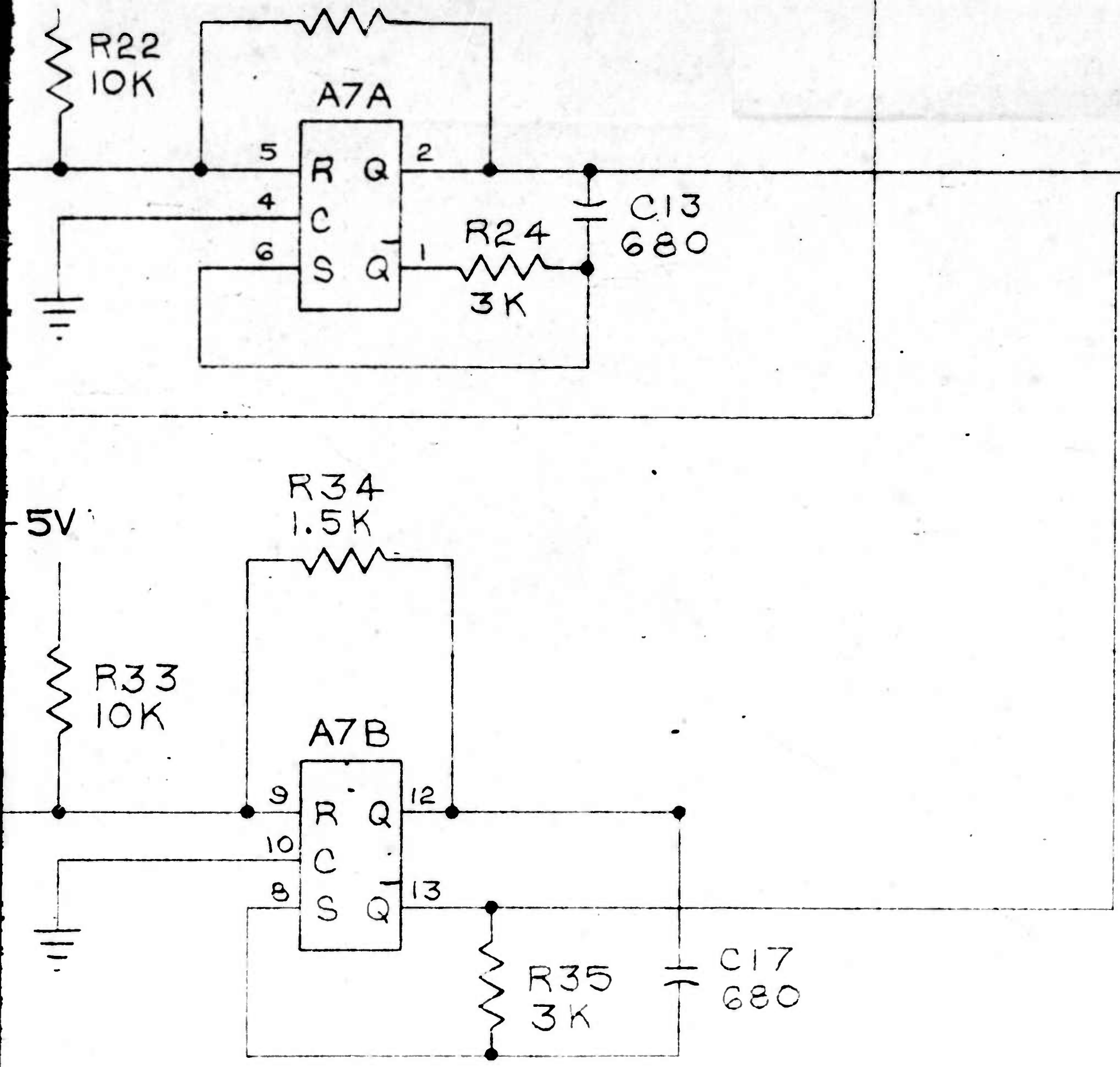
R22
10K
A7A
5
R
Q
2
4
C
6
S
Q
1
R24
3K
C13
680
-5V
R34
1.5K
R33
10K
A7B
9
R
Q
12
10
C
8
S
Q
13
R35
3K
C17
680

F

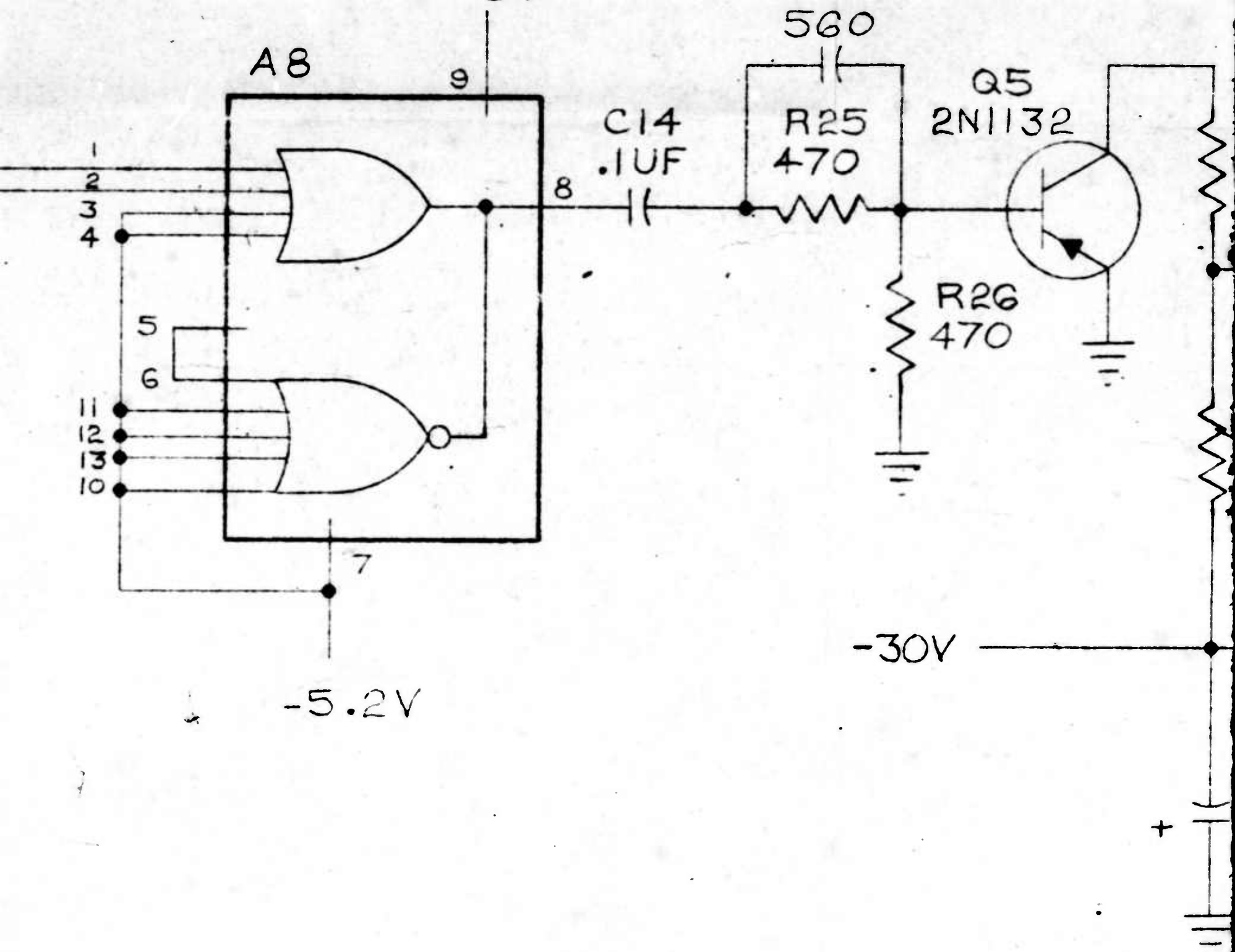

NOTES:

1. UNLESS OTHERWISE SPECIFIED
   CONNECTED TO A1-8, A4-9,
   GROUND IS CONNECTED TO
   -5.2 V IS CONNECTED TO
2. RESISTANCE VALUES ARE
3. CAPACITANCE VALUES AR

SCHEMATIC

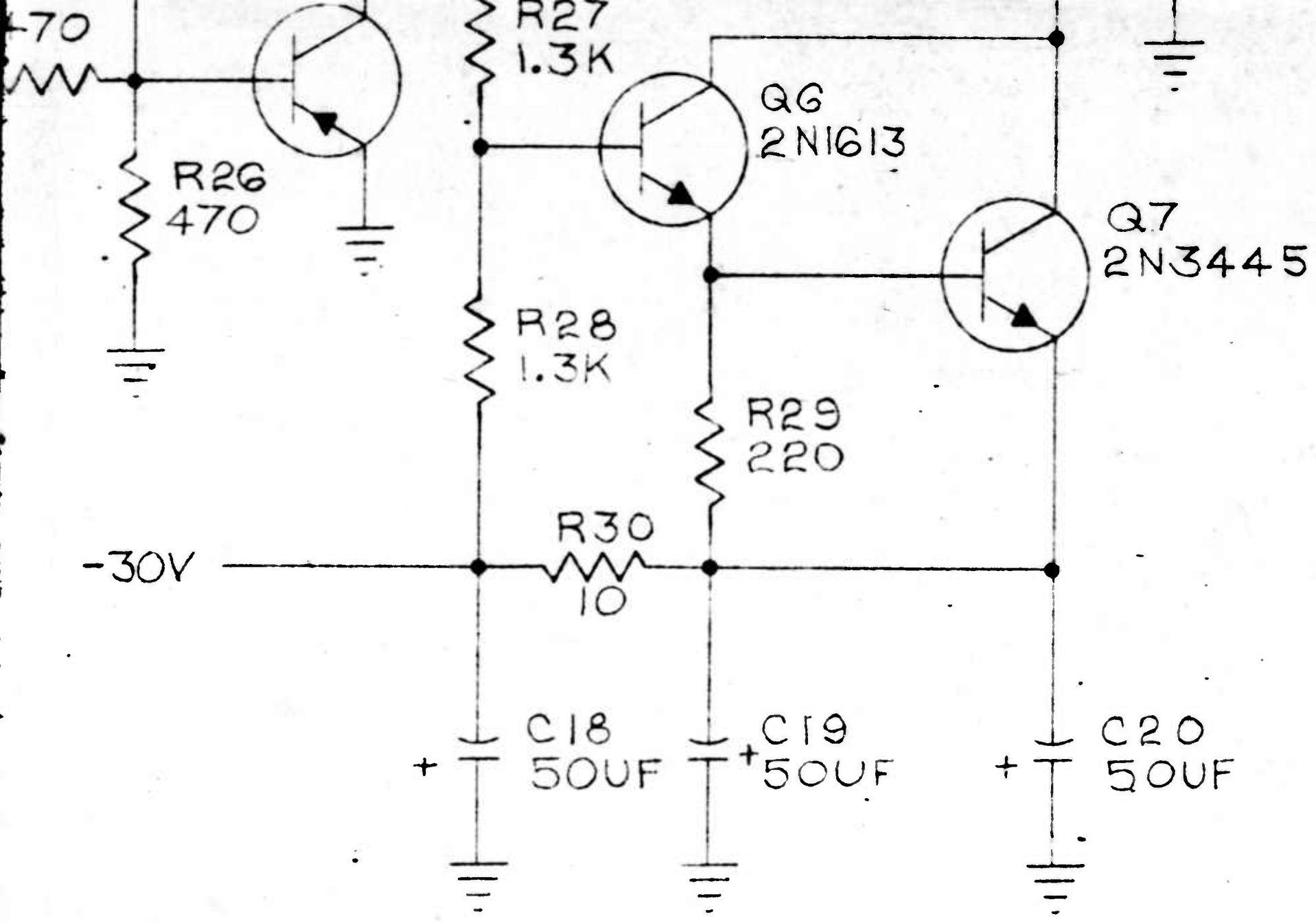

S OTHERWISE SPECIFIED +5V IS
ECTED TO A1-8, A4-9, A5-8, A8-9.
ND IS CONNECTED TO A1, A2, A3, A4, A5, A7, A8 PIN 14.
IS CONNECTED TO A1, A2, A3, A5, A7, PIN 7.
TANCE VALUES ARE IN OHMS.
CITANCE VALUES ARE IN PICOFARADS.

H

SCHEMATIC DIAGRAM
SINGLE BIT PHASE SHIFTER DRIVER

CLOCK

A

39

9 R Q 12
10 1/2MC C 1014P
8 S Q̄ 13

2K

2K

2K

39

TRIGGER

+ 200UF

SINGLE PULSE

1.5K

0.47UF

0.02UF

5 R Q 2
4 1/2MC C 1014P
6 S Q̄ 1

1 2 1/3MC 3 1007P

GRD

33

2.7K

10K

-5 V

25UF + 15V

3UF + 15V

1.5K

TO PIN 7 ON ALL INT CKTS

+5 V

0.047UF

0.02UF

INT

EXT

TRIGGER SELECT

TO PIN 14 ON ALL INT CKTS

α DELAY CIRCUIT

1.5K

4 5 1/4MC 1010P 6

33

9 R Q 12
10 1/2MC C 1014P
8 S Q 13

NORMAL

3K

1000

DELAYED α

0 1 2 3 4 5 6

B

CLOCKED COUNTER

1

2K

K

5

6 1/3MC 1007P 9

1/4MC 1010P 11 12

A

11

12 1/3MC 1007P 10 6,8

13

J A 13

MC

C

1013P

K A 1

B

5

J B 13

6,8 MC

C

10 1013P 1

K B

1/3MC 1007P 4

6 S Q 1

4 1/2MC

C

5 1014P 2

R Q

6 S

4 1/2MC

5 1014P 2

R Q

RIGGER

SELECT

13 12 11 10 4 3 2 1 13 12

1/2MC 1004P

1/2MC 1004P

1/2M 1004

8

6

8

1

UNTER

C

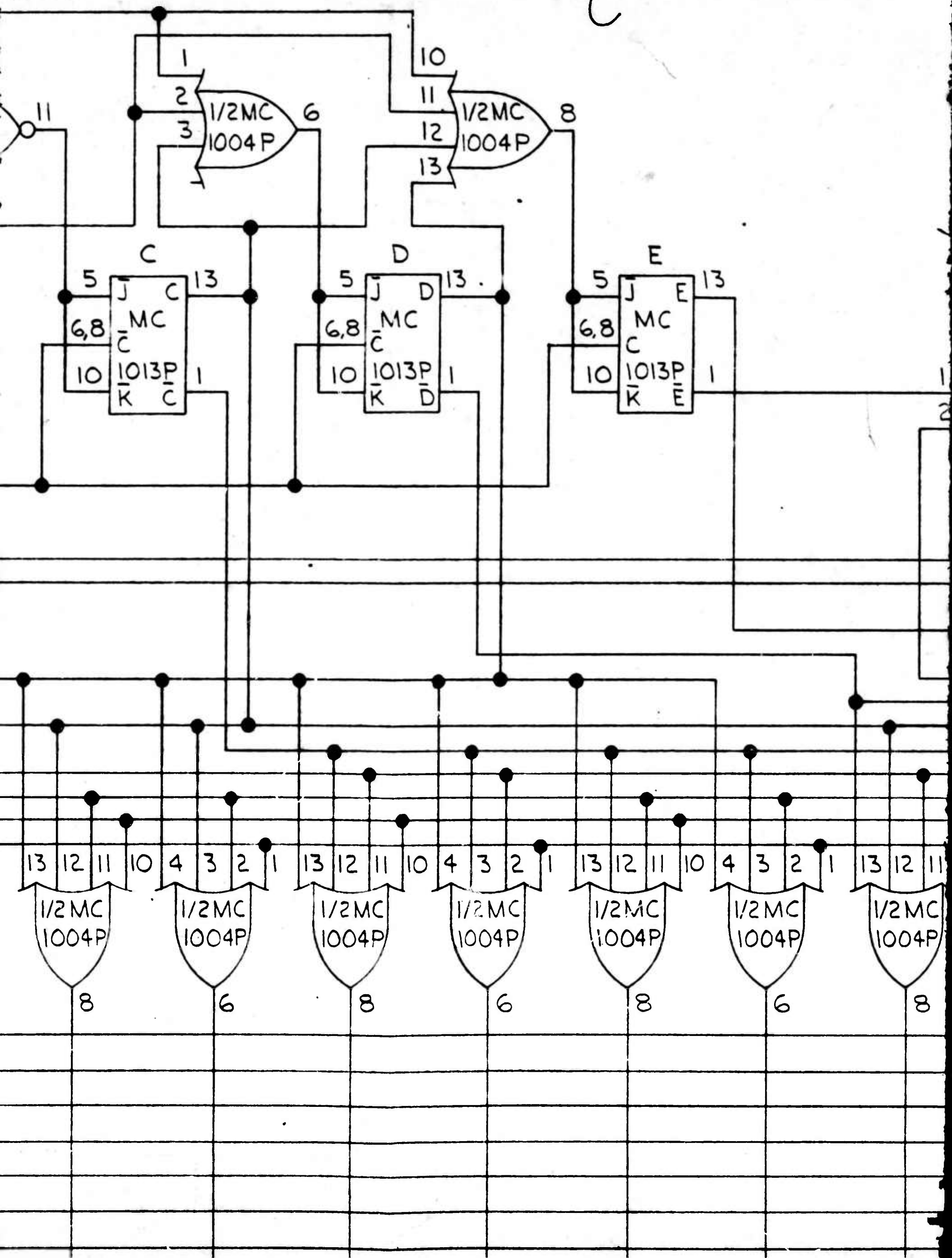
11
1
2
3
1/2MC
1004P
6
10
11
12
13
1/2MC
1004P
8
C
D
E
5
J
C
13
6,8
MC
C
10
1013P
K
C
1
5
J
D
13
6,8
MC
C
10
1013P
K
D
1
5
J
E
13
6,8
MC
C
10
1013P
K
E
1
13 12 11 10 4 3 2 1
1/2MC
1004P
8
6
8
6
8
6
8

1

D

25UF
15V
+

51
1W

2N2222

100

9

11 MC
1018P

5 4

1 1/4 MC
2 1010P
3

1 MC
2 1018P
8

5 6

12 11 10 4 3 2 1 13 12 11 10 4 3 2 1 13 12 11 10 4 3 2 1 13 12 11 10

1/2MC
1004P

8 6 8 6 8 6 8

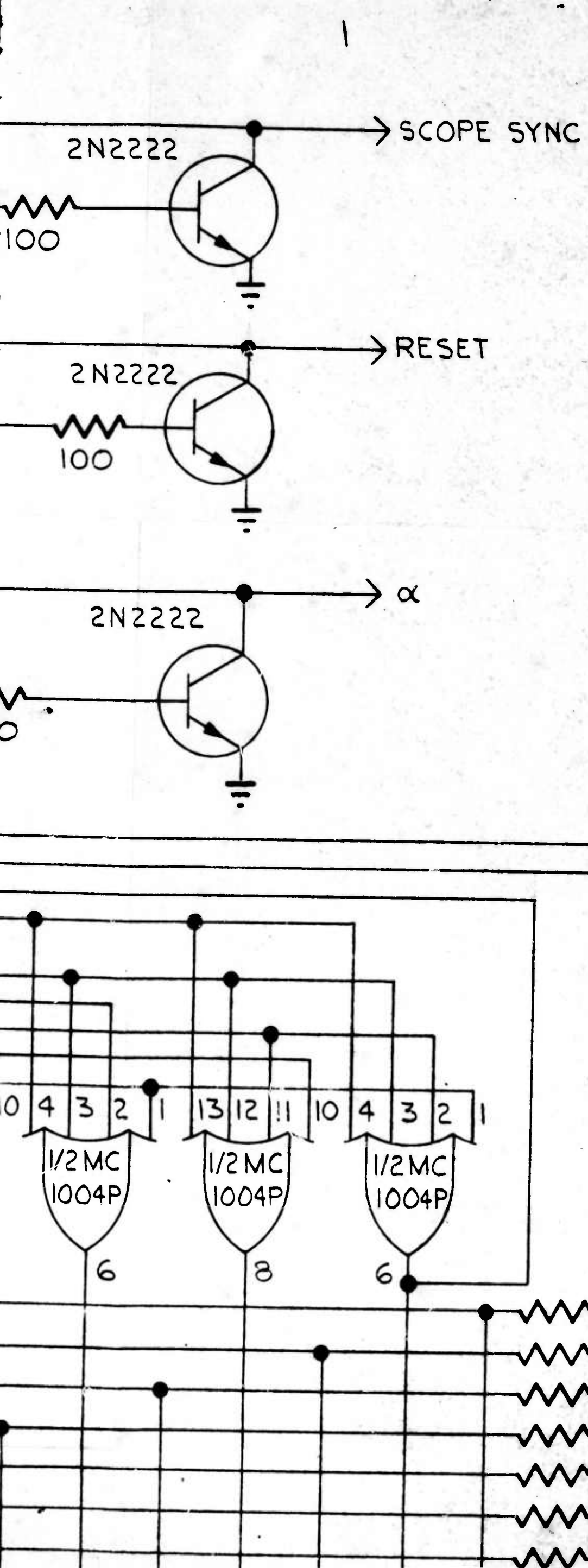
SCOPE SYNC
2N2222
100
RESET
2N2222
100
α
2N2222
1/2 MC
1004P
1/2 MC
1004P
1/2 MC
1004P
6.8K
6.8K
6.8K
6.8K
6.8K
6.8K

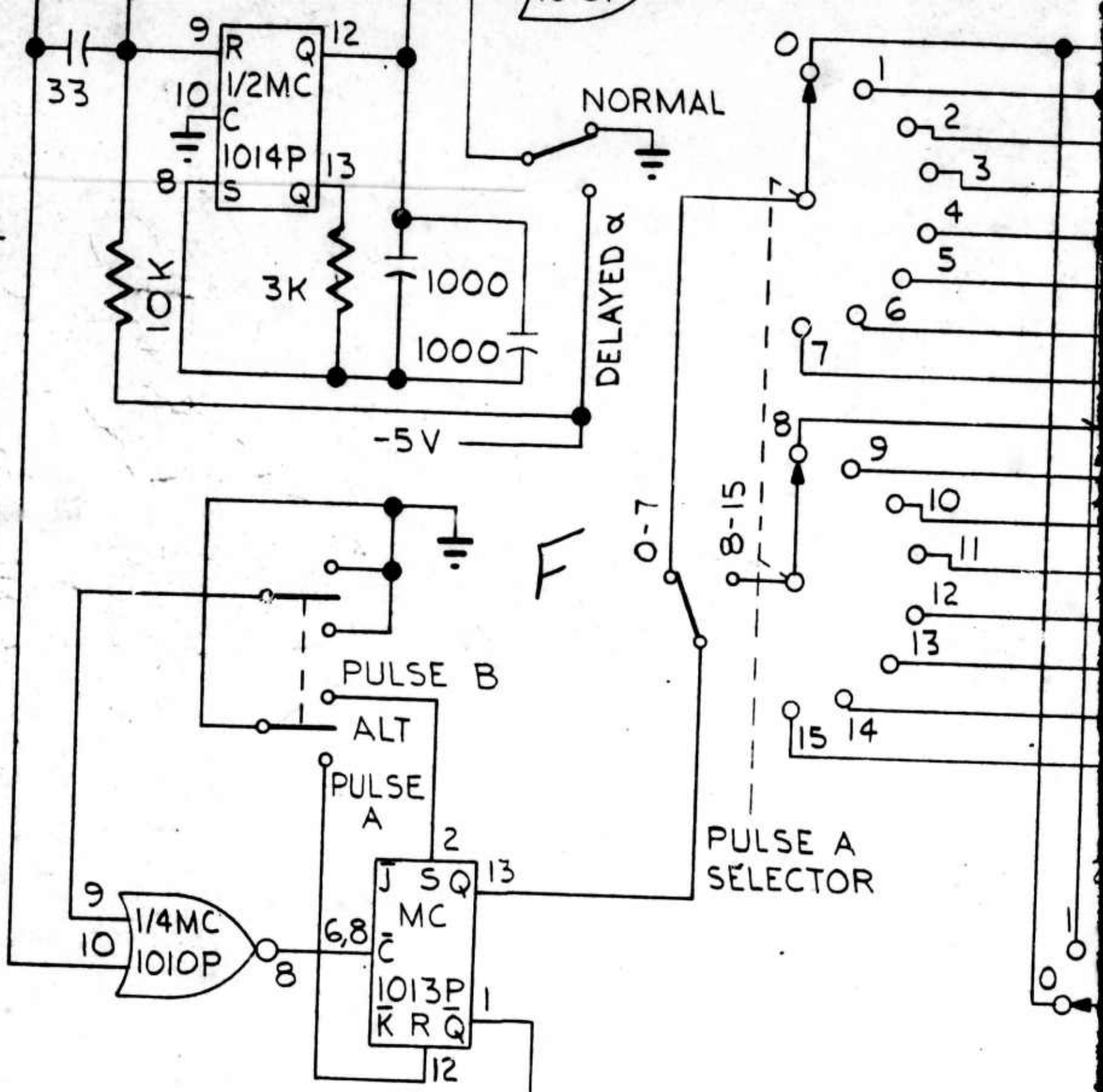

NOTES:

1. UNLESS OTHERWISE SPECIFIED; RESISTANCE VALUES ARE IN OHMS. CAPACITANCE VALUES ARE IN PICOFARADS.
2. PIN 14 ON ALL INT CKTS ARE CONNECTED TO GRD.
3. PULSE WIDTH MAY BE CHANGED BY ADJUSTING THE 2K POTS IN THE CLOCK CIRCUIT.
4. PRF MAY BE ADJUSTED BY CHANGING THE .047UF CAPACITORS IN THE TRIGGER CIRCUIT.
5. ALL RESISTORS ARE 1/4 WATT EXCEPT AS NOTED.
6. APPROXIMATE CURRENT REQUIREMENTS: +5V, 400MA; -5V, 6
7. PIN 7 ON ALL INT CKTS ARE CONNECTED TO -5 V.
8. THE α DELAY MAY BE ADJUSTED BY CHANGING THE TWO 1000 CAPACITORS IN THE DELAY CIRCUIT.
9. ACTIVE COMPONENTS: 11 - MC1004 6 - MC1013 4 - 2N
   6 - MC1007 3 - MC1014

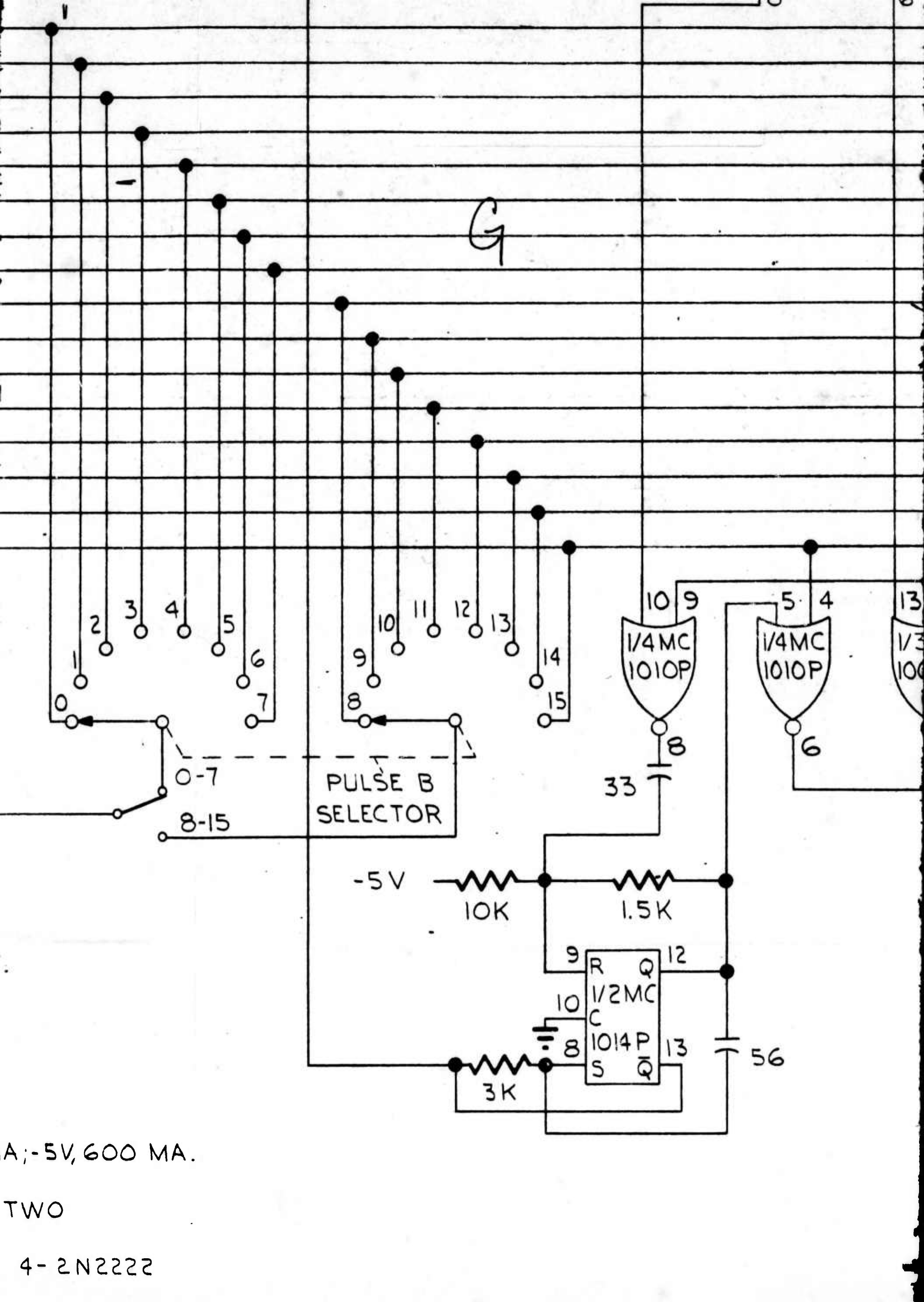

A;-5V, 600 MA.

TWO

4-2N2222

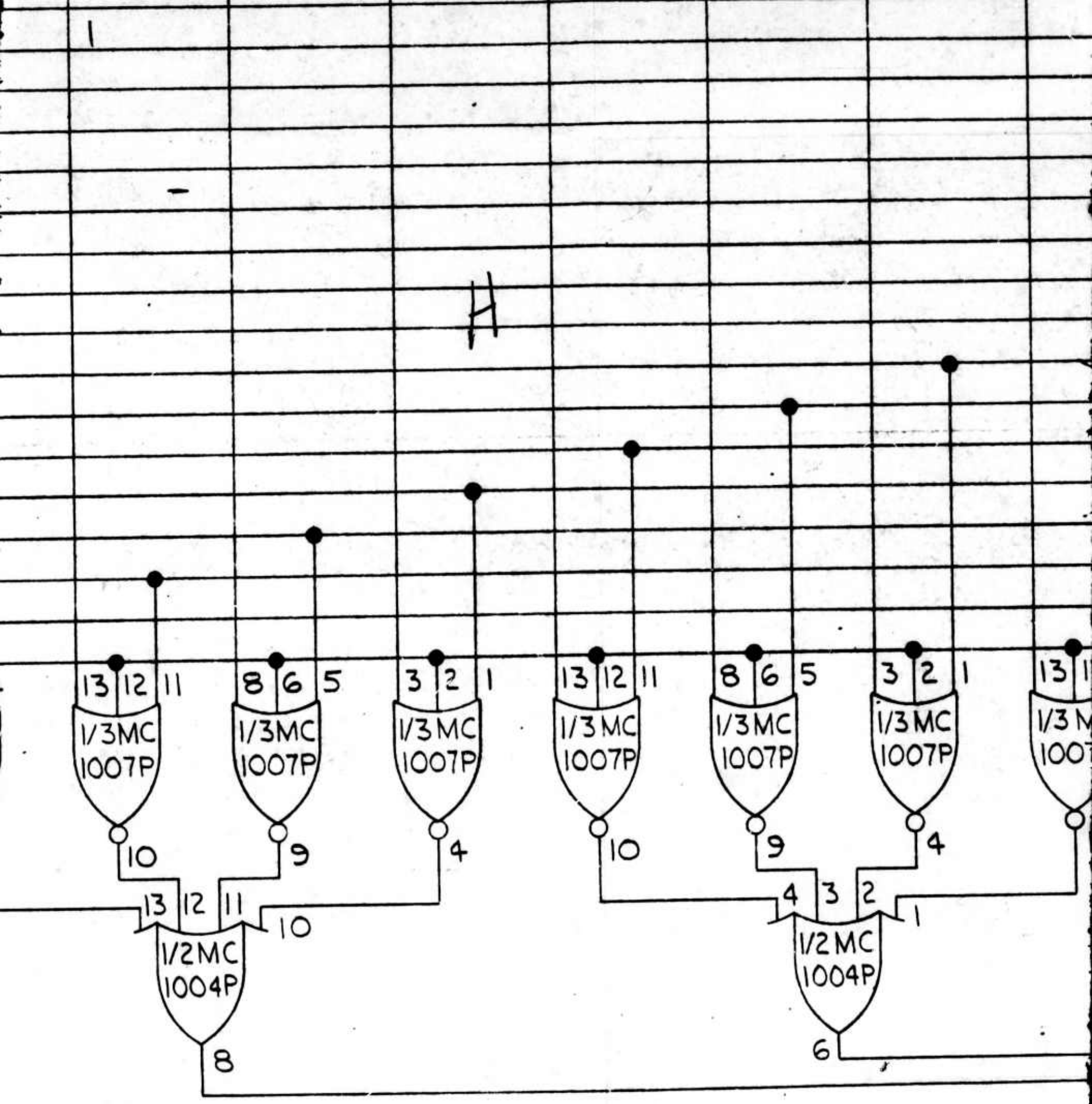
13 12 11
1/3MC 1007P
8 6 5
1/3MC 1007P
3 2 1
1/3MC 1007P
13 12 11
1/3MC 1007P
8 6 5
1/3MC 1007P
3 2 1
1/3MC 1007P
10
9
4
13 12 11
10
1/2MC 1004P
8
10
9
4
4 3 2
1
1/2MC 1004P
6

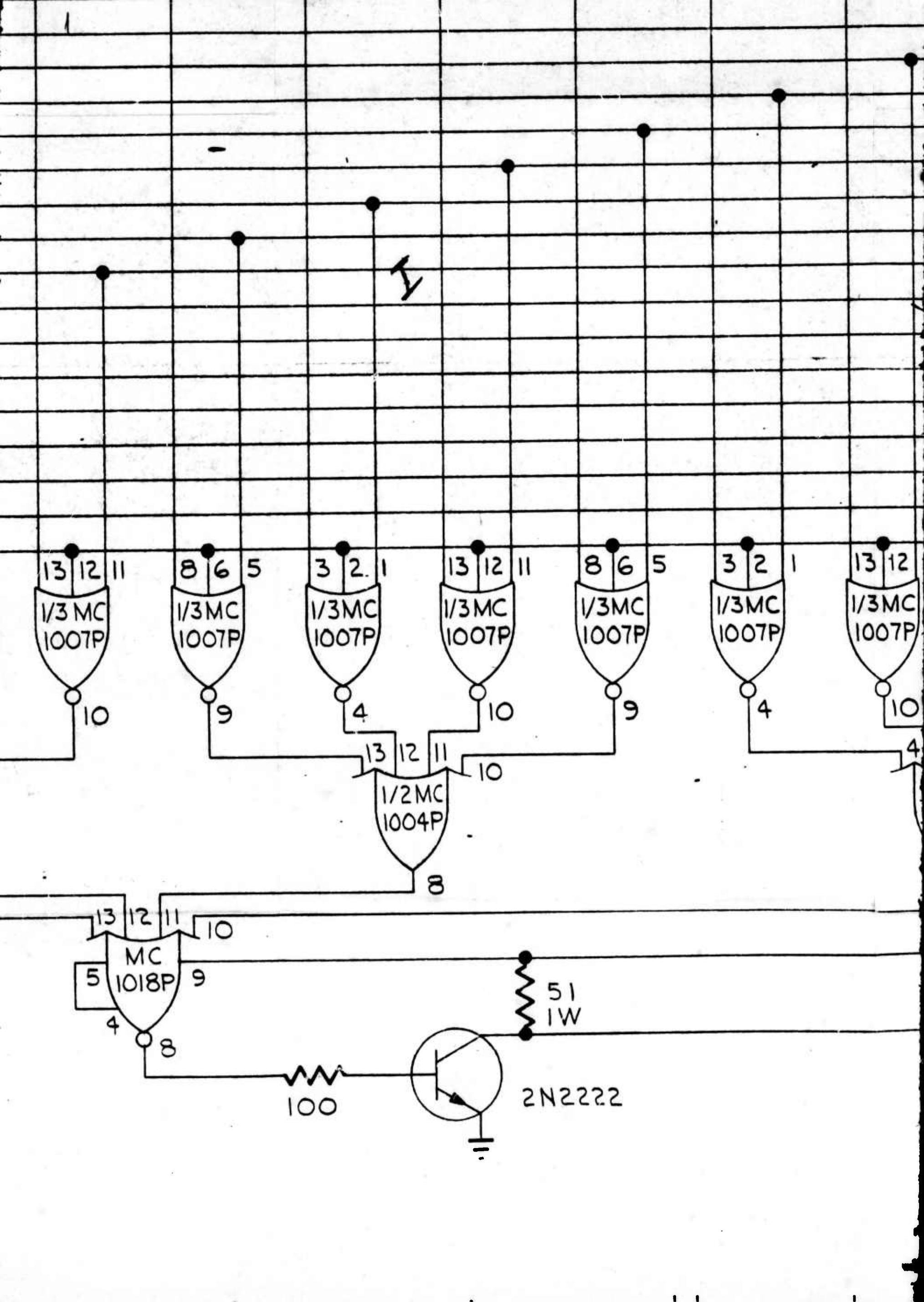
13 12 11
1/3 MC 1007P
10
8 6 5
1/3MC 1007P
9
3 2. 1
1/3MC 1007P
4
13 12 11
1/3MC 1007P
10
8 6 5
1/3MC 1007P
9
3 2 1
1/3MC 1007P
4
13 12
1/3MC 1007P
10
13 12 11
1/2MC 1004P
10
8
13 12 11
MC 1018P
10
5
9
4
8
51 1W
100
2N2222

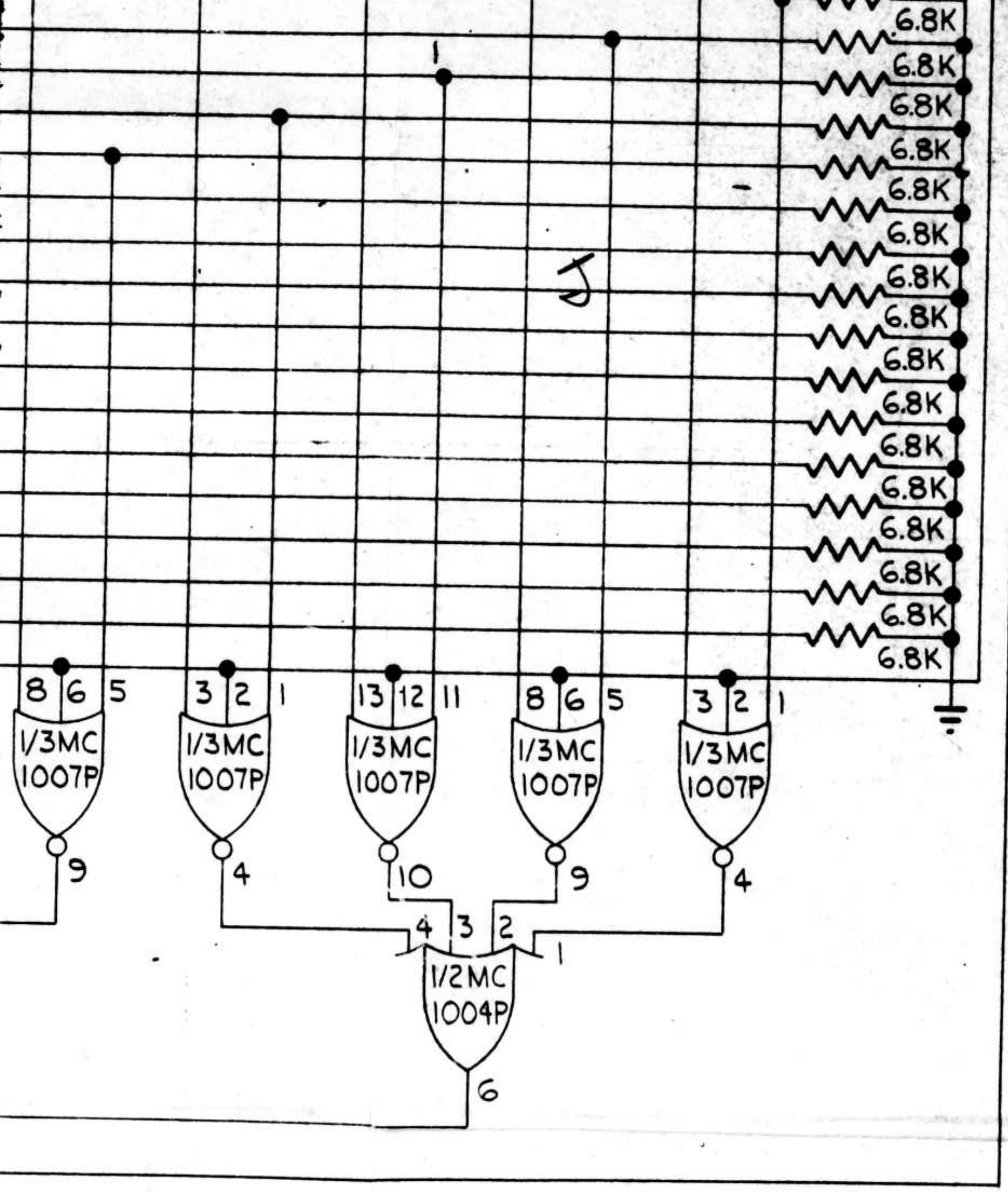

B

222

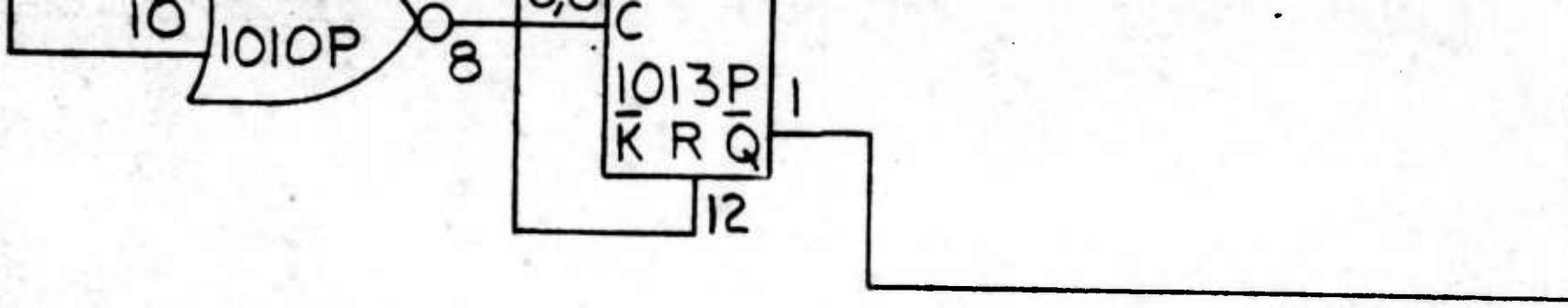

NOTES:

1. UNLESS OTHERWISE SPECIFIED; RESISTANCE VALUES ARE IN OHMS. CAPACITANCE VALUES ARE IN PICOFARADS.
2. PIN 14 ON ALL INT CKTS ARE CONNECTED TO GRD.
3. PULSE WIDTH MAY BE CHANGED BY ADJUSTING THE 2K POTS IN THE CLOCK CIRCUIT.
4. PRF MAY BE ADJUSTED BY CHANGING THE .047UF CAPACITORS IN THE TRIGGER CIRCUIT.
5. ALL RESISTORS ARE 1/4 WATT EXCEPT AS NOTED.
6. APPROXIMATE CURRENT REQUIREMENTS: +5 V, 400MA
7. PIN 7 ON ALL INT CKTS ARE CONNECTED TO -5 V.
8. THE α DELAY MAY BE ADJUSTED BY CHANGING THE 1000 CAPACITORS IN THE DELAY CIRCUIT.
9. ACTIVE COMPONENTS:

11 - MC1004	6 - MC1013
6 - MC1007	3 - MC1014
2 - MC1010	3 - MC1018

10.

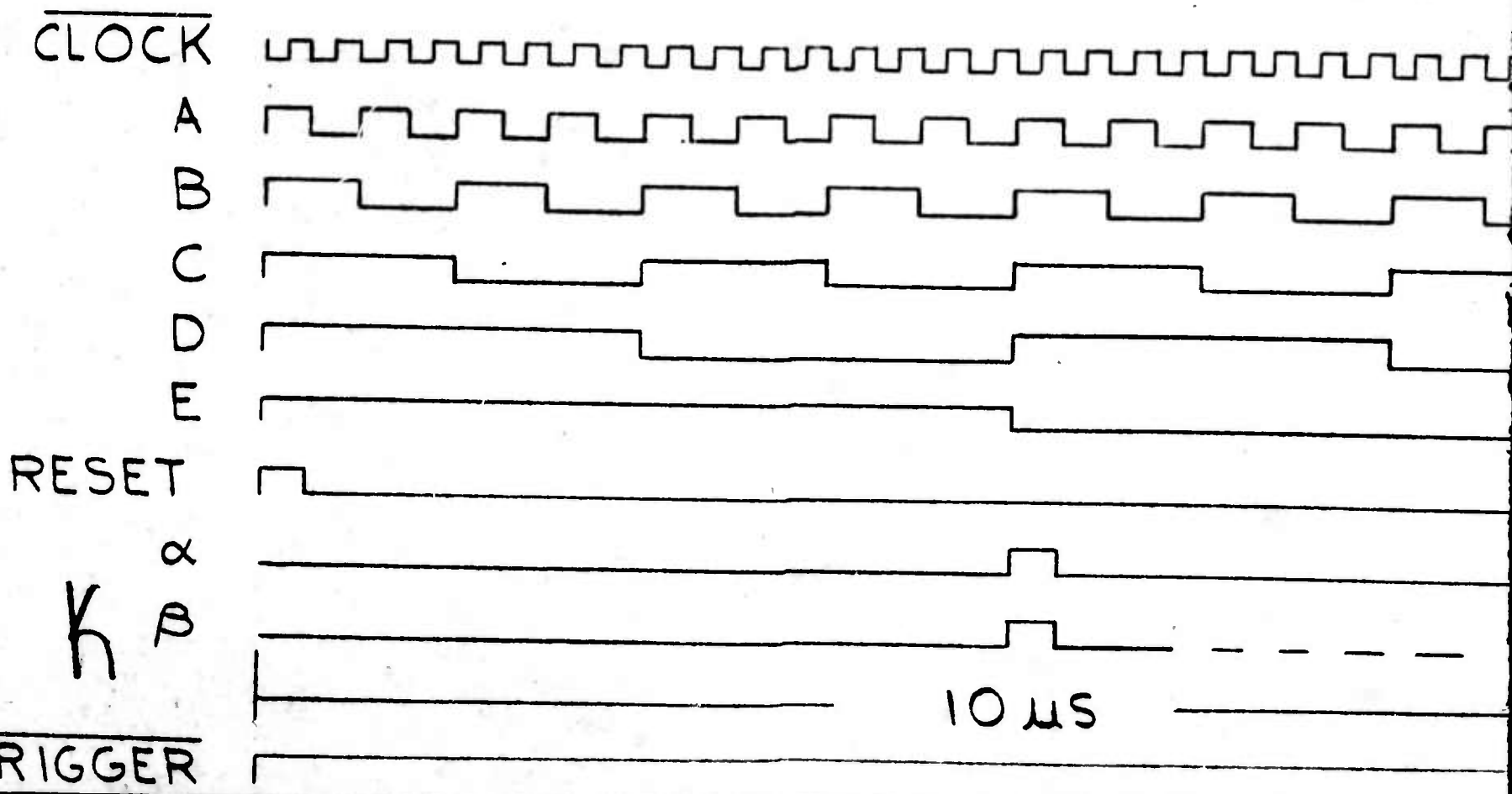

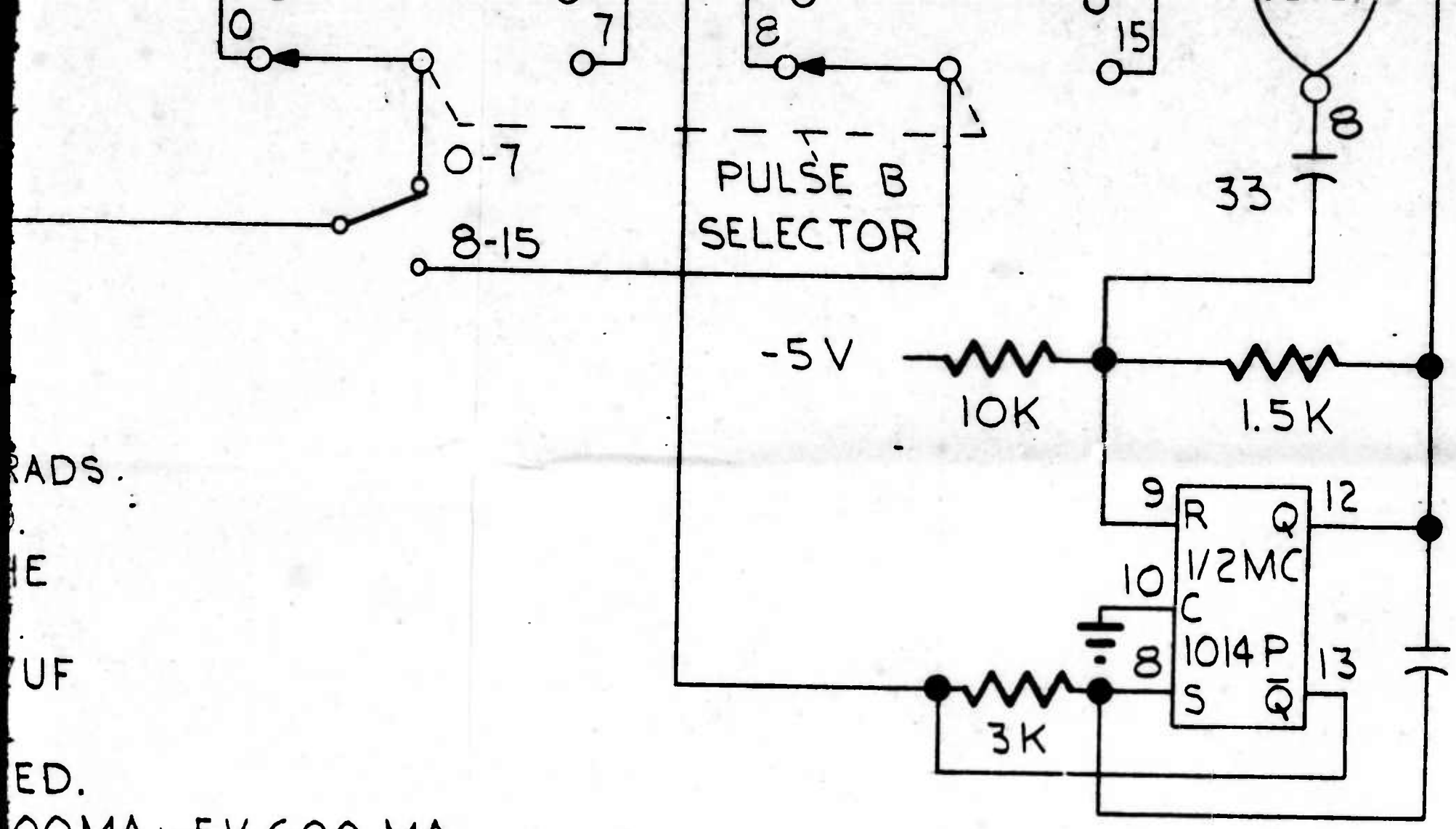

RADS.

.

HE

.

UF

ED.

OOMA; -5V, 600 MA.

V.

THE TWO

013 4-2N2222

014

018

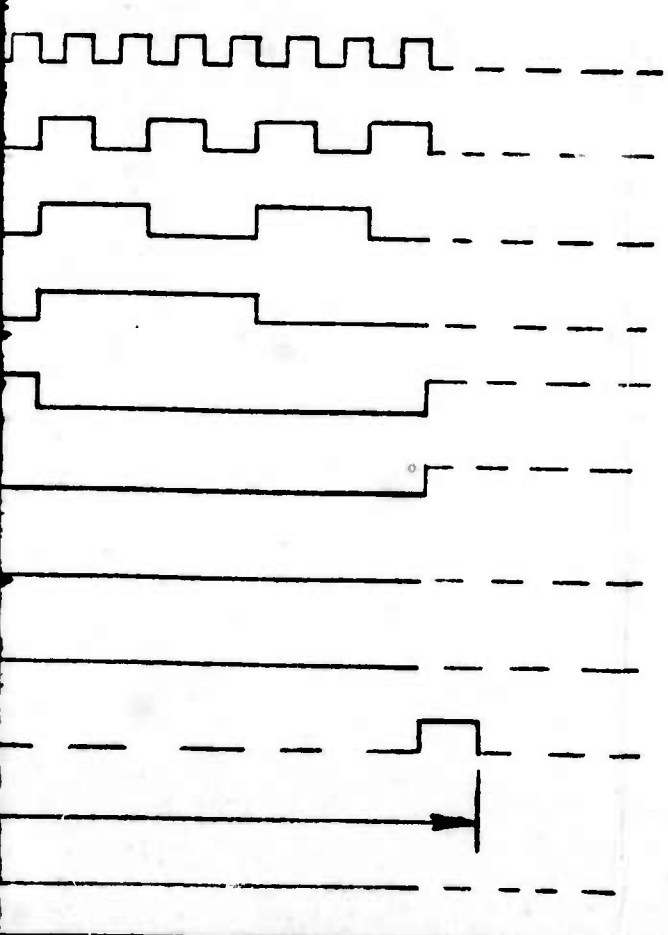

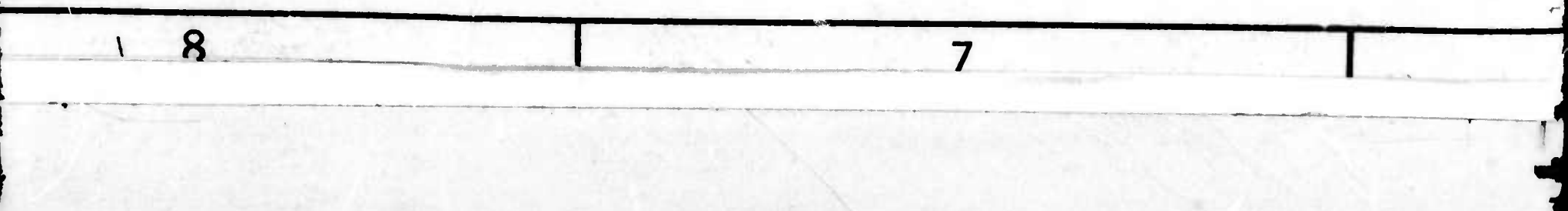

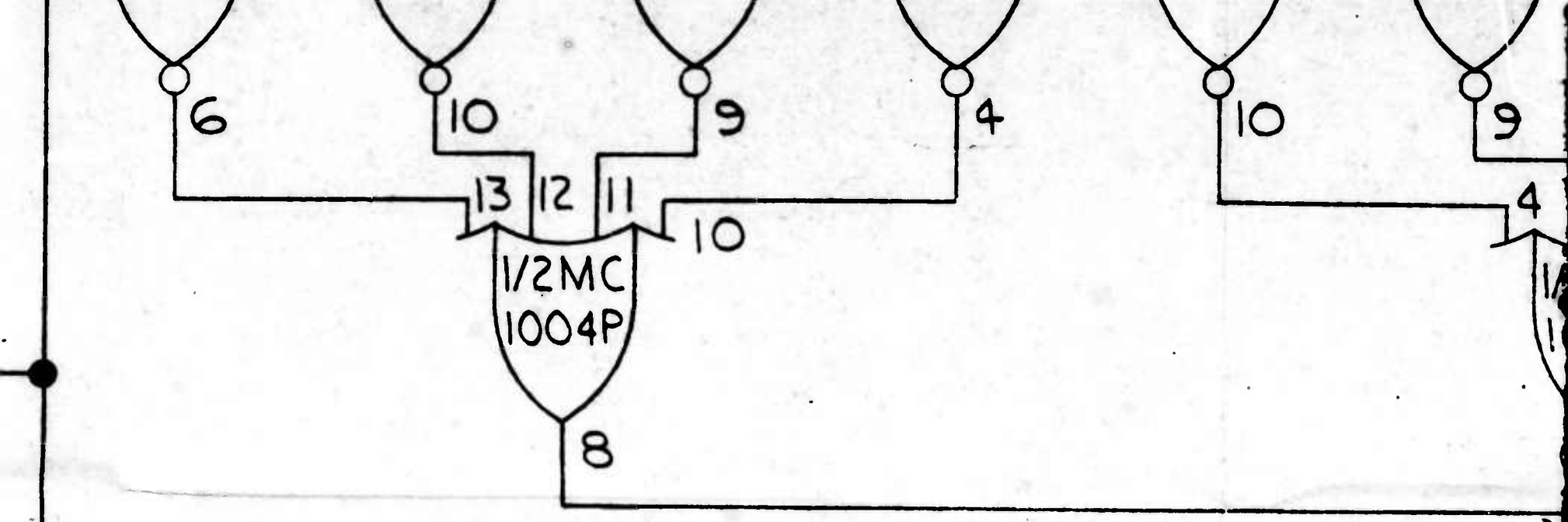

SPERRY SPEC REFERENCED

NEXT ASSY
APPLIC

6 5

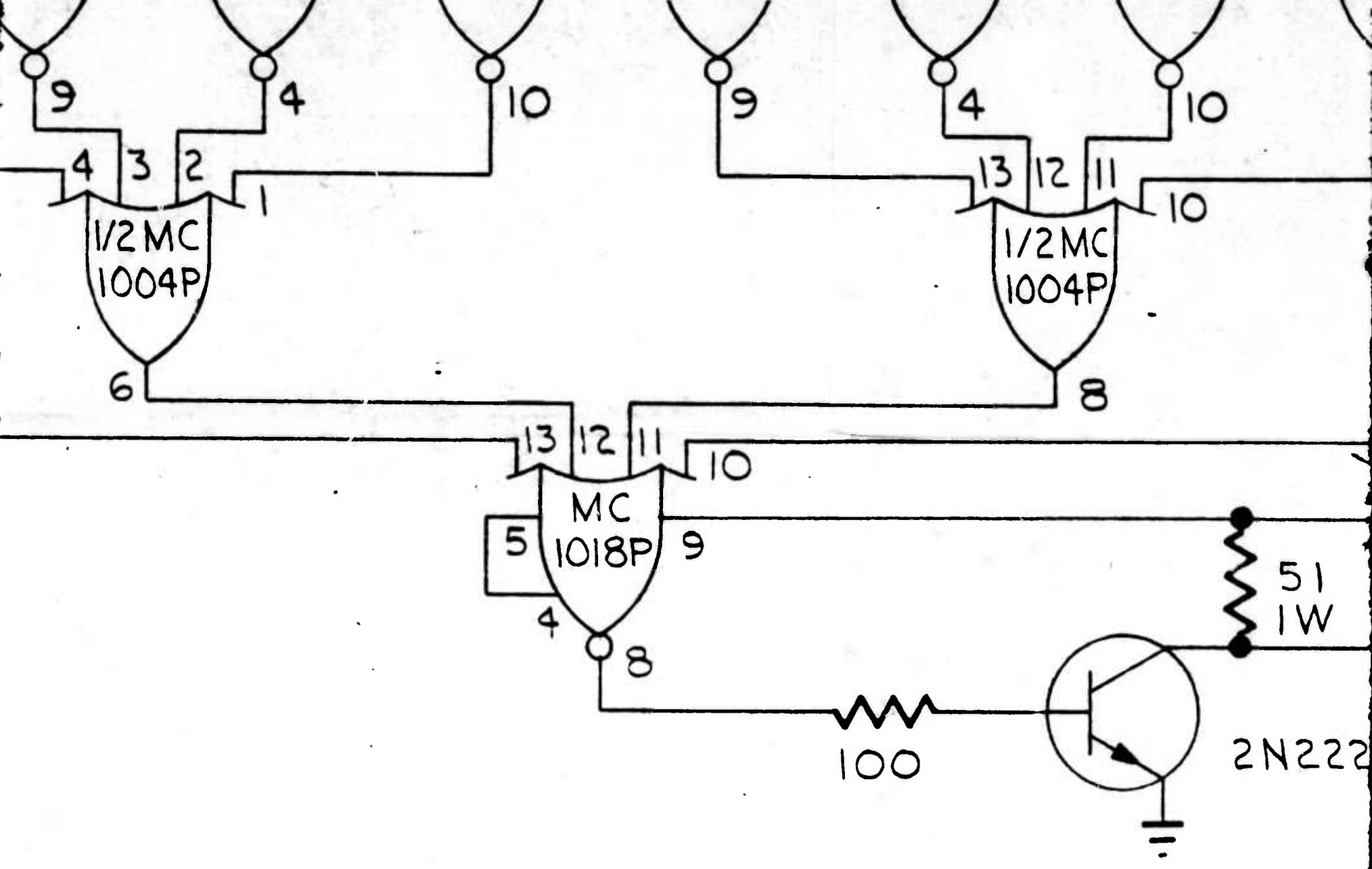

ITEM NO.	QTY REQD	CODE IDENT	MIL. OR INDUSTRY STD	DESIGN ACTIVITY NO.	NOMENCLAT OR DESCRIPT
			PART OR IDENTIFYING NUMBER		

LIST OF MATERIALS OR PARTS

65 64 63 62 61 60 59 58 57 56 55 54 53 52 51 50 49 48 47 46 45 44 43 42 41 40 39 38 37 36 35 34 33 3

SPERRY ITEM CODE	B	C	D	E	F	H

MFG REF NO.

OPERATIONAL NOTE

UNLESS OTHERWISE SPECIFIE ARE IN INCHES. TOLERANCE FRACTIONS DECIMALS

MATL PROCESS FIN.	MILITARY DESIGNATION	SPERRY REQUIREMENTS
MATL N		
PROCESS		
FIN.		

ASSY USED ON APPLICATION

4 3

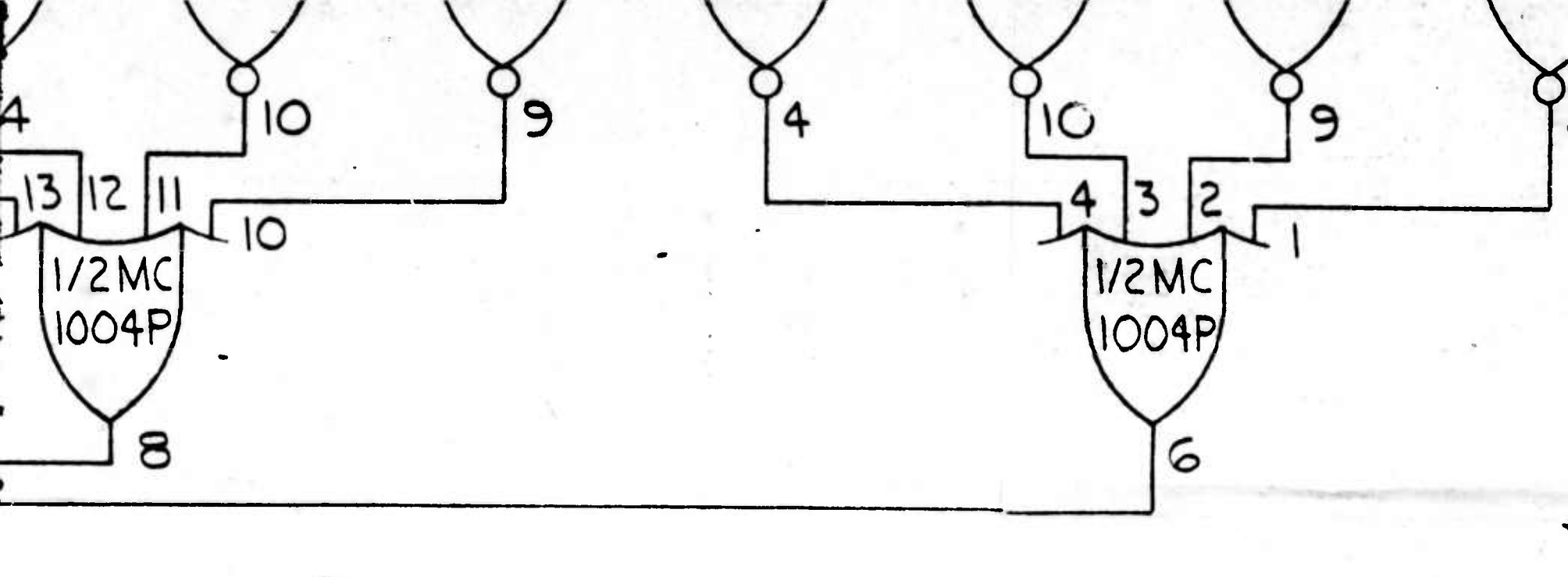

ITEM NO.	NOMENCLATURE OR DESCRIPTION	SYM	MATERIAL	MATERIAL SPECIFICATION	UNIT WT
			MILITARY MATERIAL DESIGNATION		

LIST OF MATERIALS OR PARTS LIST

UNLESS OTHERWISE SPECIFIED DIMENSIONS ARE IN INCHES. TOLERANCES ON FRACTIONS DECIMALS ANGLES

CONTRACT AO 4970-45

SPERRY MICROWA
DIVISION OF S
CLEARW

DRAWN BY DATE 29 Oct 68

CHECKED BY DATE

APPROVED FOR MFG DATE

APPROVED FOR SPERRY DATE

APPROVED FOR DATE

TITLE
LOGIC DI
PULSE G
SINGLE BIT PH

SPERRY REQUIREMENTS	REF DWG
SPERRY CLASS C	
FIRST USED ON	

SIZE	CODE IDENT NO.	DRAWIN
E	06424	

SCALE UNIT WT

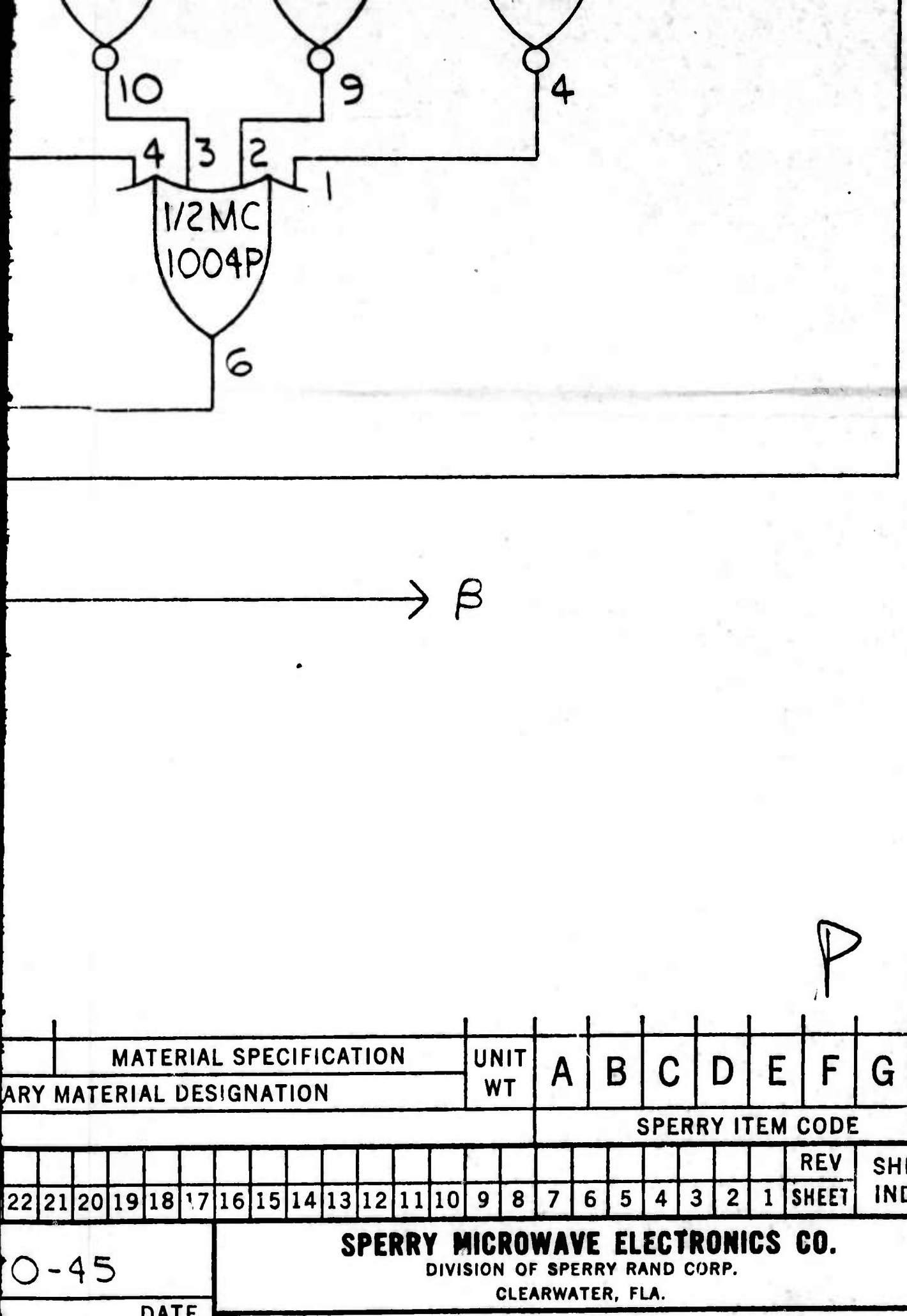

DWG NO. X2689390 SHEET

P

MATERIAL SPECIFICATION	UNIT WT	A	B	C	D	E	F	G	H
ARY MATERIAL DESIGNATION		SPERRY ITEM CODE							

22	21	20	19	18	17	16	15	14	13	12	11	10	9	8	7	6	5	4	3	2	1	REV SHEET	SHEET INDEX

O-45

DATE

- 29 Oct 68

DATE

R MFG DATE

R SPERRY DATE

R DATE

SPERRY MICROWAVE ELECTRONICS CO.
DIVISION OF SPERRY RAND CORP.
CLEARWATER, FLA.

A

TITLE

LOGIC DIAGRAM
PULSE GENERATOR
SINGLE BIT PHASE SHIFTER

SIZE	CODE IDENT NO.	DRAWING NO.	REV LTR
E	06424	X2689390	

SCALE | UNIT WT | SHEET OF

2 1

UNCLASSIFIED

Security Classification

DOCUMENT CONTROL DATA - R & D

(Security classification of title, body of abstract and indexing annotation must be entered when the overall report is classified)

1. ORIGINATING ACTIVITY *(Corporate author)*

Sperry Microwave Electronics Division
Sperry Rand Corporation
Clearwater, Florida 33518

2a. REPORT SECURITY CLASSIFICATION

UNCLASSIFIED

2b. GROUP

3. REPORT TITLE

High Power C Band Phase Shifters

4. DESCRIPTIVE NOTES *(Type of report and inclusive dates)*

Final Report - 11 July 1967 to 15 October 1968

5. AUTHOR(S) *(First name, middle initial, last name)*

L. J. Lavedan, Jr.

6. REPORT DATE	7a. TOTAL NO. OF PAGES	7b. NO. OF REFS
October 1968	80	1

8a. CONTRACT OR GRANT NO.	9a. ORIGINATOR'S REPORT NUMBER(S)
F30602-68-C-0006	(Proj. No. 0-0200-2122-D102)
b. PROJECT NO.	SJ 220-4970-6
c. ARPA Order 550	9b. OTHER REPORT NO(S) *(Any other numbers that may be assigned this report)*
d.	RADC-TR-68-557

10. DISTRIBUTION STATEMENT

This document is subject to special export controls and each transmittal to foreign governments, foreign nationals or representatives thereto may be made only with prior approval of RADC (EMATE), GAFB, NY 13440

11. SUPPLEMENTARY NOTES	12. SPONSORING MILITARY ACTIVITY
Monitored By: Rome Air Development (EMATE) Griffiss Air Force Base, New York 13440	Advanced Research Projects Agency Washington D.C. 20301

13. ABSTRACT

This report outlines all tasks performed under this program and includes techniques performed in developing high power phase shifters and a description of the hardware delivered with test results.

Structural studies have been carried out to assure compatability of designs with phased array requirements. Cross sections have been reduced to a minimum by careful location of cooling structures.

Remote driving techniques were developed with emphasis on switching efficiency. A scheme of triggering a single bit phase shifter is outlined in detail.

Studies of flux drive led to a better understanding of practical and theoretical limitations, these limitations being discussed in detail.

A direct comparison of single and multibit phase shifters is given with emphasis on microwave performance and relative cost.

DD FORM 1 NOV 65 1473

UNCLASSIFIED

Security Classification

14 KEY WORDS	LINK A		LINK B		LINK C	
	ROLE	WT	ROLE	WT	ROLE	WT
Phase shifters Ferrites						